NBS-GCR-87-536

Flexural and Shear Behavior of Reinforced Concrete Beams During Fire Tests

T. D. Lin, B. Ellingwood and
O. Piet

Portland Cement Association
Skokie, IL

November 1987

Sponsored by:
U.S. DEPARTMENT OF COMMERCE
National Bureau of Standards
Center for Fire Research
Gaithersburg, MD 20899

NBS-GCR-87-536

FLEXURAL AND SHEAR BEHAVIOR OF REINFORCED CONCRETE BEAMS DURING FIRE TESTS

T. D. Lin, B. Ellingwood and
O. Piet

Portland Cement Association
Skokie, IL

November 1987

NBS Grant No. G8-9027

Sponsored by:
U.S. DEPARTMENT OF COMMERCE
National Bureau of Standards
Center for Fire Research
Gaithersburg, MD 20899

Notice

This report was prepared for the Center for Fire Research of the National Engineering Laboratory, National Bureau of Standards Under Grant Number G8-9027. The statements and conclusions contained in this report are those of the authors and do not necessarily reflect the views of the National Bureau of Standards or the Center for Fire Research.

FLEXURAL AND SHEAR BEHAVIOR OF REINFORCED CONCRETE BEAMS DURING FIRE TESTS

PORTLAND CEMENT ASSOCIATION

RESEARCH & DEVELOPMENT BULLETIN RD 091 T

by

T. D. Lin, Bruce Ellingwood, and Olivier Piet

CONSTRUCTION TECHNOLOGY LABORATORIES
A Division of the Portland Cement Association
5420 Old Orchard Road
Skokie, Illinois 60077

October 1985

TABLE OF CONTENTS

Page

SYNOPSIS 1

INTRODUCTION 2

REVIEW OF EXPERIMENTAL WORK 4

TEST SPECIMENS 5

- Materials 7
- Fabrication 7
  - Reinforcing Bars 7
  - Thermocouples 7
  - Concrete Mix 10
  - Casting and Curing 15

TEST PROCEDURES AND RESULTS 18

- Load Measurements 18
- Temperature Measurements 23
  - Furnace Atmosphere Temperatures 23
  - Concrete Temperatures 26
  - Steel Temperatures 26
  - Stirrup Temperatures 38
- Deflection Measurements 41
- Expansion Measurements 44
- Observation During Tests 45
- General Observation 49

THERMAL ANALYSIS 49

- Thermal Properties of Concrete and Steel 49
- Analysis of Temperature Development in Beams 55

STRUCTURAL ANALYSIS 71

- Mechanical Properties of Concrete and Steel 71
- Structural Analysis and Response 77

SUMMARY 94

REFERENCES 97

FLEXURAL AND SHEAR BEHAVIOR OF REINFORCED CONCRETE BEAMS DURING FIRE TESTS

by

T. D. Lin,* Bruce Ellingwood,** and Olivier Piet***

SYNOPSIS

This report describes the results of a research program conducted by the Portland Cement Association and the National Bureau of Standards to study the behavior of reinforced concrete beams exposed to fire. Data are presented from fire tests on six full-scale concrete beams subjected to large applied loads. Also presented is a mathematical model for predicting structural response of concrete beams exposed to fire.

The objectives of the test program were:

(a) To examine flexural and shear behavior of beams exposed to fire, and

(b) To generate experimental data for validating computer programs developed for calculating thermal and structural behavior of beams exposed to fire.

Test specimens included five 21-in. deep x 9-in. wide (533x229 mm) and one 24-in. deep x 10-in. wide (610x254 mm)

---

*Principal Research Engineer, Fire Research Section, Construction Technology Laboratories, a Division of the Portland Cement Association, Skokie, Illinois 60077.

**Professor, Civil Engineering Department, Johns Hopkins University, Baltimore, MD 21218 (formerly Structural Engineering Group Leader, Center for Building Technology, National Bureau of Standards, Gaithersburg, MD 20899).

***Engineer, Service des Voies Navigables due Nord et du Pas de Calais, Douai, France (formerly Guest Worker, Center for Building Technology, National Bureau of Standards).

beams. All beams measured approximately 27 ft (8.2 m) in length, with a 20-ft (6.1 m) span exposed to fire and an unexposed cantilever loaded so as to provide continuity over one support. They were fabricated with normal-weight concrete.

Four beams were exposed to the standard fire specified in ASTM Designation: E119.(1) The remaining two beams were tested using a exposure denoted as a Short Duration High-Intensity (SDHI) fire. During testing, beams were loaded to produce a negative moment equivalent to 59% of their respective nominal negative flexural strength at the continuous support. A few hairline cracks developed across top and side surfaces of the beam over the continuous support.

In all tests, diagonal shear cracks developed near the continuous support at 1-1/2 hr after the start of the fire and flexural cracks formed in the maximum positive moment region approximately one-half hour later. As the test progressed, shear cracks remained essentially unchanged, but flexural cracks rapidly worsened and surpassed the shear cracks in magnitude during the third hour of the test. All beams formed flexural failure mechanisms that caused the termination of tests. The length of the fire tests were: 3 hr 40 min for Beam No. 1; 3 hr 26 min for Beam No. 2; and 4 hr for Beam Nos 3 to 6.

INTRODUCTION

The provision of fire resistance for reinforced concrete components usually is treated indirectly in structural design. Fire ratings of structural components in the United States traditionally have been measured by tests conducted in accordance with provisions of ASTM Designation: E119.(1)* These tests, which form the basis for most building code requirements for fire resistance, are very costly, and cannot be employed on a wide enough scale to develop general fire-resistant design criteria. These tests provide only a limited basis for extrapolating to situations not covered by the limited test data. Moreover, the ASTM E119 time-temperature curve represents only one type of fire exposure, and may lead to excessively conservative fire ratings in some instances.

To extend the use of the limited available test data, analytical procedures have been developed (e.g., 2, 13) to calculate thermal and structural response of building elements exposed to fire. The availability of analytical procedures makes it possible to design structures for other, more realistic fire exposures than the ASTM Designation E119 exposure. Such designs might well lead to cost savings in construction and better performance of structures exposed to fires. However, with the increasing reliance on computer modeling in analysis and design, it is essential that these analytical procedures be validated using experimental data.

This report describes the results of a combined experimental and analytical program at the Portland Cement Association and the National Bureau of Standards to study the behavior of full-size concrete beams exposed to fire. Structural fire tests were conducted in the Fire Research Laboratory of the Portland

Cement Association. Measured data included steel and concrete temperatures, applied loads, and beam deformations such as deflections, expansions, and slopes throughout each fire test. Thermo-mechanical calculations of beam behavior were performed at NBS, and were compared to the behavior observed experimentally. This study has shown that thermo-mechanical structural analysis, coupled with appropriate values for material properties, can accurately predict the structural behavior of reinforced concrete members exposed to fire. Such analyses can provide an improved basis for fire-resistant structural design.

REVIEW OF EXPERIMENTAL WORK

Numerous fire tests of reinforced concrete beams have been conducted at the PCA Fire Research Laboratory during the last 20 years. These tests have been carried out in accordance with the ASTM Designation: E119 standard test method. In one test series,(3) 40-ft (12.2 m) long simply supported prestressed and reinforced concrete beams were tested with uniform loads. These beams invariably failed in flexure when a hinge formed at midspan after several hours of exposure. In another fire test series,(4) different continuity conditions were simulated by applying a uniform load on the portion of the beam exposed to fire and point loads at one or both unexposed cantilever portions of the beam. In these tests, flexural behavior also governed the failure condition.

In both series, the shear-moment strength ratio of the beams was small. There has been little experimental investigation of the possibility that the appropriate limit state for certain beams during fire would be related to shear rather than flexure. Stresses due to thermal strains frequently cause a concrete beam or column to crack or spall and lead to a reduction in concrete area available to resist shear forces. In contrast to flexural failures, which are usually ductile, shear failures often occur without warning. It was theorized that a reinforced concrete beam designed to fail in flexure under ambient conditions might fail in shear at elevated temperatures. One objective of the experimental program was to see if this would occur.

TEST SPECIMENS

Six reinforced concrete beams were cast at the Construction Technology Laboratories, of the Portland Cement Association. Dimensions of beams and reinforcing steel details were provided by the Center for Building Technology of the National Bureau of Standards. All beams had a 20-ft (6.1 m) span and a 6-ft (1.8 m) cantilever. Figure 1 shows details of the beam specimens.

Grade 60 reinforcing bars used in the fabrication conformed to requirements of ASTM Designation: A615.(5) Beams were fabricated using a normal-weight concrete with a nominal compressive strength of 4000 psi (2.76 MPa).

Approximately 75 thermocouples were installed in each specimen to measure concrete and steel temperatures during fire tests. Two Monfore-Type hygrometer wells(6) for measuring relative humidity (RH) of the concrete were provided at the centerline of the west end of each beam, as shown in Fig. 1.

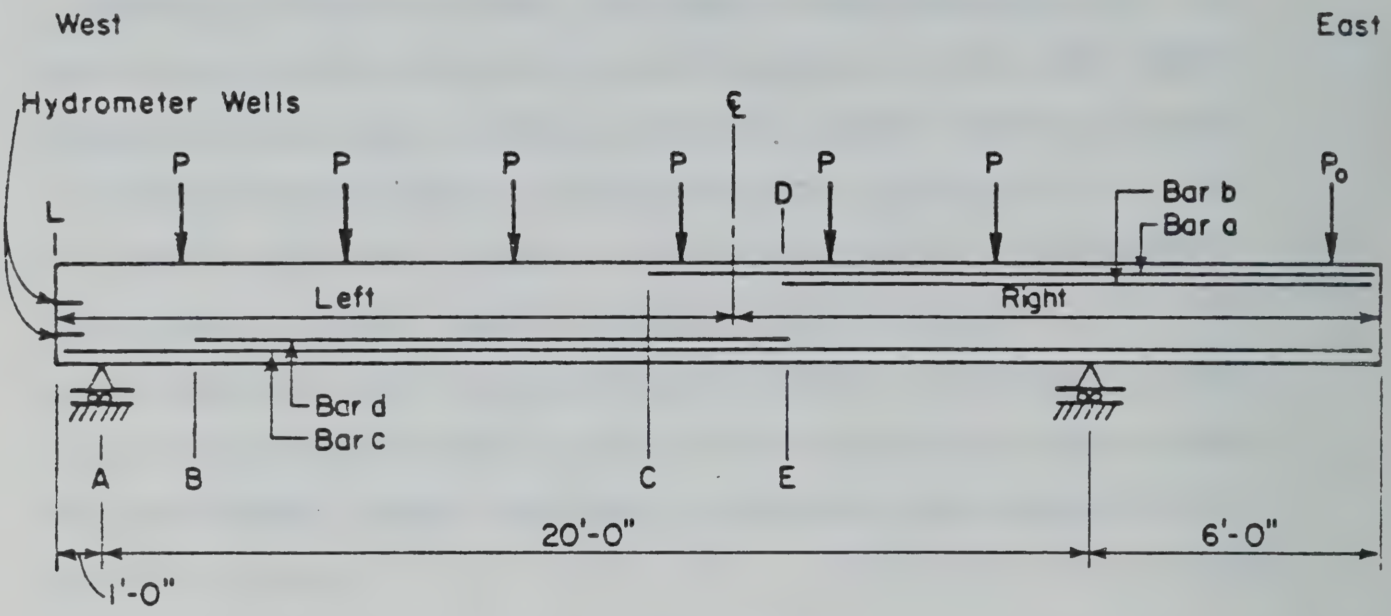

Specimen	Bar Size					Bar End Location, from L				
	a	b	c	d	e	A	B	C	D	E
1,2,3,5,6	#8	#8	#7	#7	—	1'	2'-2"	12'-10"	15'-7"	15'-11"
4	#8	#8	#7	#7	#8	1'	2'-8"	12'-8"	15'-4"	15'-5"

Specimen	Cross Section H x W	Cover, in.	Dividing Line for F Stirrup	Stirrup Spacing	
				Left	Right
1,2,5	21"x9"	1-1/2	15'-7"	8-1/2"	5-3/4"
3,6	21"x9"	2-1/4	15'-7"	8-1/2"	5-3/4"
4	24"x10"	1-1/2	13'-11"	10"	4"

Fig. 1 Specimen Details

Material

Concrete was made with Type I portland cement and calcareous sand and gravel from McHenry, Illinois. The maximum size of coarse aggregate was 1 in. (25 mm). Table 1 gives the physical properties of the aggregate.

Reinforcing bars were tested to determine their tensile strength. Measured stresses and strains at yield and ultimate are listed in Table 2.

Thermocouples used were made from 20-gage chromel-alumel duplex wires.

Fabrication

Details concerning fabrication and curing of specimens are given in the following paragraphs:

Reinforcing Bars

All beams were reinforced with No. 8 bars at top, No. 7 bars at bottom, and No. 3 bars for stirrups. In the first step of fabrication, main bars and stirrups were tied together to form a steel cage. The steel cage was then hoisted by a crane and carefully positioned in the form.

Thermocouples

To utilize effectively the thermocouples available for measuring temperatures in each test beam, eight thermocouple frames were fabricated and installed at locations, as shown in Fig. 2. All eight thermocouple frames were distributed in an exposed portion of the beam starting from 1 ft 8 in. (0.56 m)

TABLE 1 - PHYSICAL PROPERTIES OF AGGREGATE

Property	
Specific Gravity of Sand	2.67
Specific Gravity of Gravel	2.68
Moisture Content of Sand, %	5.0
SSD(a) Unit Wt. of Gravel, lb/ft^3	102.4
SSD(a) Unit Wt. of Sand, lb/ft^3	109.5
Fineness Modulus of Fine Aggregate	2.7
Fineness Modulus of Coarse Aggregate	6.97

(a) SSD = Saturated Surface Dry

TABLE 2 - STRESS AND STRAIN DATA FOR STEEL

Bar Size	Yield		Ultimate	
	Stress, ksi	Strain in./in.	Strength ksi	Strain in./in.
3	70.1	0.0028	114.9	0.0763
7	69.8	0.0025	111.3	0.1347
8	73.9	0.0028	121.5	0.1150

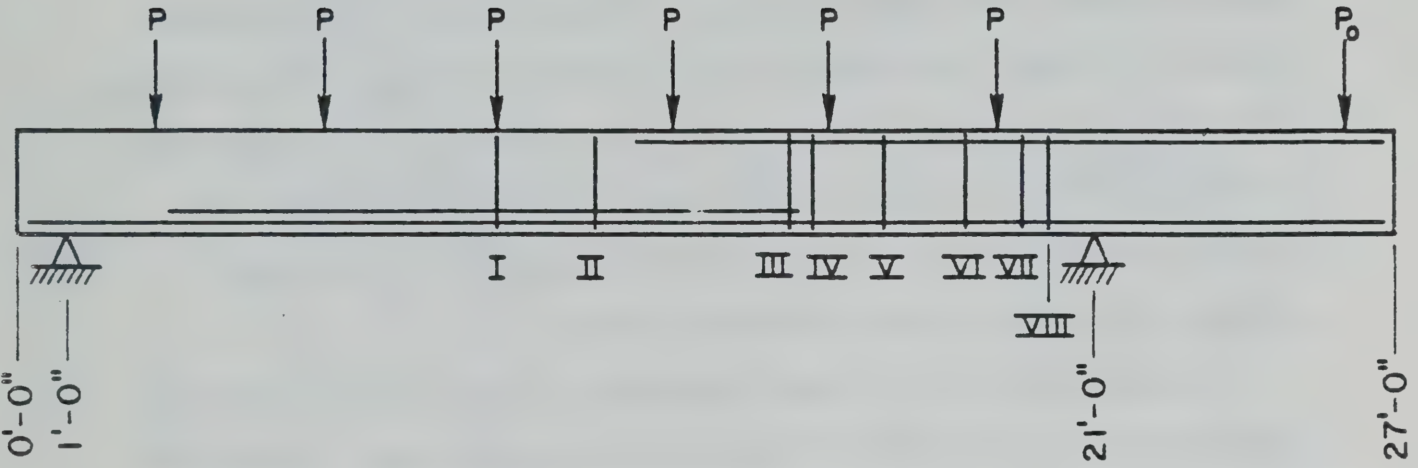

T/C frame	T/C locations	Beams 1,2,3,5,6 from west end	Beam 4 from west end
I	Main bars	9'-4"	9'-4"
II	Concrete	11'-0"	11'-0"
III	Stirrup	15'-¼"	15'-1"
IV	Main bars	15'-11"	15'-5"
V	Stirrup	17'-2"	17'-1"
VI	Stirrup	18'-7¼"	18'-5"
VII	Stirrup	19'-6¾"	19'-5"
VIII	Stirrup	20'-½"	19'-9"

Fig. 2 Location of Thermocouple Frames

west of the mid-span to the east support. This is the region where the maximum flexural and shear stresses were expected to occur.

Figure 3 shows details of thermocouple Frames I and IV for measuring main bar temperatures. Thermocouples were mounted directly on the side surfaces of the bars. Paired thermocouples that were symmetrically located on either side of the vertical centerline of the cross-section were connected together to obtain an average temperature of bars located at the same elevation measured from the beam bottom.

Thermocouple Frame II was designed for measuring concrete temperatures in one-half of the beam cross-section. This particular thermocouple frame was constructed with five thermocouple trees, each containing eight measuring points. Figure 4 shows the numbering sequence and locations of these 40 thermocouples.

Since one objective of the program included the study of the shear behavior of beams exposed to fire, stirrup temperatures were measured on five selected stirrups. Figure 5 shows designated Thermocouple Frames III, V to VIII, and their thermocouple numbers.

Concrete Mix

Ready-mixed concrete was used for all specimens. The water/ cement ratio for the mix was 0.4. Batch quantities, data on fresh concrete, and average 28-day concrete compressive strength are listed in Table 3.

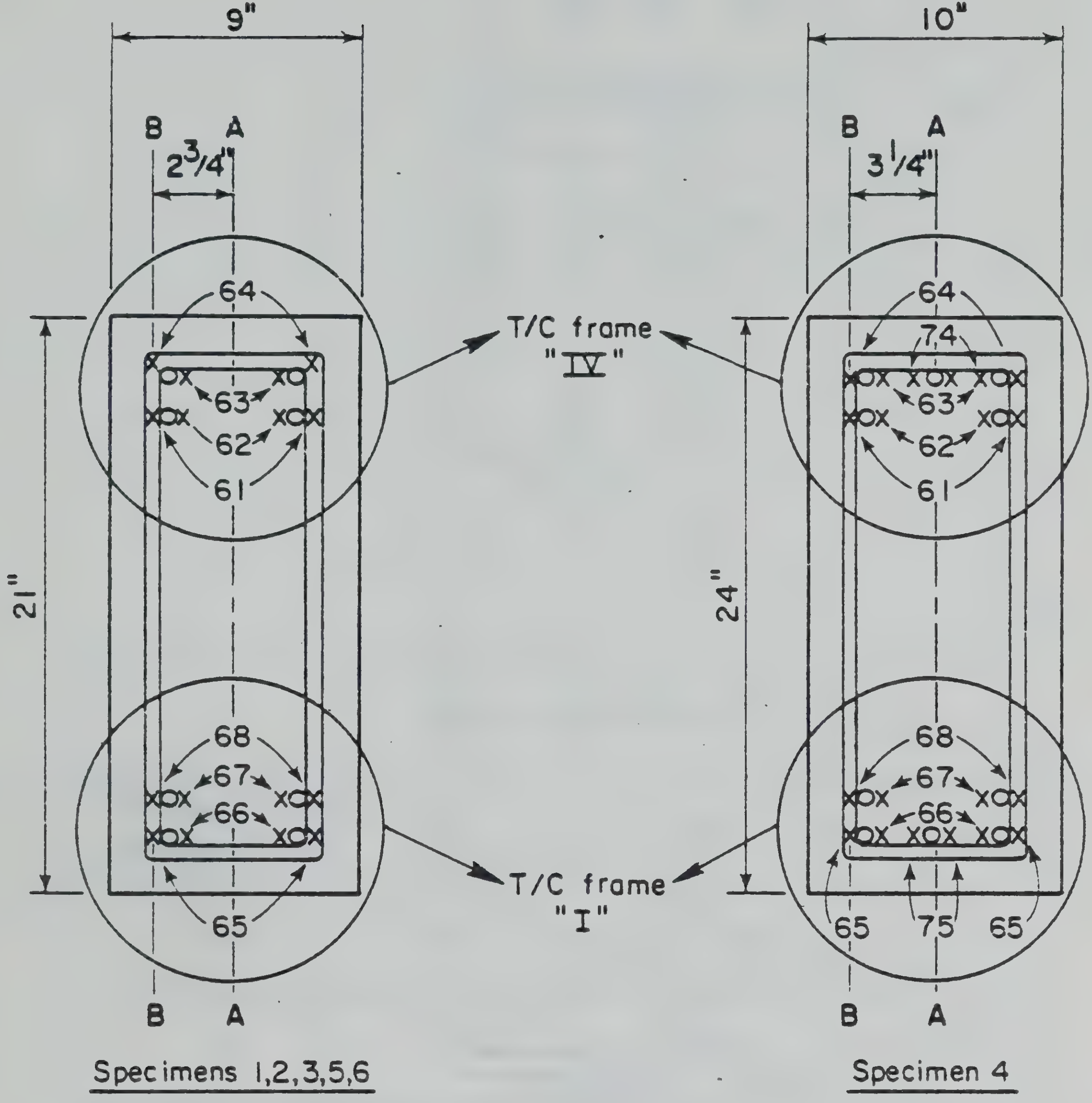

Fig. 3 Thermocouples for Measuring Main Bar Temperatures - T/C Frames I and IV

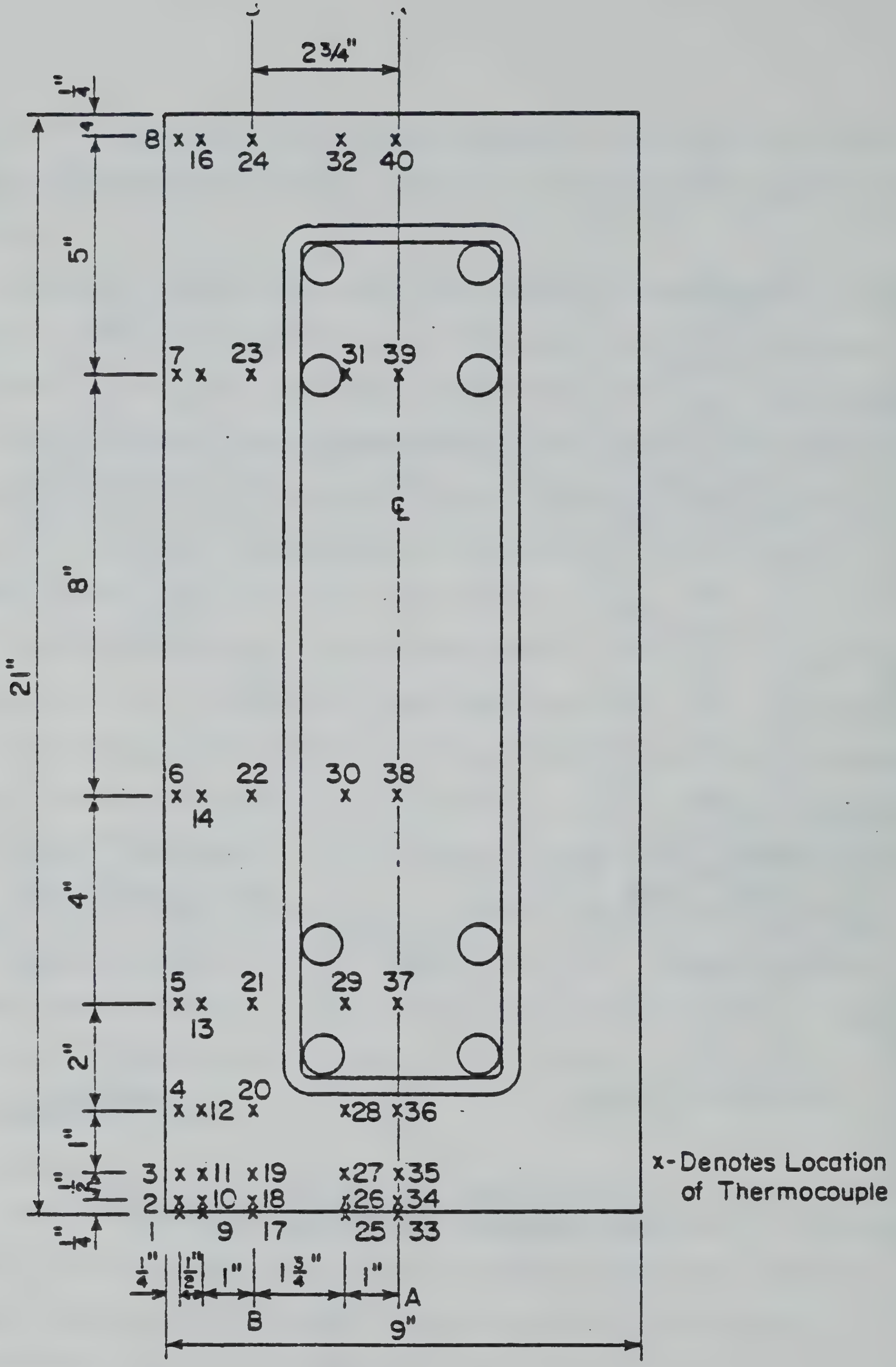

Specimens 3,6

Fig. 4 Thermocouple Frame II

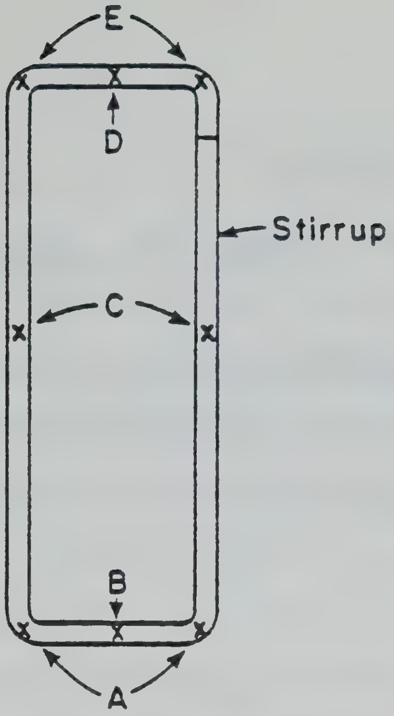

	Thermocouple Number				
Frame Designation	III	V	VI	VII	VIII
A	56	51	46	41	69
B	57	52	47	42	70
C	58	53	48	43	71
D	59	54	49	44	72
E	60	55	50	45	73

X-Denotes location of thermocouple

Fig. 5 Thermocouple Locations and Numbering Sequence-Stirrup Temperatures

TABLE 3 - CONCRETE DATA

Item	lb/cu yd
Cement	517
Coarse Aggregate	1840(a)
Sand	1345(a)
Water	252
Darex, Fl. Oz.	6
Average Air Content, %	4.7
Average Unit Weight, lb/cu ft	148.2
Average Slump, in.	3.8
Average Compressive Strength at 28 days, psi	4520

(a) Saturated Surface Dry Weight

Casting and Curing

Six inserts were embedded along the longitudinal centerline of the top surface of each beam. Two lifting inserts were located 3 ft 6 in. (1.1 m) from each end. Four safety inserts for attaching lifting chains were positioned near mid-span.

Concrete was placed with a 6-cu ft dump bucket, and was consolidated with internal vibrators and finished with wood floats. Concrete placement is shown in Fig. 6.

Concrete was cured in the form under damp burlap for 7 days. Following removal of the form, concrete beams were immediately transported to a room in which the temperature and relative humidity (RH) were maintained at 70° to 75°F (21° to 24°C) and 30 to 40%, respectively, for moisture conditioning.

A summary of the beams tested is given in Table 4. All beams were designed according to ACI Standard 318-77.(10) Beam Nos. 1 and 2 are nominally identical and have the same minimum allowable bar cover. These two beams were tested to assess the reproducibility of beam behavior during fires. Beam No. 3 had bar cover of 2-1/4 in. (57 mm). A comparison of the behavior of Beam No. 3 with that of Beam Nos. 1 and 2 would show the effect of concrete cover on beam behavior during the fire. Beam No. 4 had a larger cross-sectional area than the other beams, and was tested to study the effect of shear stress on the fire endurance of beams.

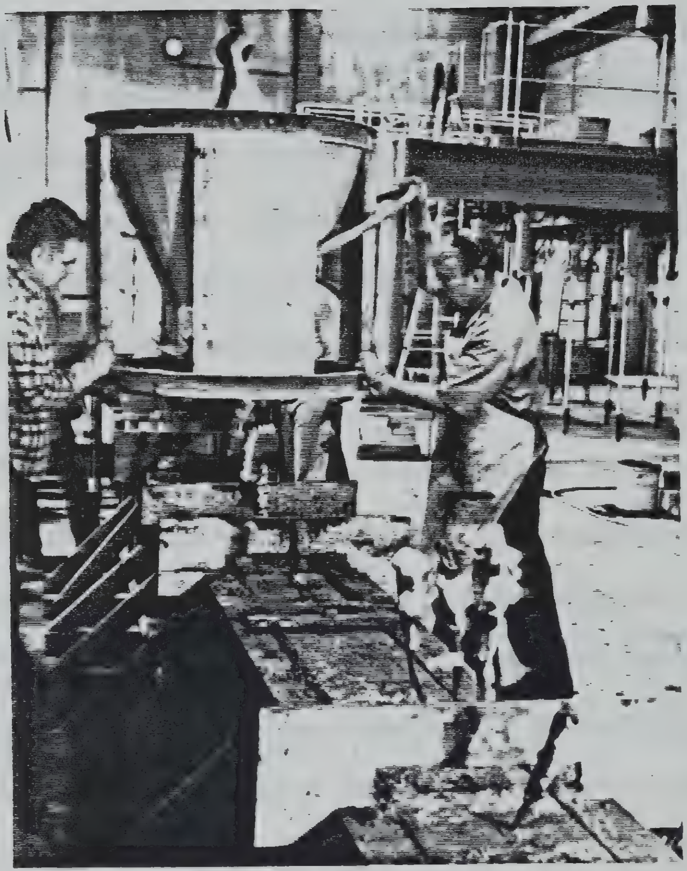

Fig. 6 Casting Beam Specimen

TABLE 4 - DETAILS OF BEAM TEST CONDITIONS

Beam No.	Test Date Mo-Day-Yr	Fire Exposure Type	Specimen Age, Days	Loads		f'_c at Test psi	Concrete Cover, in.	% RH(2) at Test	Test Duration Hr:Min
				P, kip	P_o, kip				
1	12-07-79	ASTM	298	10	26	4040	1-1/2	74	3:40
2	03-03-80	ASTM	369	10	26	4490	1-1/2	73	3:26
3	04-08-80	ASTM	375	10	25	4300	2-1/4	76	4:03
4	04-23-80	ASTM	361	16	39	4970	1-1/2	74	4:08
5	08-21-80	SDHI[1]	526	10	26	4890	1-1/2	80	4:03
6	10-20-80	SDHI	520	10	25	5010	2-1/4	74	4:03

(1) Short Duration High Intensity Fire
(2) Relative Humidity

Beam Nos. 5 and 6 were tested using a Short Duration High Intensity (SDHI) fire exposure, the general characteristics of which are more realistic(12) than the ASTM E119 fire exposure. In fires which are naturally ventilated, temperatures increase rapidly for a finite period of time and then decrease over an extended period after the fuel supply has been consumed. Comparisons of the behavior of Beam No. 5 to Beam Nos. 1 and 2 (or Beam Nos. 6 to 3) show the effect on behavior of the SDHI rather than the ASTM fire exposure.

TEST PROCEDURES AND RESULTS

About one week prior to each fire test, the test beam was moved from the conditioning room to the furnace room for instrumentation. The test beam was positioned in the furnace, as shown in Fig. 7. After the furnace top was closed and sealed, instruments for measuring beam deflections and rotations were installed.

A tabulation of measured data for the six test beams is given in Reference.(7) Details of testing procedures and test results are given in the following paragraphs.

Load Measurements

Superimposed loads, P, and cantilever load, P_o, were applied alternatively in four stages through the hydraulic system. Load application points are shown in Fig. 8. Full loads were maintained on the beam for at least 40 min before the fire started.

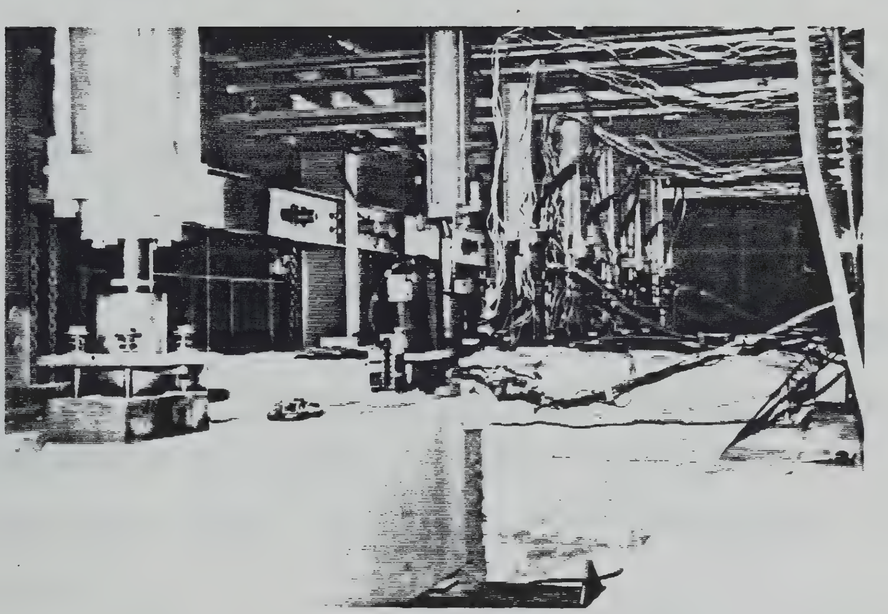

Fig. 7 Test Beam in Furnace.

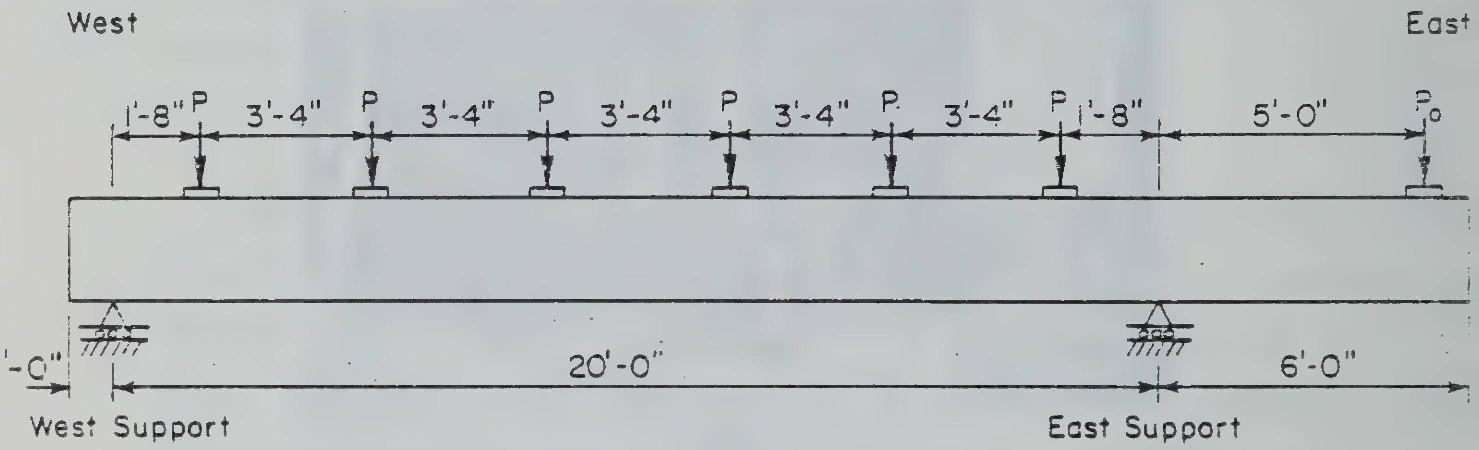

Fig. 8 Ram Locations.

The magnitude of superimposed loads, P, was determined by assuming that loads on the floor system were equal to the full unfactored design loads. These loads were held constant throughout the test. The cantilever load, P_o, applied at the start of the test was determined so that the induced negative moment was equal to 59% of the negative nominal moment strength at the continuous support. Initial loads for all tests are given in Table 4.

Specimens were tested to simulate an end span of a continuous beam. This was accomplished by maintaining the cantilever end of the beam at a constant elevation during the course of the fire test by changing the cantilever load as required. The cantilever load was further controlled so that the induced negative moment did not exceed 85% of the negative nominal flexural strength at the support. Beyond this point, the cantilever end was allowed to deflect under the maximum cantilever load.

Figure 9 shows cantilever loads measured for the six beams. The lower curve represents average cantilever loads for the five beams that had a 21-in. x 9-in. (533x229 mm) cross-section. The measured cantilever loads for these five beams all increased rapidly during the first 50 min, and reached the maximum at about 1 hr of fire exposure. After the first hour, cantilever loads remained fairly constant or increased slightly.

The upper curve in Fig. 9 shows the measured cantilever load for Beam No. 4. This beam had a cross-section of 24-in.

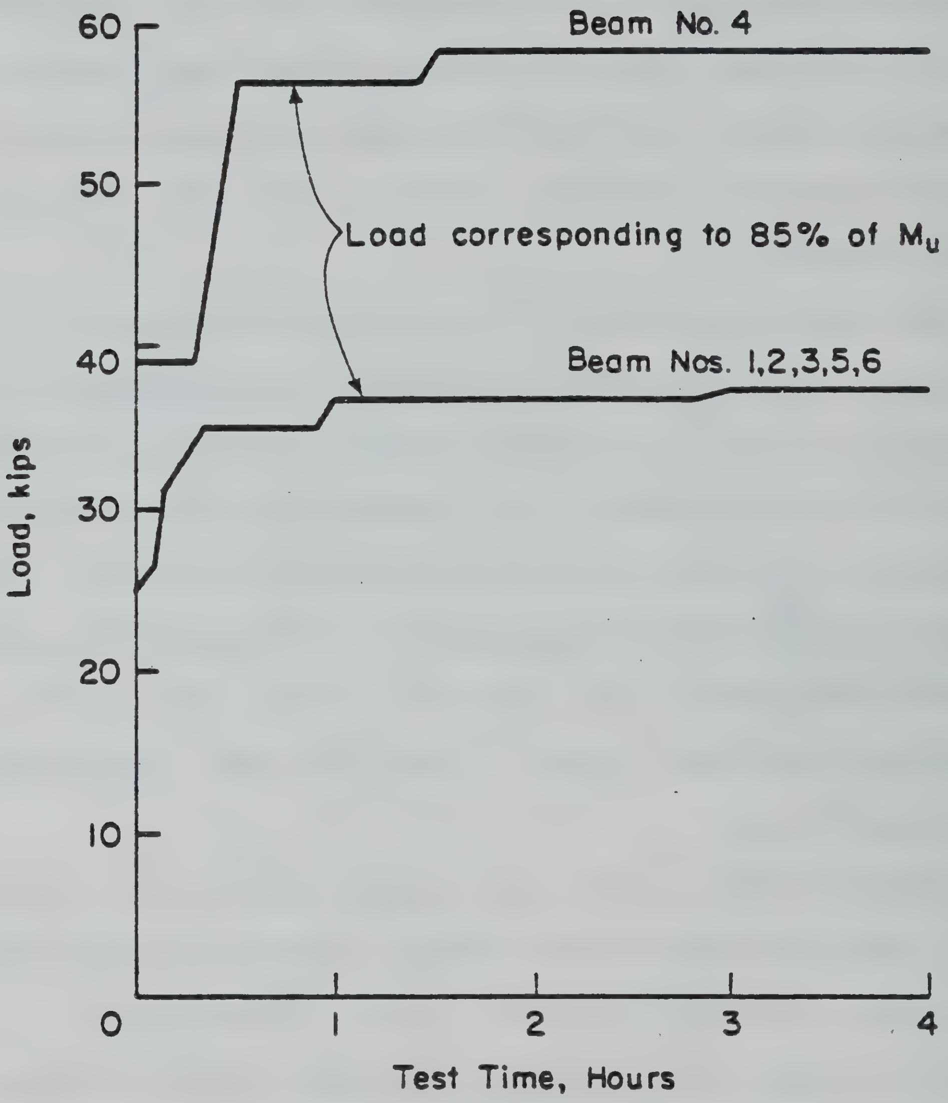

Fig. 9 Measured Cantilever Loads

deep by 10-in. wide (610x254 mm), and a flexural stiffness equal to 166% of Beam No. 1. Interestingly, the cantilever load for Beam No. 4 did not increase during the first 15 min of fire. It increased rapidly in the following 10 min and then remained constant for nearly 1 hr. At 1-1/2 hr of test time, the cantilever load increased about 4 kips (17.8 kN) and then remained constant until the end of the test.

Temperature Measurements

Temperatures of the furnace atmosphere and in the concrete, main reinforcing steel, and stirrups were measured during each of the six fire tests.

Furnace Atmosphere Temperature

Six thermocouples protected and positioned in accordance with the requirements of ASTM Designation: E119 were used to measure and control furnace temperatures.

Four beams were exposed to the ASTM Designation: E119 time-temperature relationship. The remaining two beams were exposed to a Short Duration High-Intensity Fire.(8,12)

Figure 10 shows average furnace temperatures measured in the four tests that used the ASTM Designation: E119 Curve. Average furnace temperatures for the two tests using the Short Duration High-Intensity Fire developed at the National Bureau of Standards are shown in Fig. 11.(12) The measured temperatures were about 100 to 200°F cooler than the ASTM standard fire curve (or Short Duration High-Intensity curves in the first 15 min of

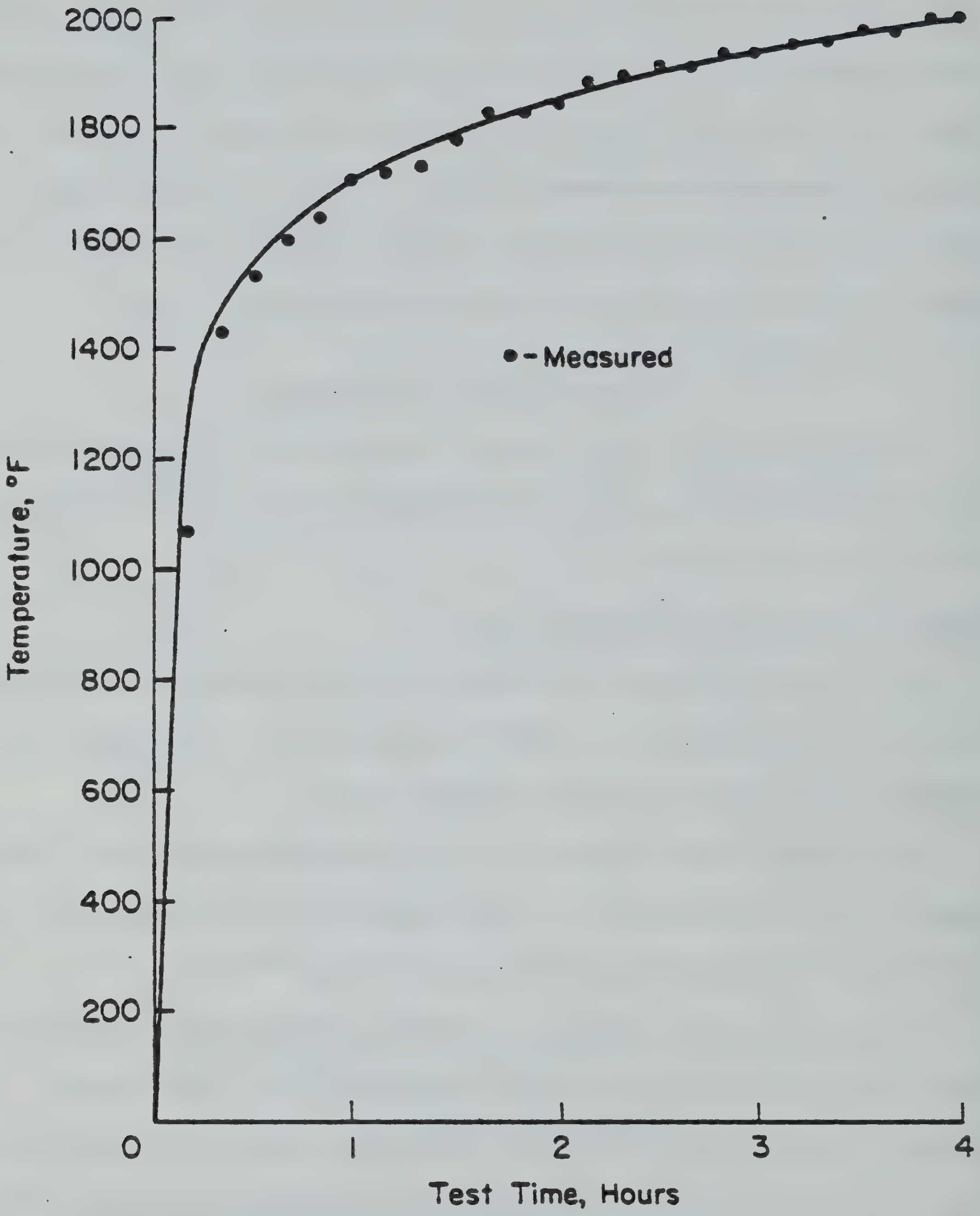

Fig. 10 Furnace Atmosphere Temperatures - ASTM Fire

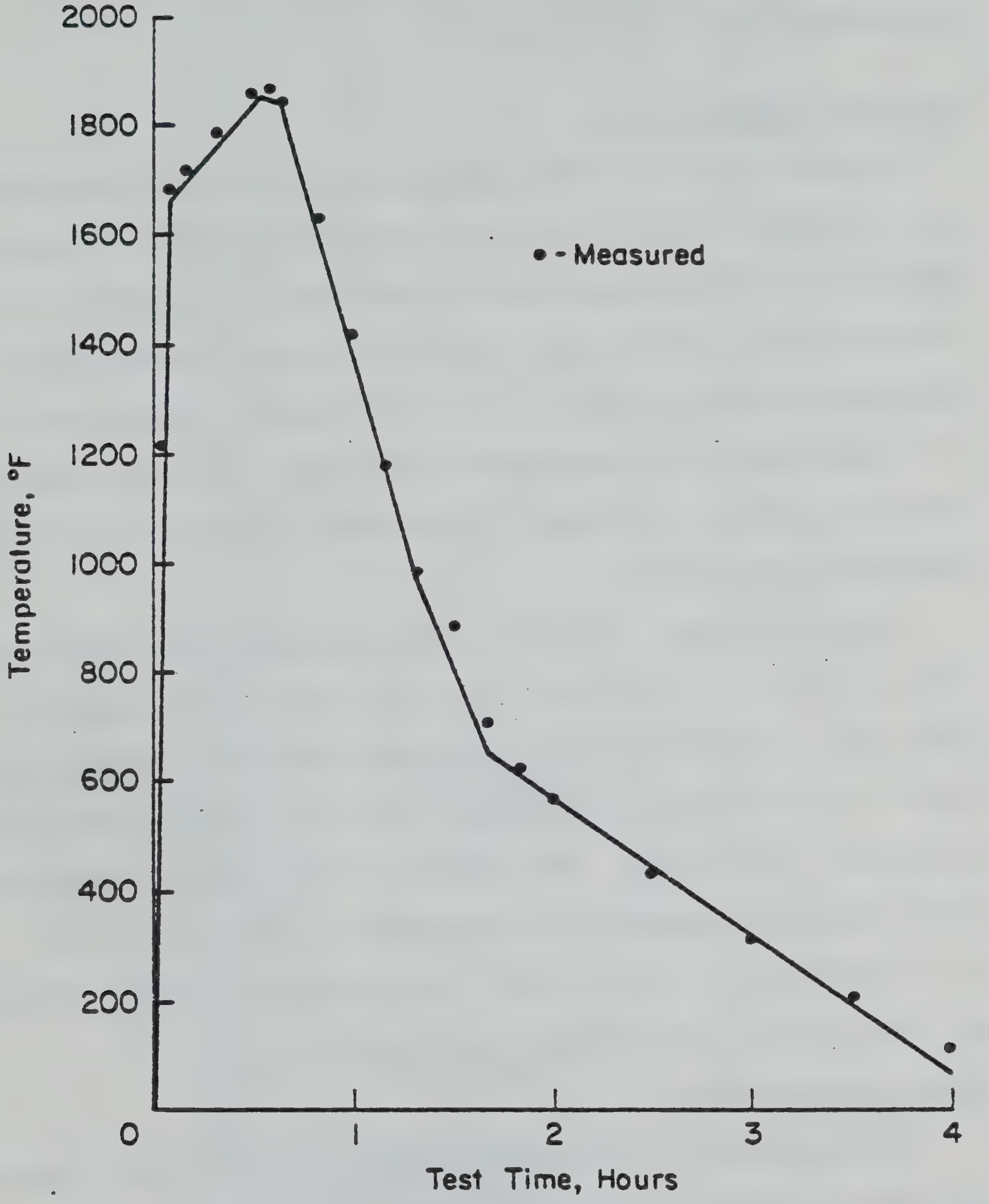

Fig. 11 Measured Furnace Temperatures - SDHI Fire

time. Subsequently the differences were so small that the furnace temperature correction required by ASTM E119 was found unnecessary for these tests.

Concrete Temperatures

Figures 12 to 15 show temperature distributions measured at test times of 1/2, 1, 2, and 3 hrs, in Beam No. 1 exposed to ASTM fire. These isothermal curves were constructed by interpolating temperatures measured at the thermocouple locations shown in Fig. 4. All isothermal curves were plotted for temperature of even-number hundreds. In areas where the thermal gradient was small, isothermal curves at odd number hundreds were added.

Likewise, Figs. 16 to 20 show isothermal curves at test time of 1/2, 1, 2, 3, and 4 hrs for Beam No. 5 exposed to the SDHI fire. The SDHI fire increases from room temperature to 1860°F in the first 45 minutes, and then rapidly cools off to 600°F at 1 hr-40 min. The effect of decreasing temperatures on the isothermal curves is illustrated in Figs. 18 to 20. At test times of 2, 3 and 4 hrs, the isothermal curves change from an open-end to a closed-end configuration.

Steel Temperatures

Temperatures of reinforcing bars in a test beam influence the beam's flexural strength. For this reason temperatures were measured for each bar. Figures 21 and 22 show the measured temperatures for Beam Nos. 1 and 5 exposed to the ASTM fire and SDHI fire, respectively. Temperatures in the bottom steel at midspan are shown by the two upper curves marked as 1st and

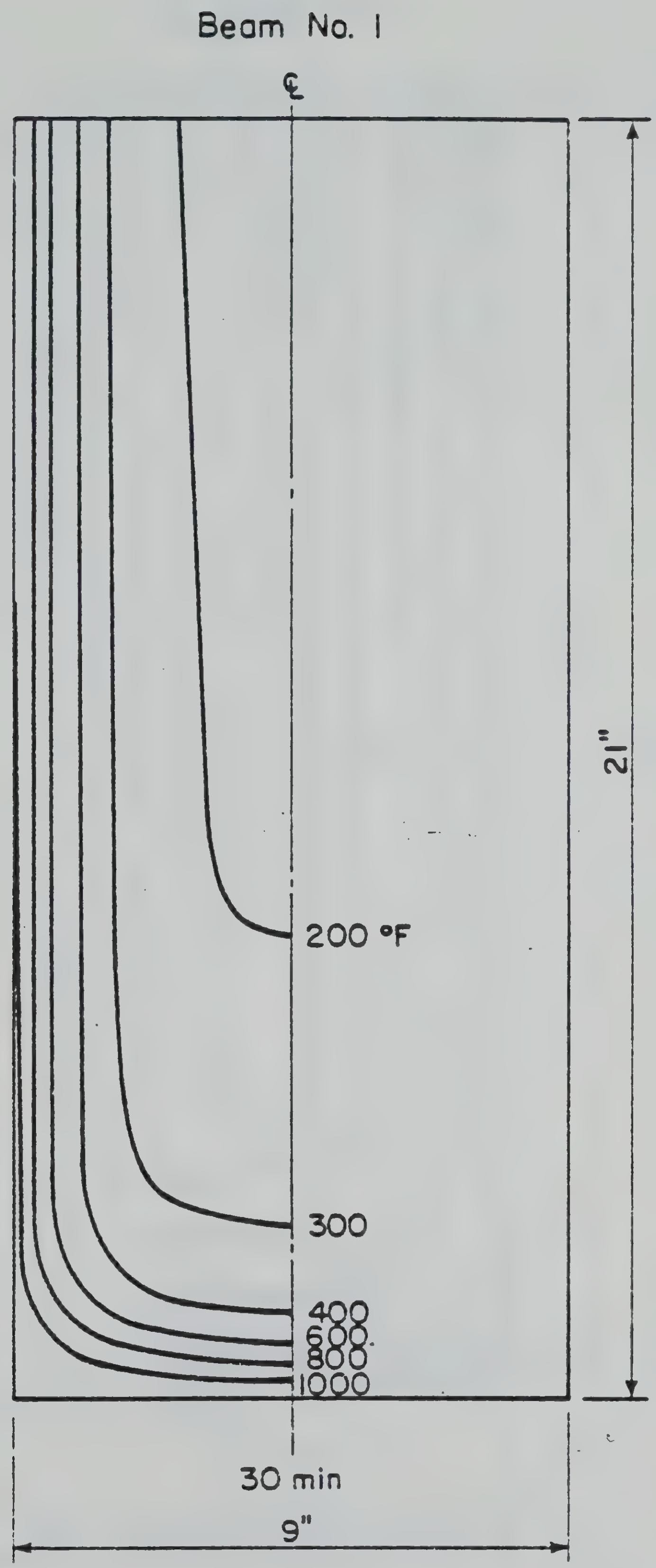

Fig. 12 Temperature Distribution - Beam No. 1 @Test Time 30 min

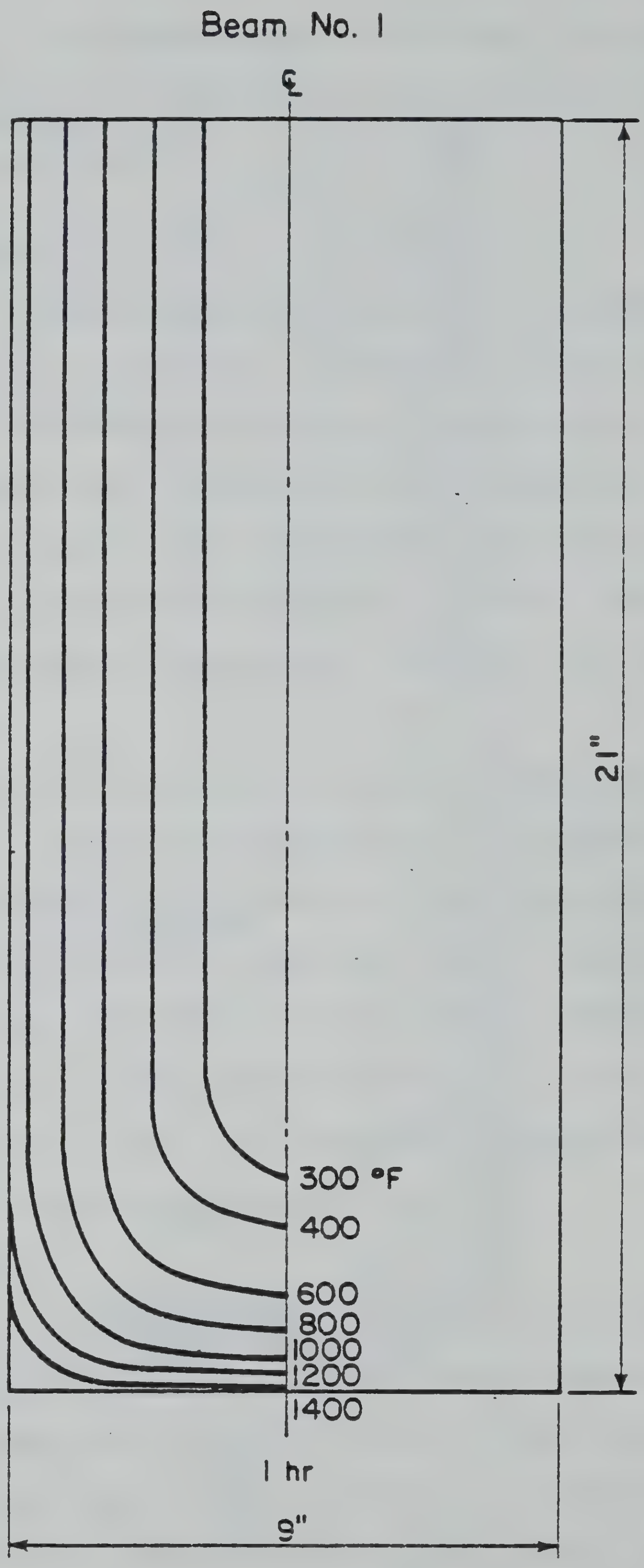

Fig. 13 Temperature Distribution - Beam No. 1
@Test Time 1 hr

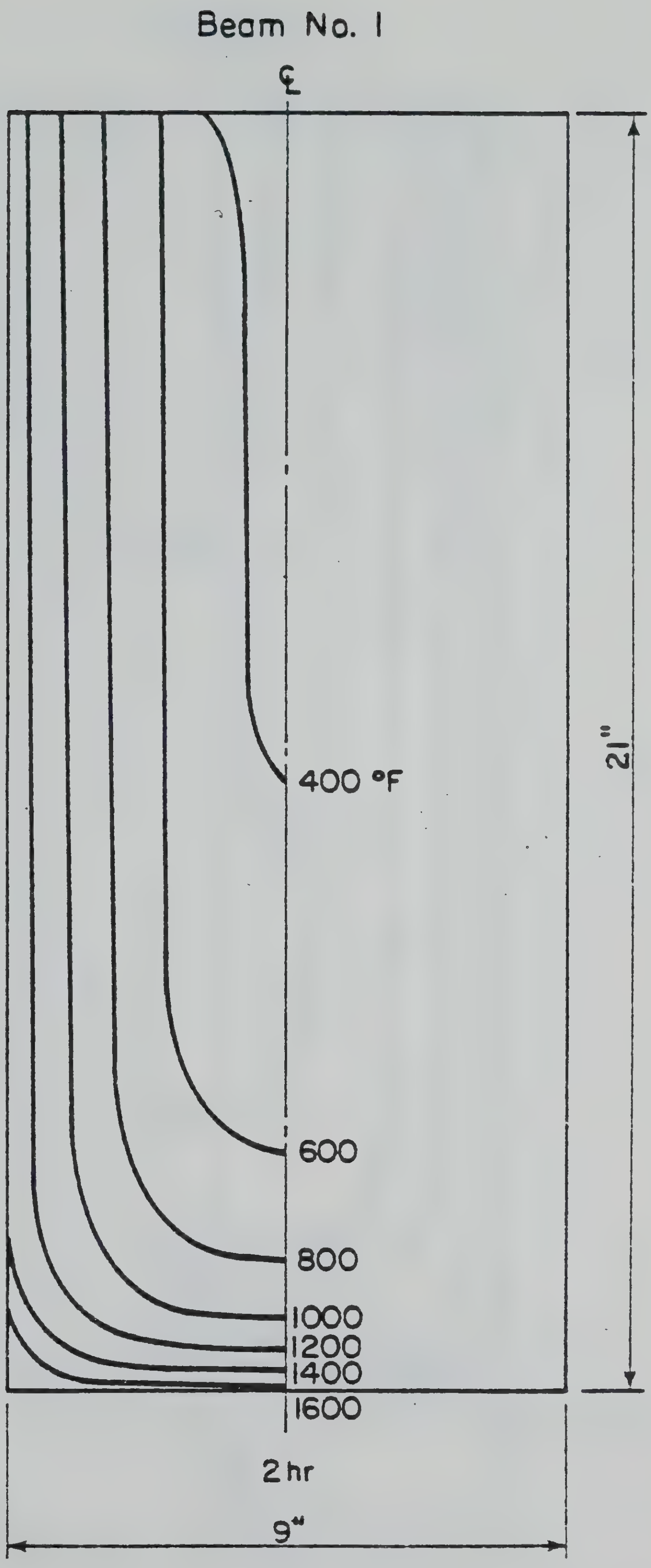

Fig. 14 Temperature Distribution - Beam No. 1
@Test Time 2 hr

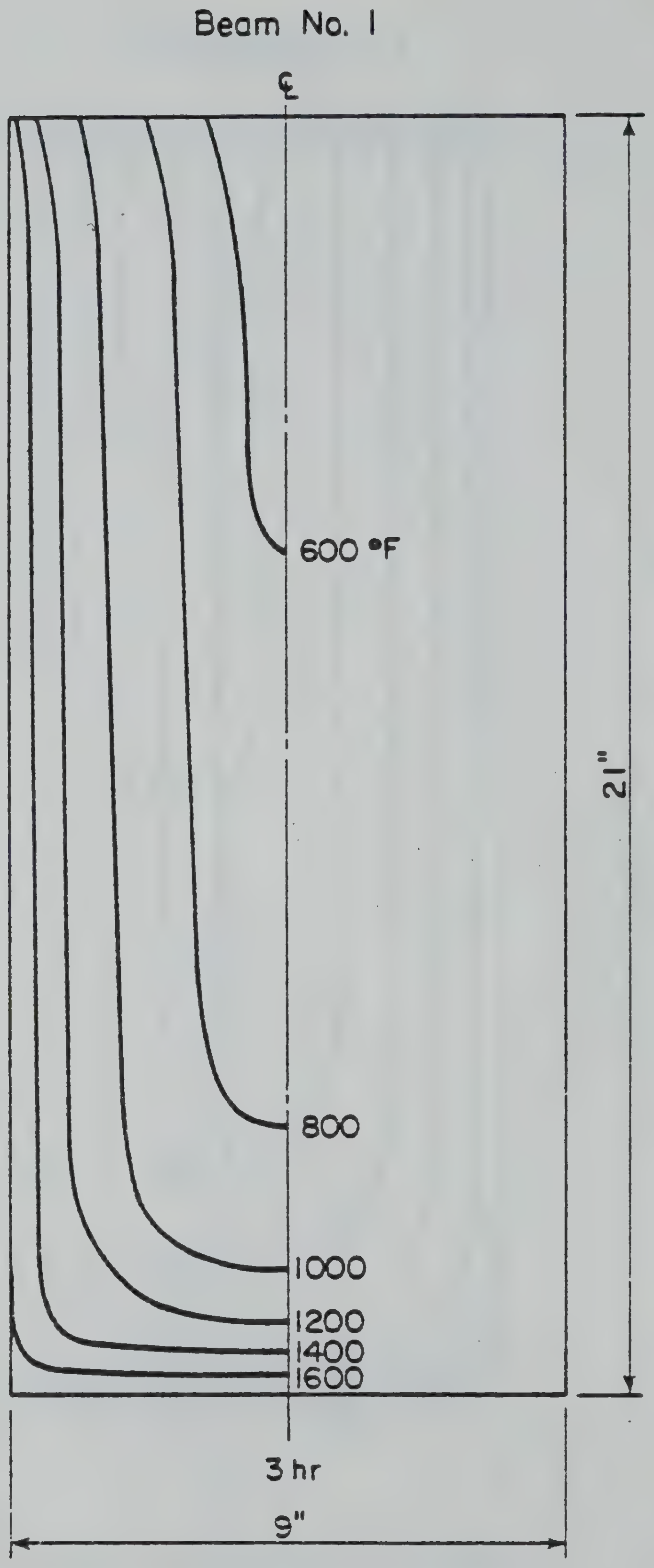

Fig. 15 Temperature Distribution - Beam No. 1 @Test Time 3 hr

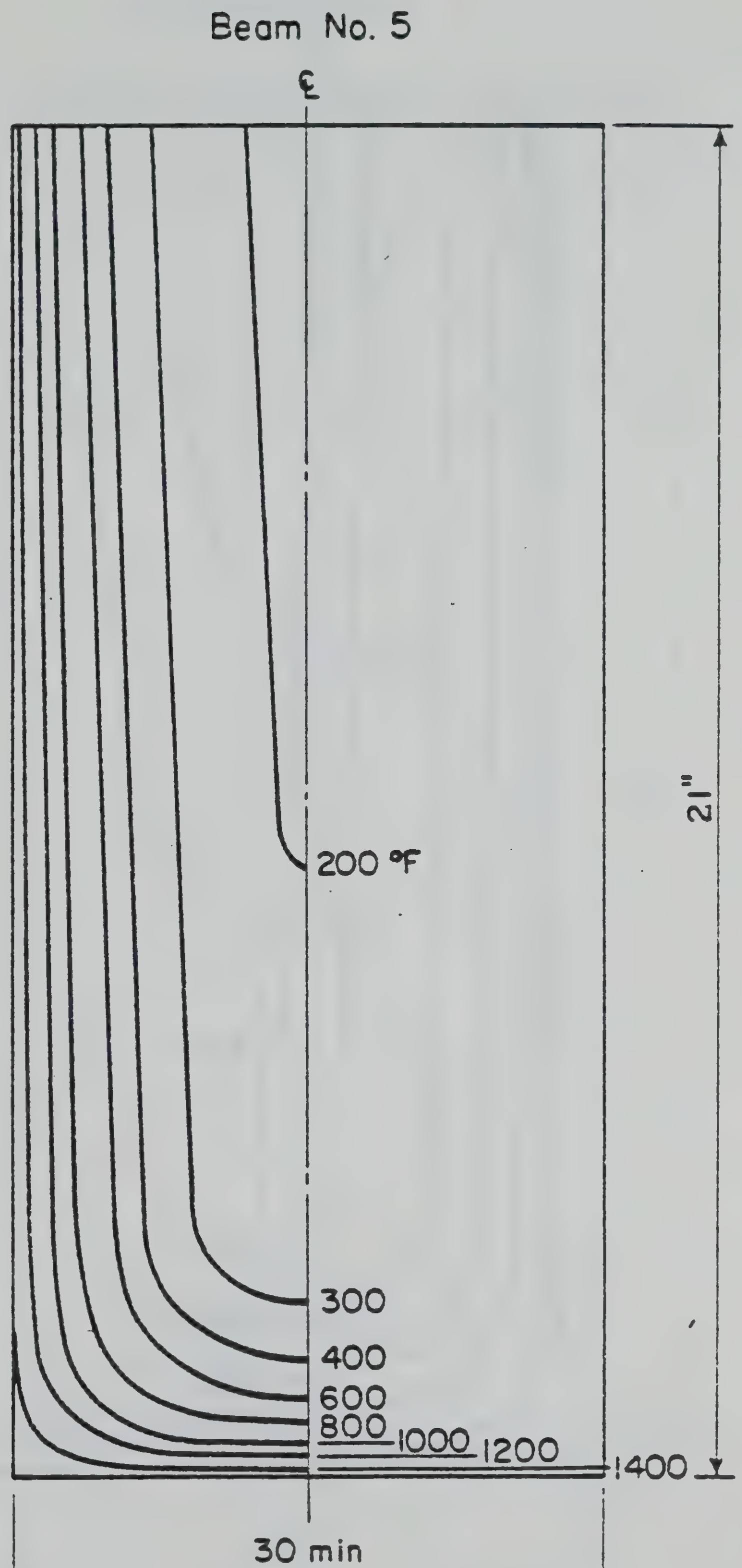

Fig. 16 Temperature Distribution - Beam No. 5
@Test Time 30 min

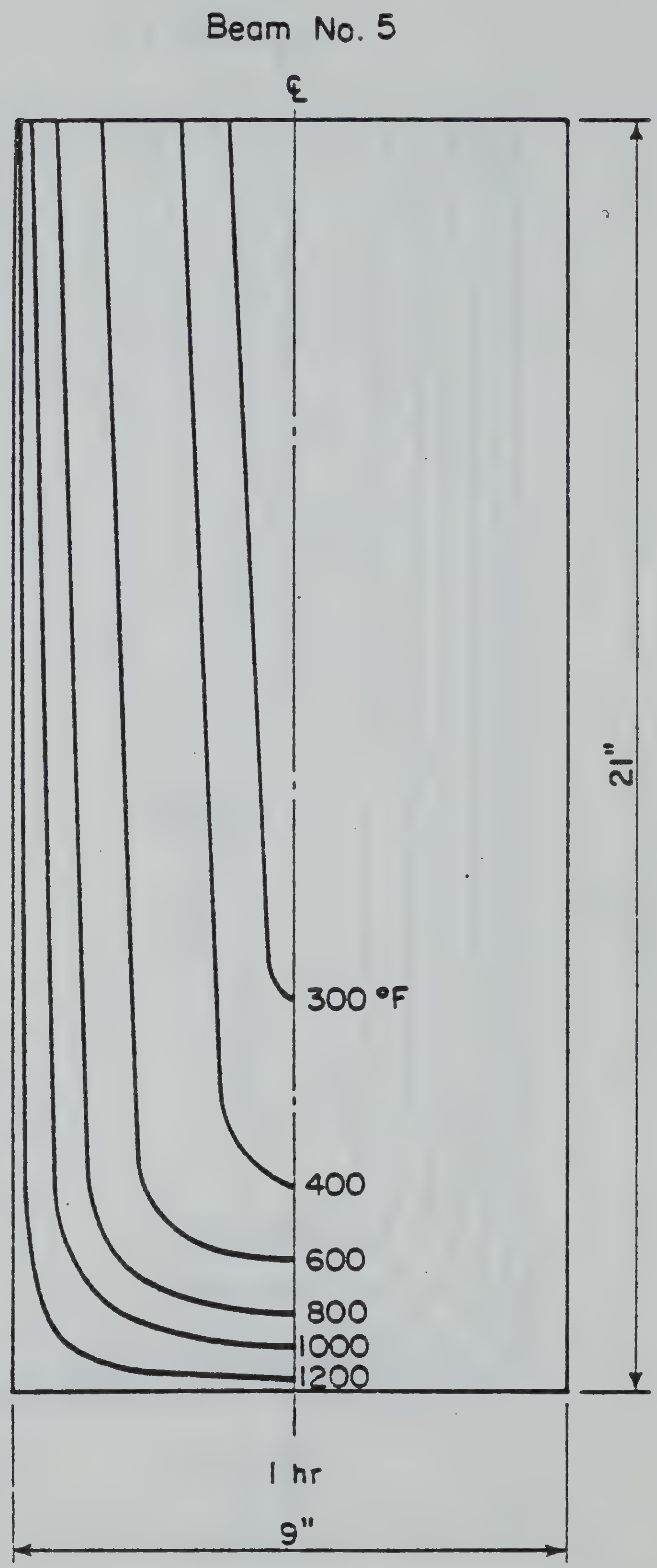

Fig. 17 Temperature Distribution - Beam No. 5
@Test Time 1 hr

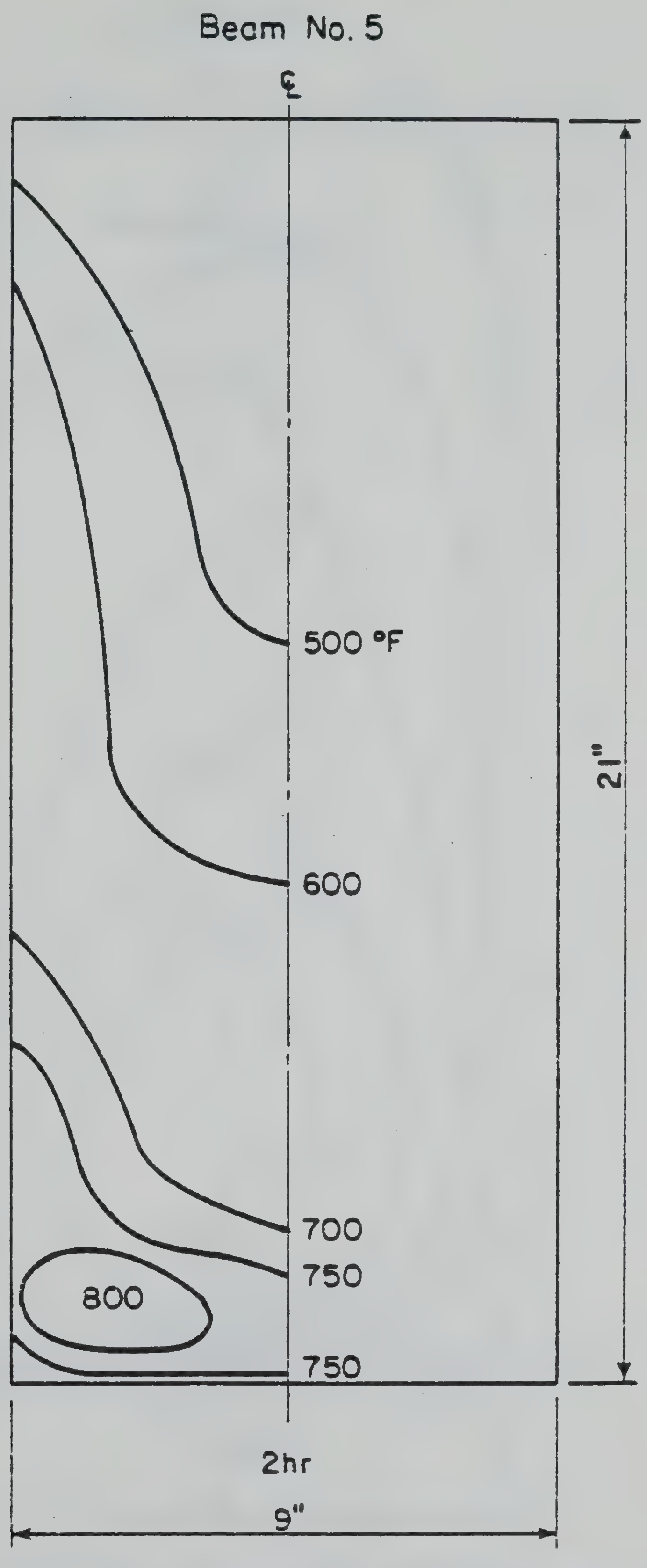

Fig. 18 Temperature Distribution - Beam No. 5 @Test Time 2 hr

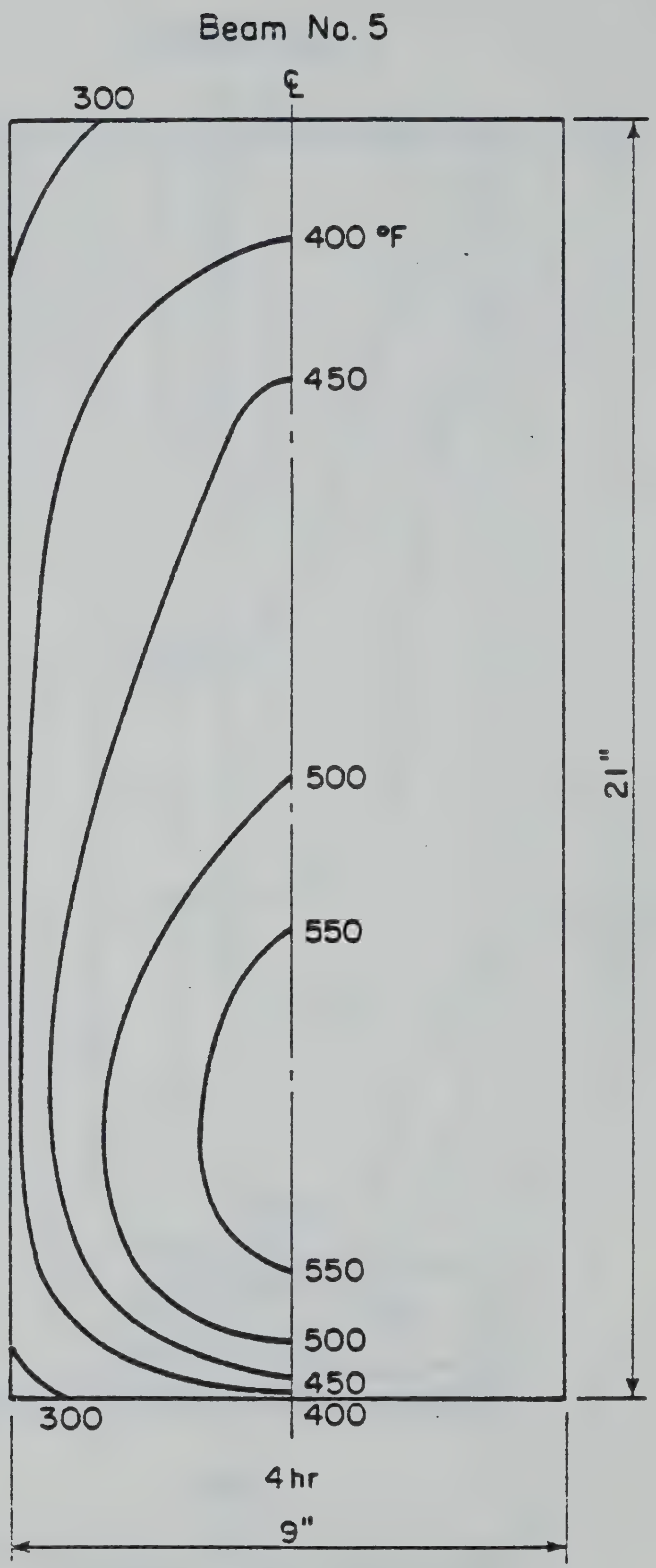

Fig. 19 Temperature Distribution - Beam No. 5 @Test Time 3 hr

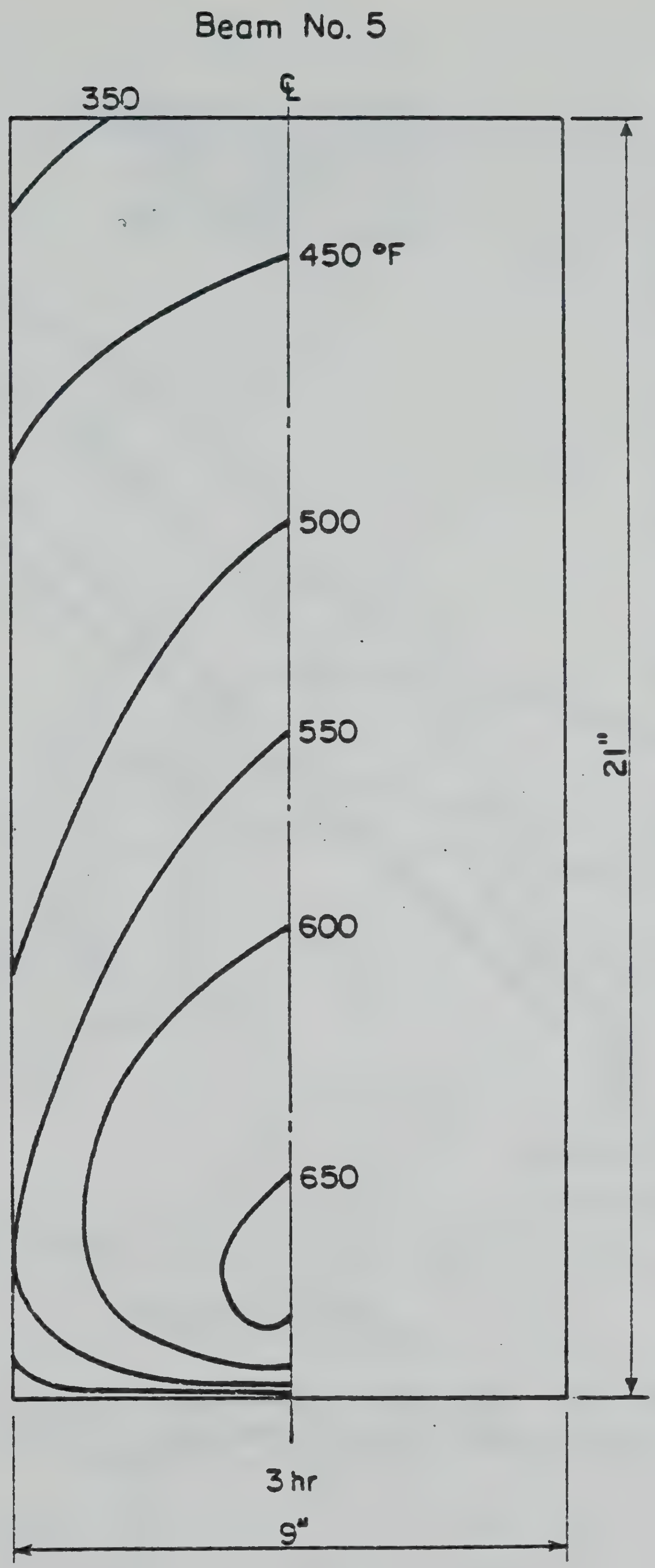

Fig. 20 Temperature Distribution - Beam No. 5
@Test Time 4 hr

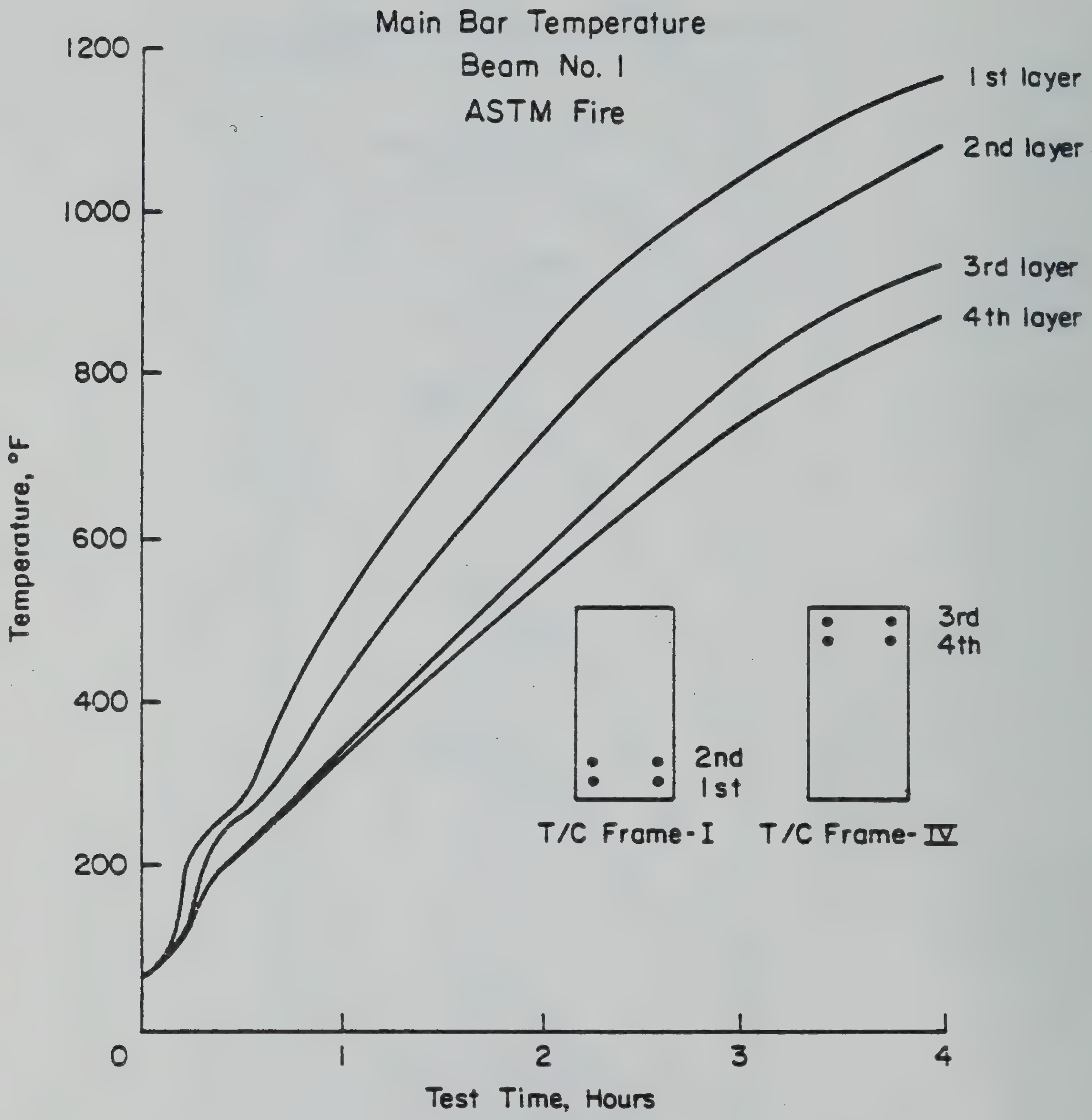

Fig. 21 Main Bar Temperature - Beam No. 1
Exposed to ASTM Fire

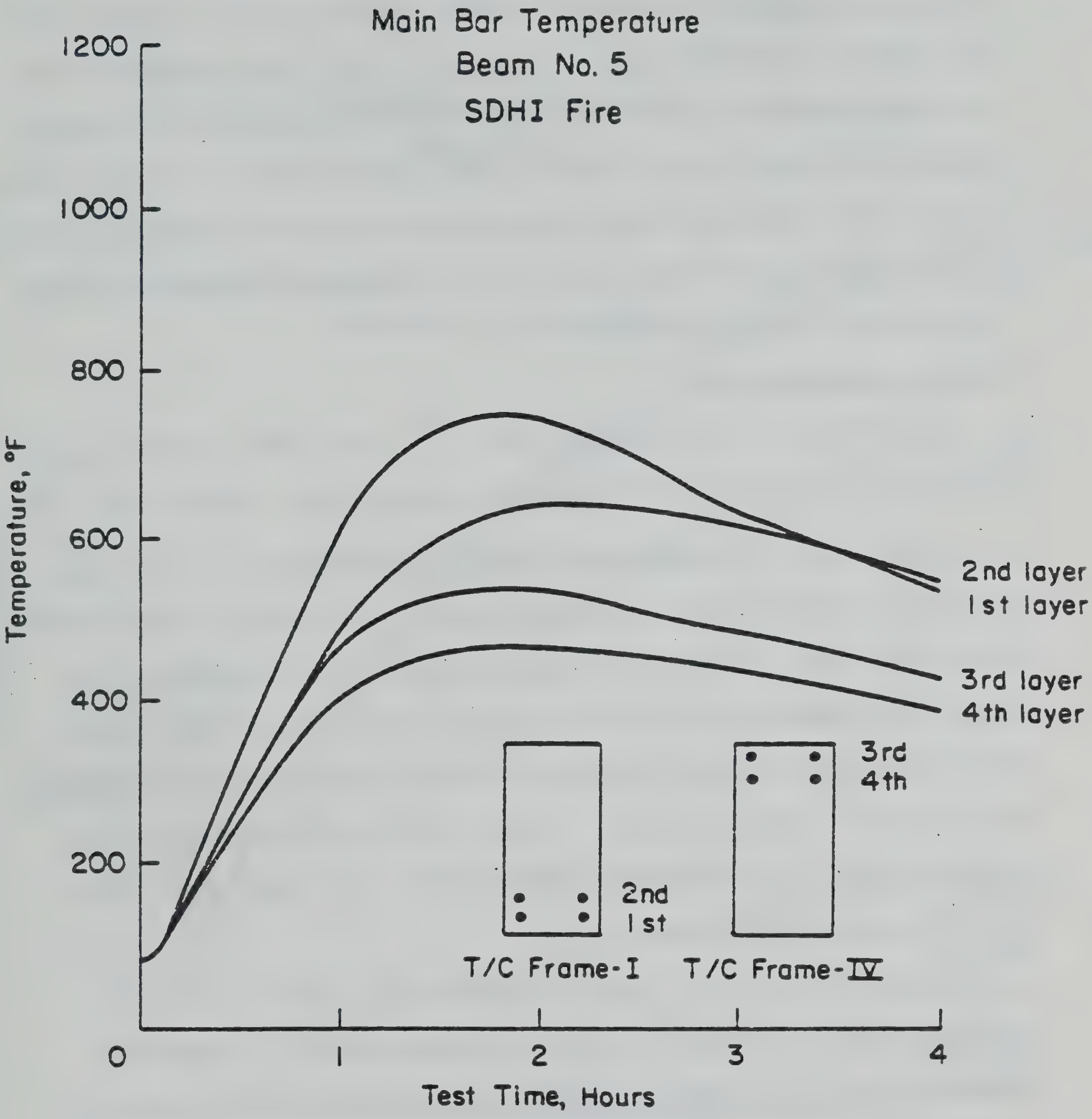

Fig. 22 Main Bar Temperature - Beam No. 5
Exposed to SDHI Fire

2nd layer, while temperatures in the top steel over the continuous support are shown by the lower curves, the 3rd and 4th layers. In Beam Nos. 1 through 4, the steel temperatures increased monotonically throughout the fire test, and the bottom bars were always hotter than the top bars. In Beam Nos. 5 and 6 the measured steel temperatures showed a rapid increase in the first 1 hr 40 min period, and gradually decreased for the remaining test period.

Stirrup Temperatures

According to ACI Standard 318,(10) the shear stress assigned by the concrete generally should not exceed $2\ f'_c$. As a result, shear reinforcement must be designed to resist the remaining portion of the shear stress. To predict nominal shear strength at elevated temperatures, it is necessary to know the temperatures of the stirrups during the fire test. Figures 23 and 24 show measured stirrup temperatures for Beam Nos. 1 and 5, respectively. These curves are similar to the longitudinal reinforcement temperatures, in that they follow the furnace temperature.

In each test beam, five stirrups were instrumented with thermocouples to measure stirrup temperatures at locations shown in Fig. 2. Three thermocouple frames, III, V, and VI, were located near the midspan of the beam where the fire intensity was quite uniform. The measured temperatures from these three thermocouple frames agreed reasonably well. However, the temperatures measured by thermocouple Frame VII were cooler than those measured at midspan. The cooler

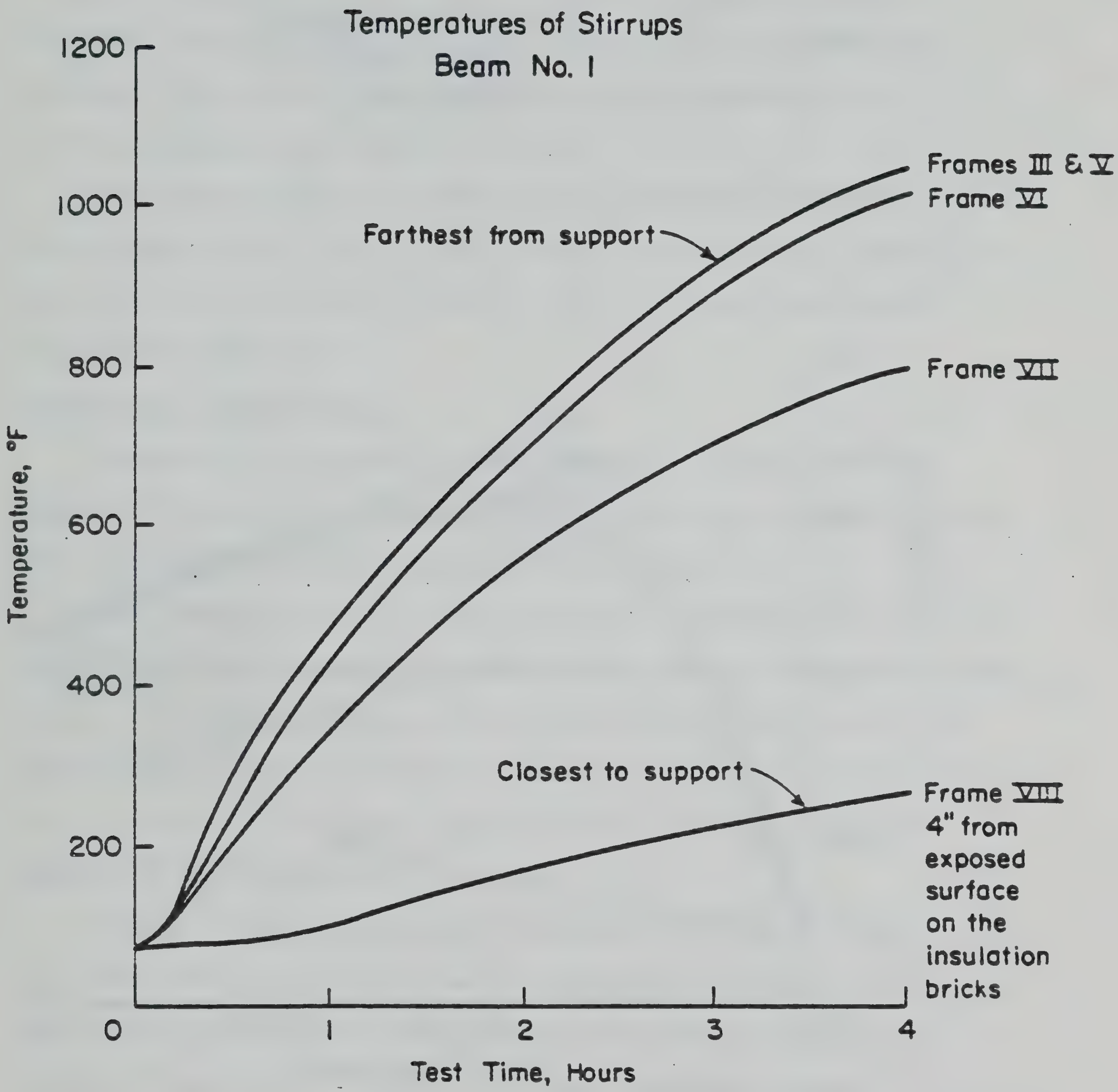

Fig. 23 Stirrup Temperatures - Beam No. 1
Exposed to ASTM Fire

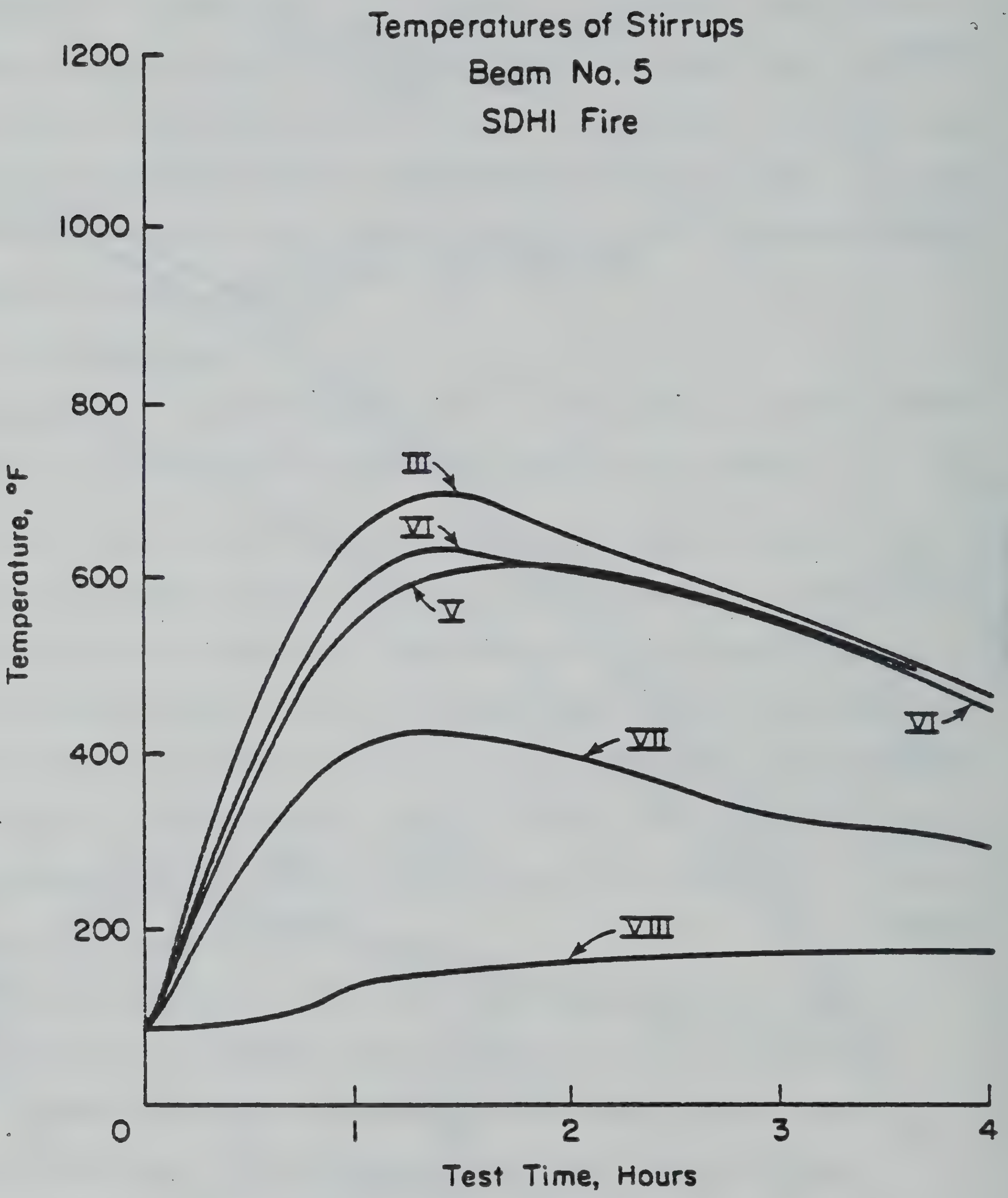

Fig. 24 Stirrup Temperatures - Beam No. 5
Exposed to SDHI Fire

temperatures were due to the fact that T/C Frame VII was located only 3 in. (76 mm) away from the furnace wall. The temperatures measured at T/C Frame VIII indicated only a minimal rise throughout the fire test. T/C Frame VIII was located right above the fire bricks of the furnace wall, 4 in. (102 mm) beyond the exposed surface.

The maximum stirrup temperatures measured during the fire tests were 1030°F (554 C) at 4 hours for Beam No. 1 exposed to the ASTM Fire, and 700°F (371 C) at 1-1/2 hour for Beam No. 5 exposed to SDHI fire.

Deflection Measurements

Deflection measurements were taken at eleven points by means of rotary potentiometers. All measurements were printed on recording charts at 3 minute time intervals.

The maximum deflection of each beam was observed continually during the test because the rate of increase in deflection provided the warning signal of a collapse of the test beam into the furnace. All tests were terminated when the rate of deflection reached 0.1 in./min; at this time, structural collapse generally was imminent.

Figure 25 shows measured deflection profiles of Beam No. 1 at test times of 0, 1/2, 1 and 3 hrs. The deflection profiles for the remaining five beams are somewhat similar to those of Beam No. 1. Figure 26 shows measured maximum deflections for all six beams. Figure 26(a) compares the maximum deflections of three identical beams: Beam Nos. 1 and 2 exposed to ASTM fire and Beam No. 5 exposed to SDHI fire.

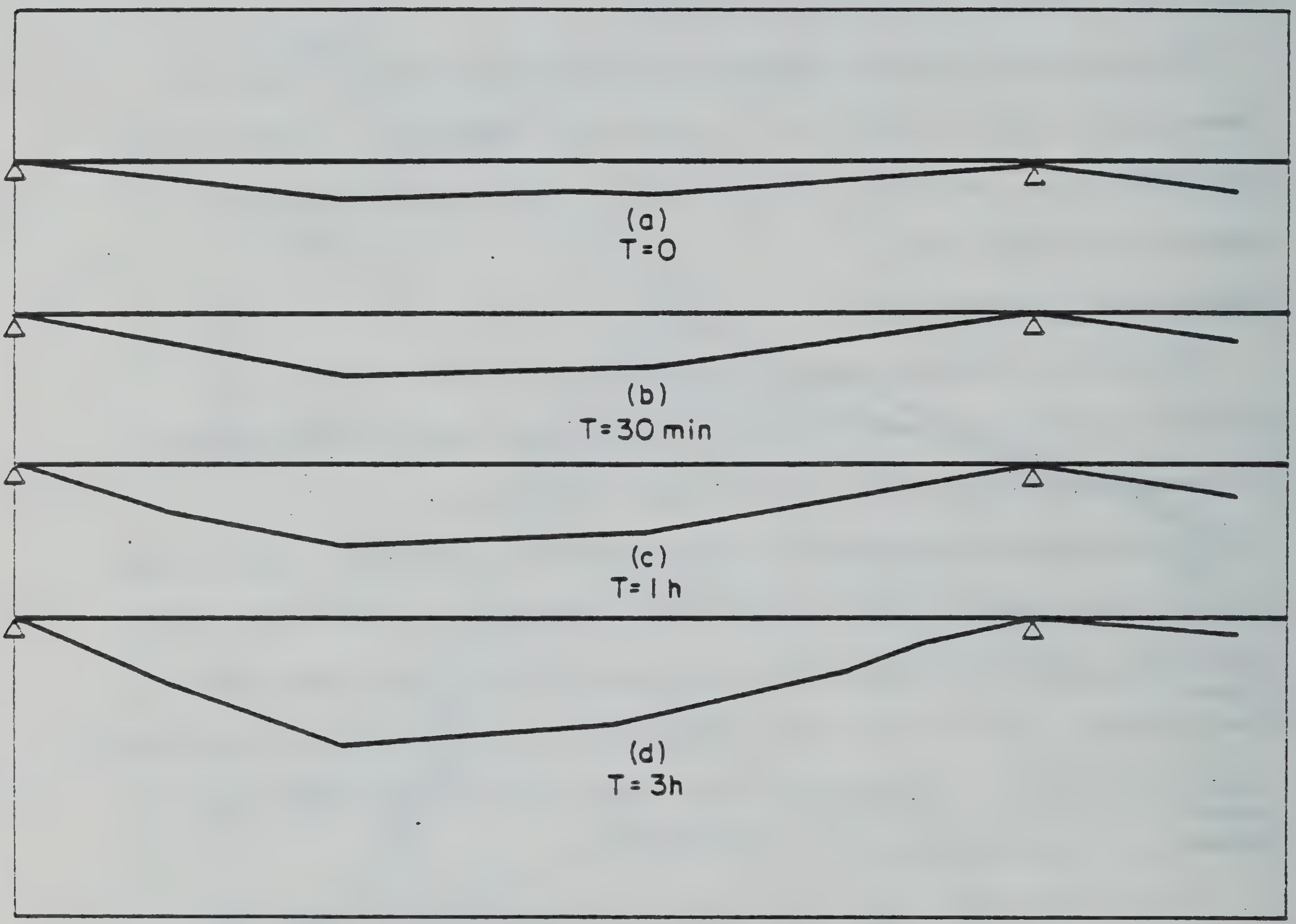

Fig. 25 Measured Deflection Profiles - Beam No. 1

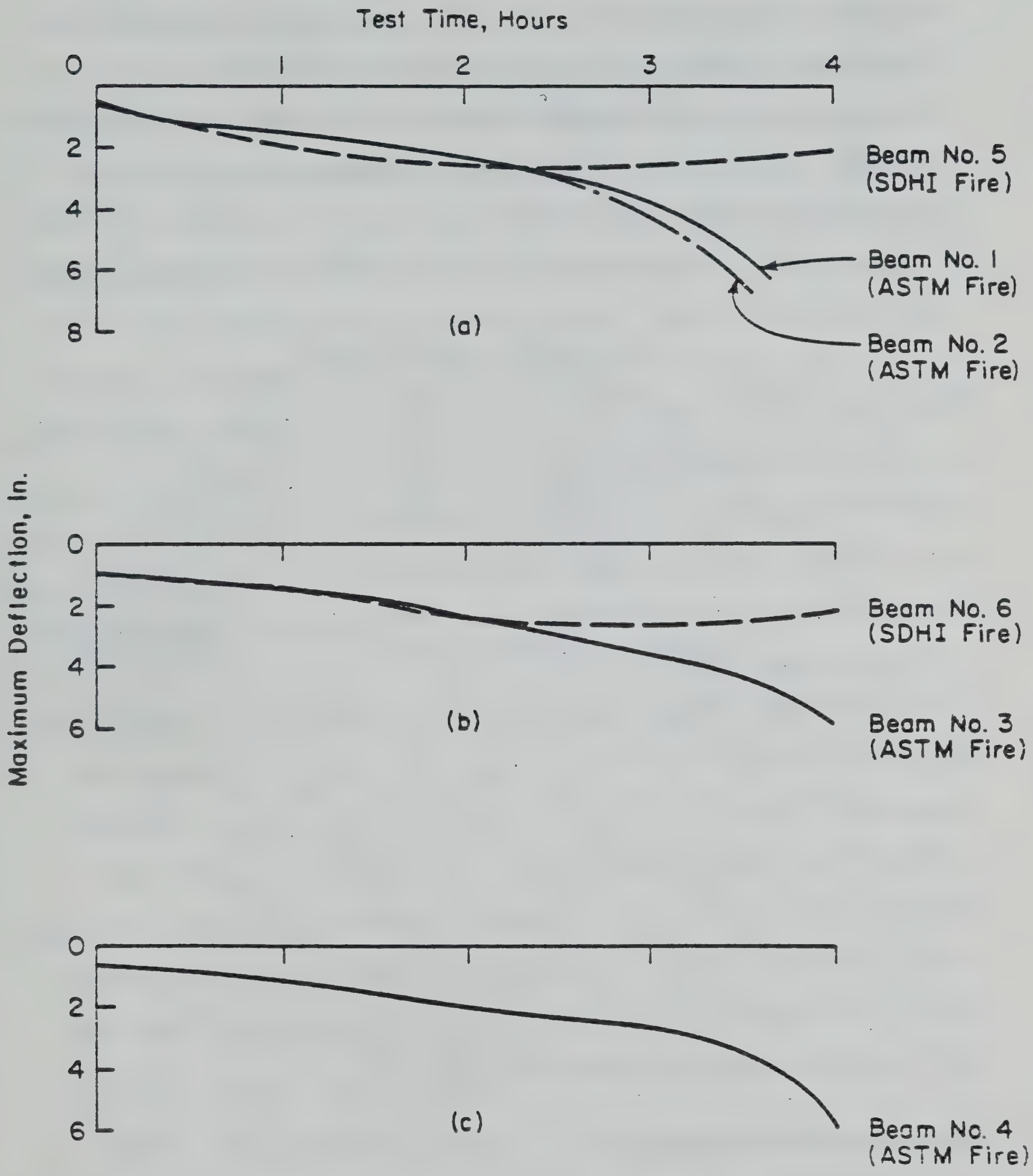

Fig. 26 Measured Maximum Deflection During Fire Tests

Beams that were exposed to the SDHI fire deflected slightly more than beams exposed to the ASTM fire for the first 2 hrs. After that, deflections of beams exposed to SHDI fire stabilized, while the deflections of beams exposed to ASTM fire continued to increase. Figure 26(b) compares measured deflections of Beam Nos. 3 and 6.

Beams for Fig. 26(a) had 1-1/2 in. (38 mm) concrete cover over the bottom steel whereas beams for Fig. 26(b) had 2-1/4 in. (57 mm) cover. It appears that the thickness of concrete cover has little effect on the deflection of beams during fire if they are designed in accordance with ACI Standard 318.(10) The maximum deflection measured on these beams prior to the start of fire was approximately 1 in. (25 mm). This deflection was basically due to the applied superimposed and cantilever loads.

Figure 26(c) shows the deflection of Beam No. 4 exposed to the ASTM Standard E119 fire. Beam No. 4 had a cross-section deeper and wider than that of the other five beams. However, its test load was proportionally increased to a level that developed the same ratio of applied moment to flexural strength as in the other beams. Consequently, the measured deflection curve for Beam No. 4 is close to the deflections of Beam Nos. 1, 2, and 3, shown in Figs. 26(a) and (b).

Expansion Measurements

Longitudinal expansions of beams during the fire tests were measured continuously through the use of potentiometers attached to the roller plates that supported the test beams. Figure 27 shows the measured expansions at the bottom of each beam for all 6 beams. The difference in expansions of beams in Figs. 27(a) and (b) is caused by the difference in concrete cover. All measured expansions were less than 3 in. (76 mm). The expansions observed at the start of the fire were due to the flexural bending of the beam bottom under the vertical loads.

Observations During Tests

Since all beams were tested to simulate a one-end continuous beam exposed to fire, similar behavior was observed in all tests. Observations of Beam No. 1 during its test, which was typical of the beams exposed to the ASTM E119 fire, are described below:

Test Time	Observation (See Fig. 28)
0:40	Full superimposed loads and a cantilever load were applied. Three fine vertical cracks occurred near the east support on the cantilever portion. Cracks extended 6 in. (152 mm) down from the top edges of the beam. Three or four hairline cracks roughly 4- to 5-in. (102-127 mm) long were seen at the positive moment region, about 5 ft (1.5 m) from the west support.
0:00	Start of fire test
0:01	All hairline cracks in the positive moment region closed.

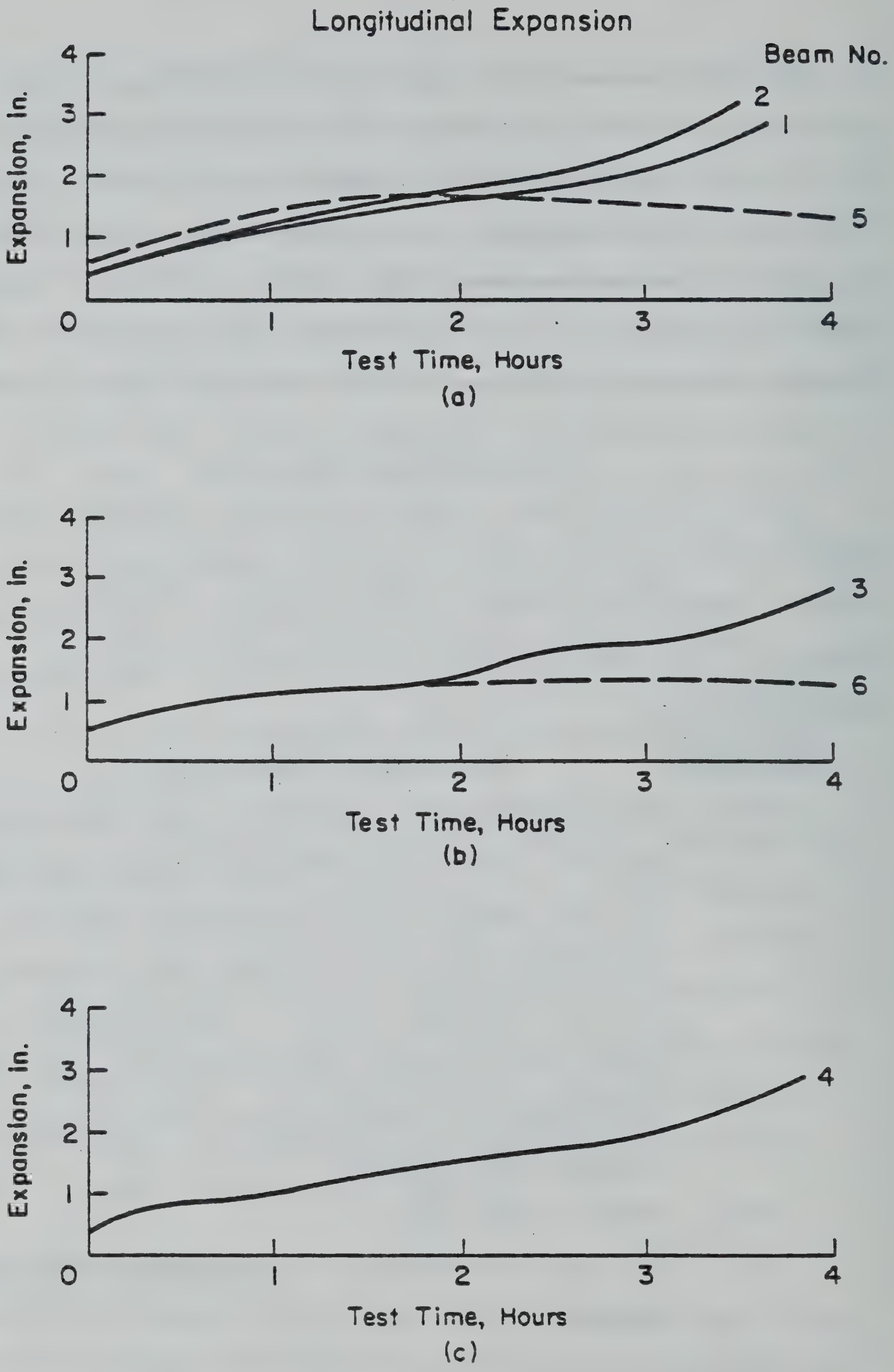

(a)

(b)

(c)

Fig. 27 Measured Longitudinal Expansions During Fire Tests

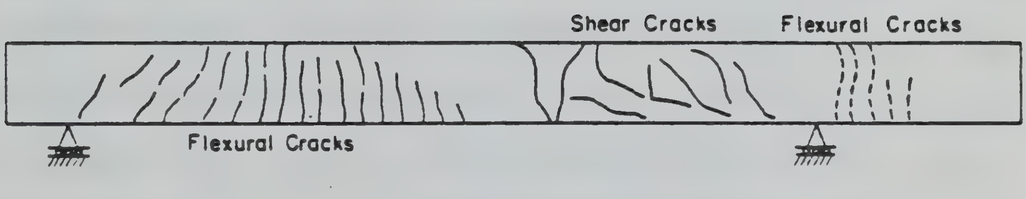

Fig. 28 Representative Crack Pattern Developed in Beams During Fire Tests

0:10 Two or three additional cracks were seen in the cantilever region near the east support.

0:15 Cracks in the cantilever region widened.

0:25 Steam and water oozed out through the cracks from the top surface of the beam.

0:30 Bottom edges of the beam glowed.

1:00 Maximum deflection was slightly over 1-1/2 in. (38 mm)

1:30 A diagonal shear crack, about 3 to 4 in. (76-102 mm) long, appeared in the lower portion of the beam, about 4 ft (1.2 m) from the east support toward the furnace.

1:35 Top surface was dry.

1:45 A second shear crack developed. This new crack was rather long. The bottom part of the crack extended horizontally 2 in. (51 mm) above the bottom edge of the beam.

2:05 Flexural cracks in the positive moment region reopened.

2:10 Two additional shear cracks developed. The existing cracks lengthened. The estimated maximum crack width was about 1/16 in. (1.6 mm)

2:15 Flexural cracks widened.

2:30 No new shear cracks developed. The existing shear cracks extended diagonally upward to the beam top.

3:00 Additional flexural cracks developed; the maximum width of cracks reached nearly 1/4 in. (6 mm)

3:40 The worst flexural crack was about 1/4 in. (6 mm) wide. The maximum deflection increased with a rate of about 0.1 in./min. Test was terminated.

General Observations

Spalling did not occur in beams during fire tests. The maximum deflection of beams at the end of each test was about 6 in. (152 mm) for beams exposed to the ASTM fire and was less than 3 in. (76 mm) for beams exposed to the SDHI fire.

After beams cooled down to room temperature, cracks were darkened with a felt-tipped pen to make them more visible when photographed. Figure 29 shows Beam No. 1 after the fire test. The crack pattern for Beam No. 2 was almost identical to that of Beam No. 1. Figures 30 to 33 show Beam Nos. 3 through 6 after the fire tests. A corner piece of Beam No. 4 dropped off during the cooling period, not during the fire test.

THERMAL ANALYSIS

Thermal Properties of Concrete and Steel

The surface heat transfer coefficient, thermal conductivity, k, and volumetric specific heat, ρC_p, of the structural materials govern the temperature distribution in beams. The temperature distribution governs the thermal strains. Thermal properties of concrete and steel have been established through laboratory testing.(11) However, test data on thermal properties of concrete may differ

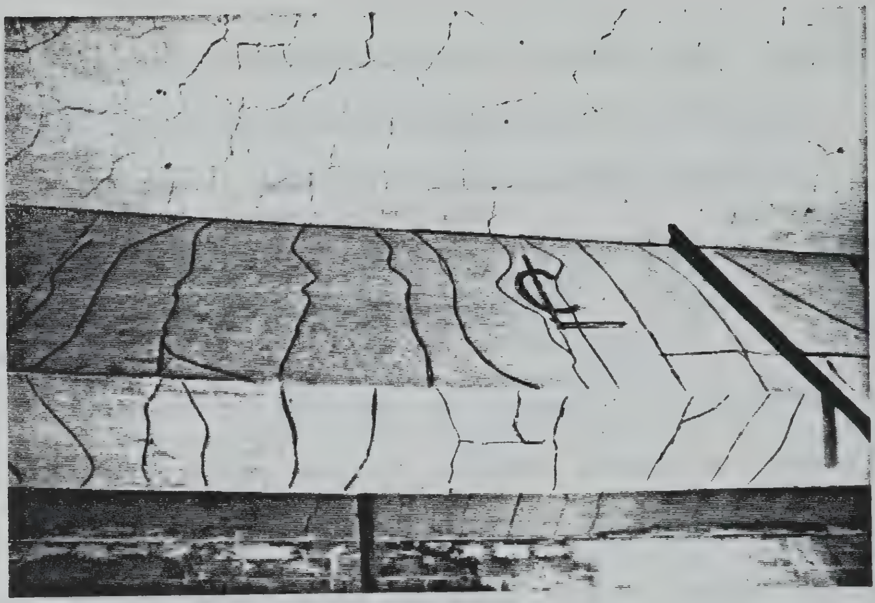

Flexural Cracks

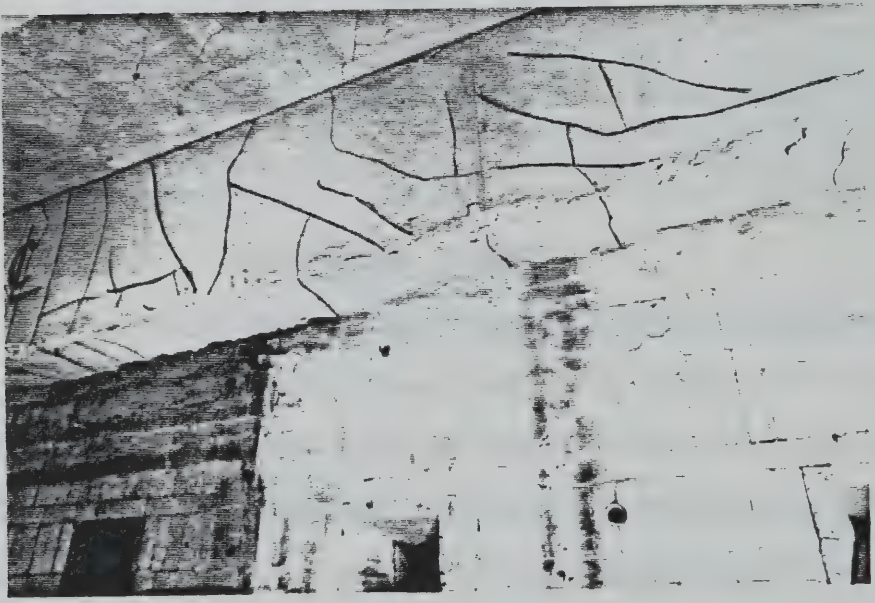

Shear Cracks

Fig. 29 Beam No. 1 After Fire Test.

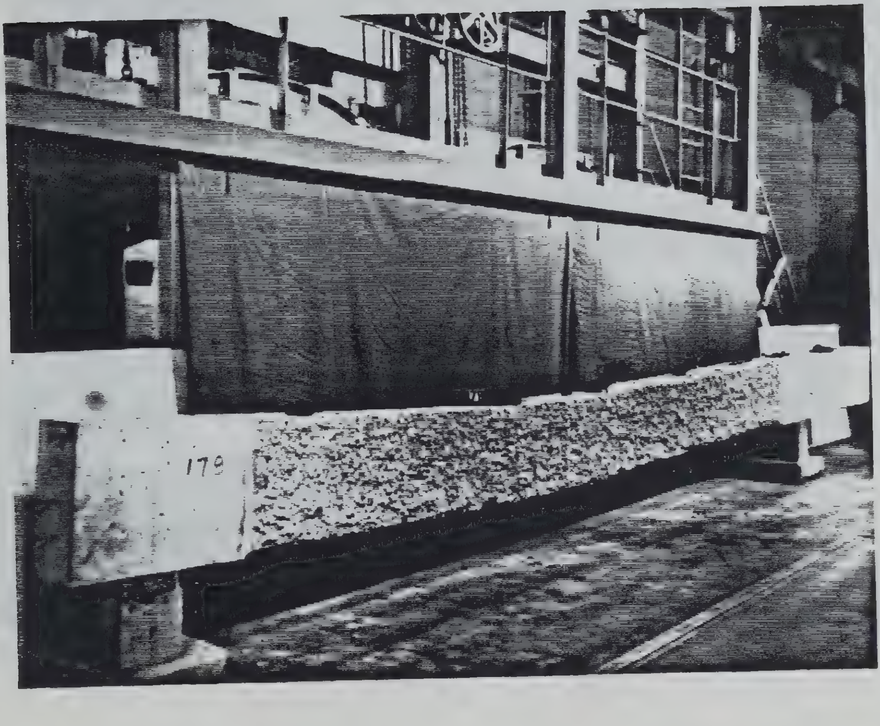

Fig. 30 Beam No. 3 After Fire Test.

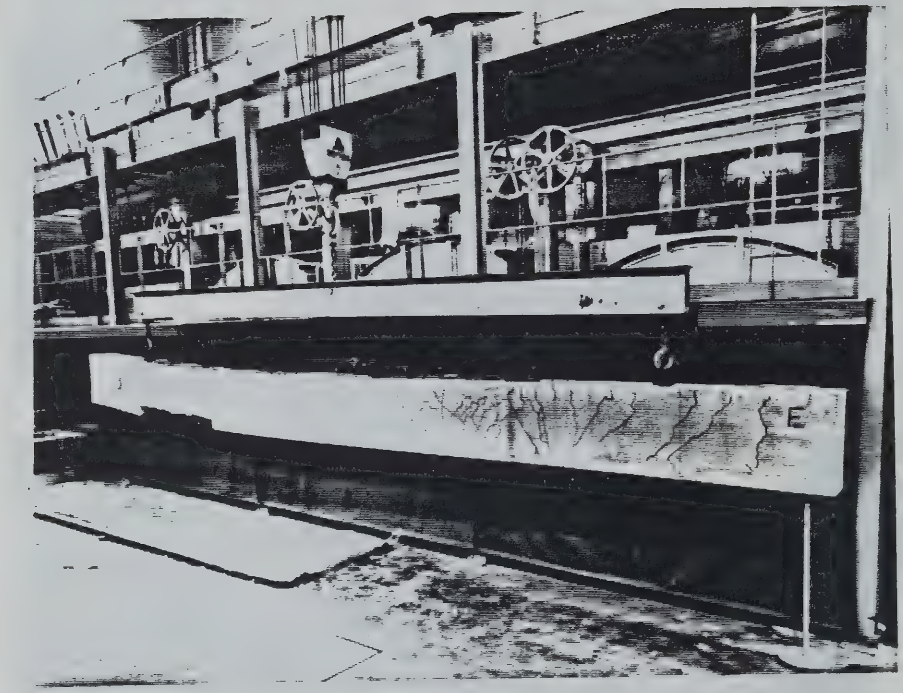

Fig. 31 Beam No. 4 After Fire Test.

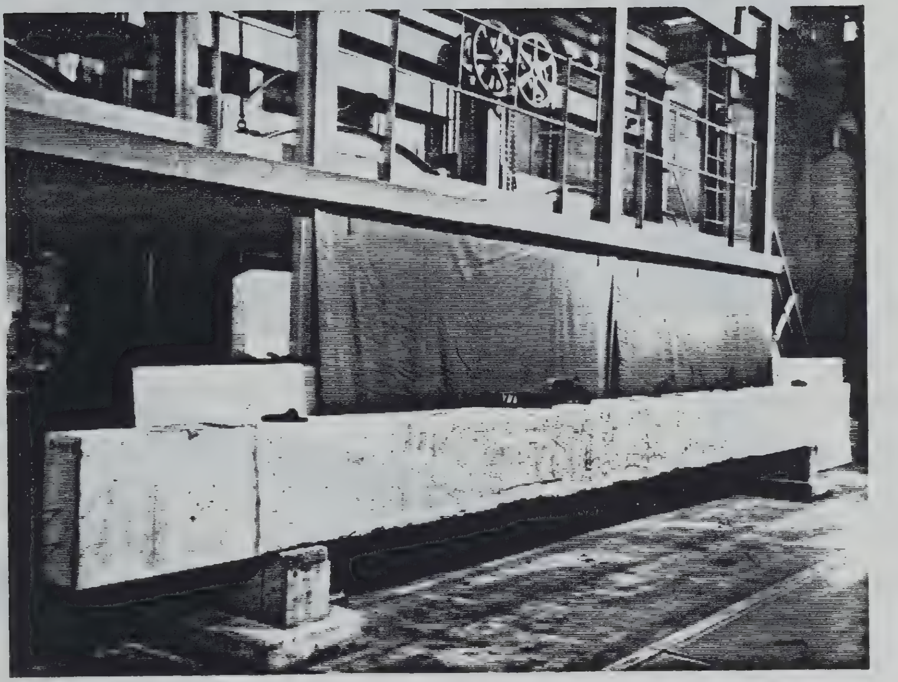

Fig. 32 Beam No. 5 After Fire Test.

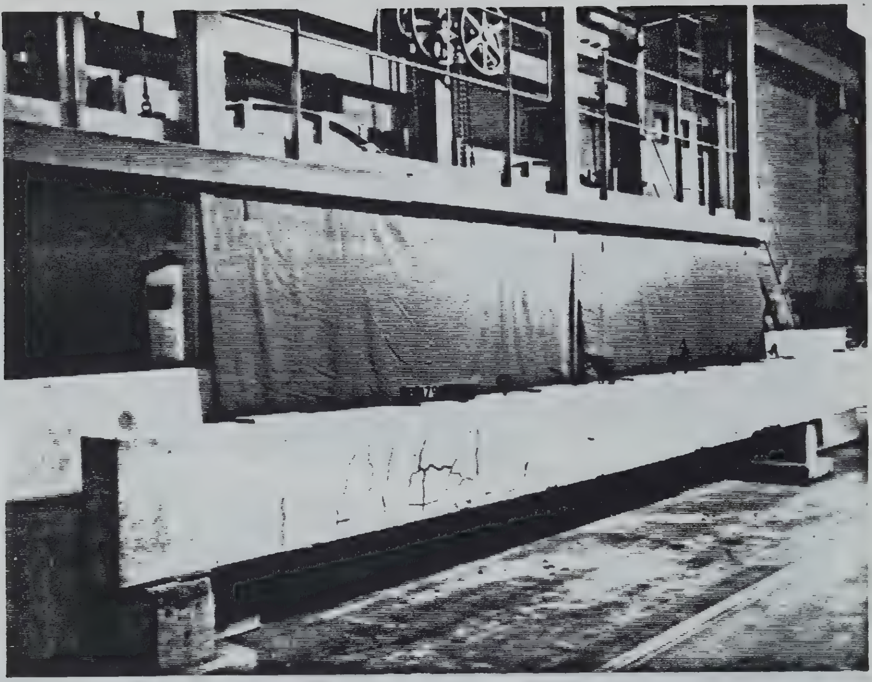

Fig. 33 Beam No. 6 After Fire Test.

considerably from one laboratory to another, even at room temperature. In general, thermal conductivity decreases with increasing temperature, while volumetric specific heat shows a tendency to increase. Figures 34 and 35 show the thermal conductivity and volumetric specific heat used in the thermal analysis. There is considerable scatter associated with both k and ρC_p.

Analysis of Temperature Development in Beams

The thermal analysis is based on the two-dimensional heat flow equation,

$$\rho C_p \frac{\partial T}{\partial t} = \frac{\partial}{\partial x} (k \frac{\partial T}{\partial x}) + \frac{\partial}{\partial y} (k \frac{\partial T}{\partial y}) \qquad (1)$$

in which ρC_p is volumetric specific heat, k is thermal conductivity, T is temperature and t is time. It is assumed that the material is homogenous and there are no phase changes or cracking during the fire. Assuming that heat flow across the exposed boundary of the section is caused by both convective and radiative mechanisms, the boundary condition for the solution of Eq. 1 is,

$$-k \frac{\partial T}{\partial n} = h_c (T_s - T_a) + \epsilon\sigma (T_s^4 - T_a^4) \qquad (2)$$

in which n is the direction of heat flow normal to the boundary, h_c is the convection coefficient, ϵ is resultant emissivity, σ is the Stefan-Boltzman constant, and T_a, T_s are absolute air and surface temperatures.

Analytical solutions to Eqs. 1 and 2 are difficult to obtain. Instead, solutions were obtained using a finite difference approach.(13) This leads to a matrix equation,

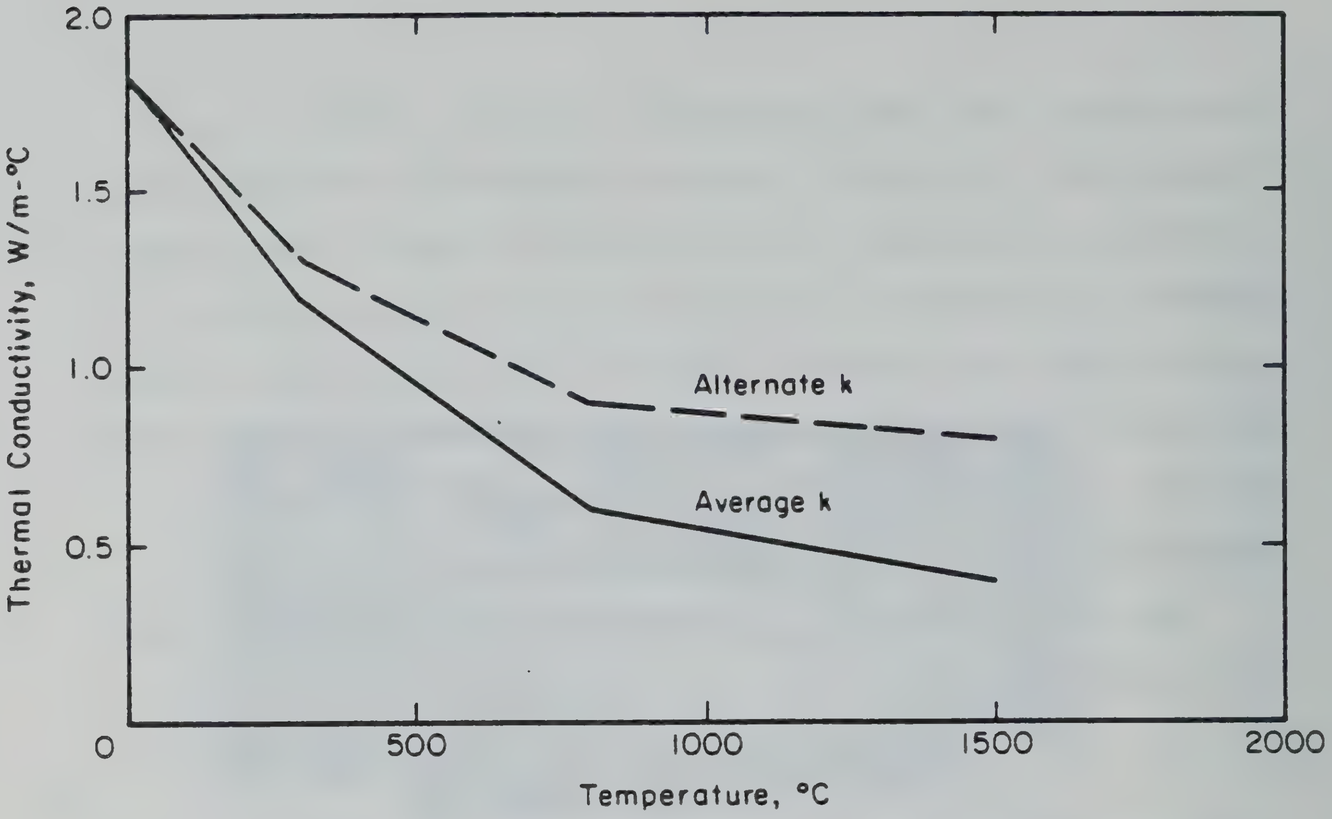

Fig. 34 Thermal Conductivity of Concrete

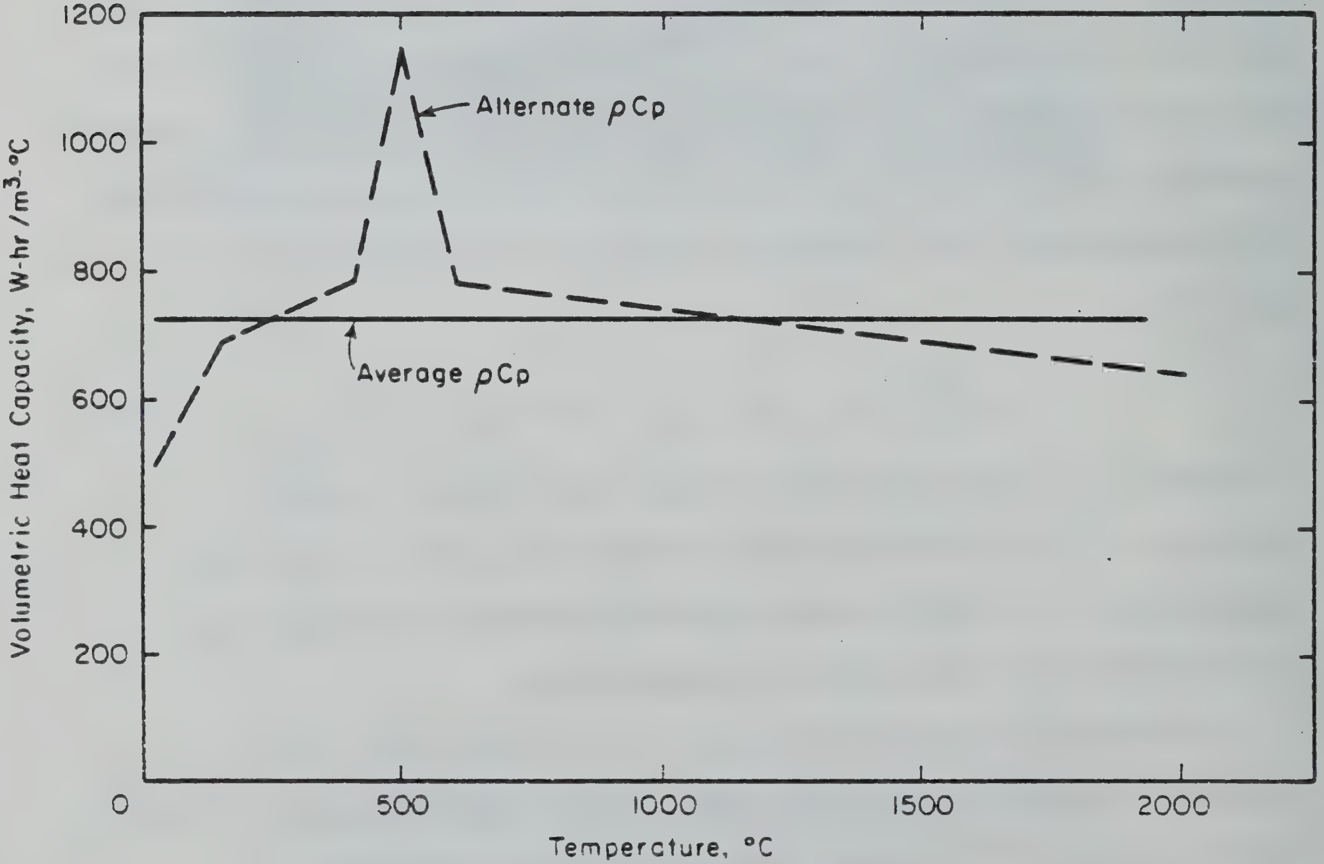

Fig. 35 Volumetric Specific Heat of Concrete

$$[C]\dot{\underline{T}} + [k]\underline{T} = \underline{Q} \tag{3}$$

in which the dot represents differentiation with respect to time, $\underline{Q}$ is the heat input vector and [C] and [K] are heat capacity and conductivity matrices derived from ρC_p and k for each element. $\underline{Q}$ is defined at the boundary nodes by Eq. 2. The temperature vector $\underline{T}$ is obtained at a sequence of time steps. Criteria exist to ensure the stability of the solution.

Grid lines used in the finite difference computation basically coincided with the thermocouple layouts as shown in Figs. 3 and 4. A finer grid was employed in regions where the thermal gradient was expected to be steep. Due to symmetry with respect to the centerline of the cross-section, only one-half the cross-section was needed for the analysis.

The calculated and measured temperature distributions were compared at test times of 1/2, 1, and 2 hrs for Beam No. 1. Figures 36 and 37 show temperature profiles along the vertical centerline and a parallel line 2-3/4 in. (70 mm) from the centerline, respectively (Sections A-A and B-B in Figures 3 and 4). The comparison shows a reasonable agreement throughout the test except in the first 30 min of fire exposure.

It has been found(12) that reinforcing bars have an insignificant effect on the temperature distribution within the concrete when the reinforcement ratio is less than about 0.04. Accordingly, their presence has been ignored in computing the temperature distributions. The thermal analysis tends to overpredict the temperature rise on the bottom of the beam.

However, the thermocouples at the exposed boundary might not give accurate readings. Those thermocouples are often damaged by oxidation at extremely high temperatures.

The actual k and ρC_p for concrete used in fabricating the beams were not known. Accordingly, most of the thermal analyses performed as a part of this research were conducted using the "average" values shown in Figs. 34 and 35, which were obtained from other studies.(12) To determine the sensitivity of the solutions to assumed values of k and ρC_p, two separate analyses were performed using, one at a time, the relations labeled "alternate" in Figs. 34 and 35. The predicted temperatures so obtained also are shown in Figs. 36 and 37.

Figures 38 and 39 compare the measured temperatures at the centerline of the cross section for Beams 1, 2, and 3. Other than the additional 3/4 in. (19 mm) concrete cover over the longitudinal reinforcement in Beam 3, all three beams were essentially identical. The test variability appears to be of the same order as the variability in predicted temperatures obtained assuming different (but reasonable) relations for k and ρC_p (Figs. 36 and 37).

Within the normal range of experimental scatter, the temperature distributions in these three beams are the same. Note that the different position of the reinforcement in Beam 3 does not change the overall temperature distribution.

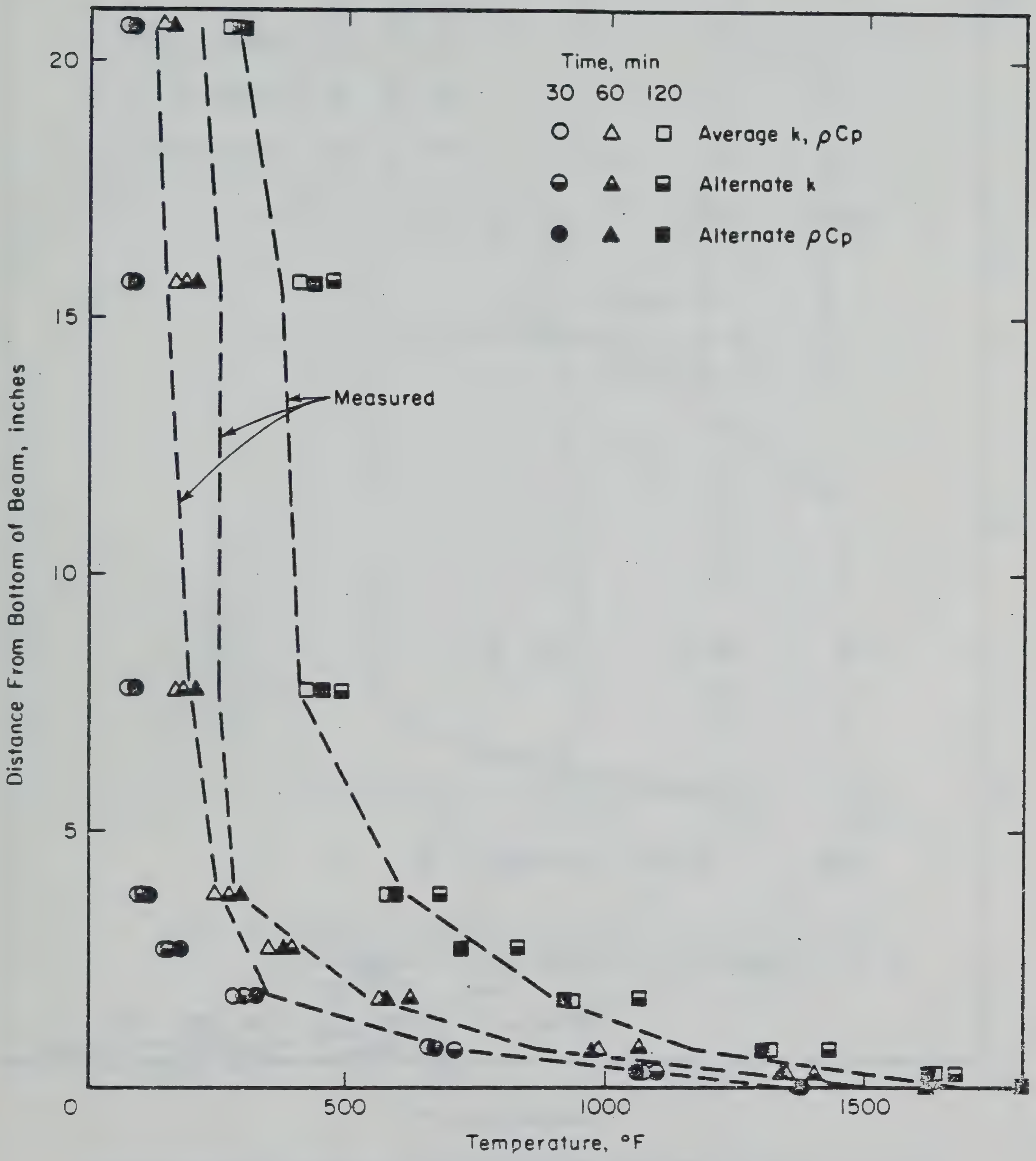

Fig. 36 Comparison of Predicted and Measured Temperatures on Centerline of Cross-Section of Beam No. 1 (ASTM Fire)

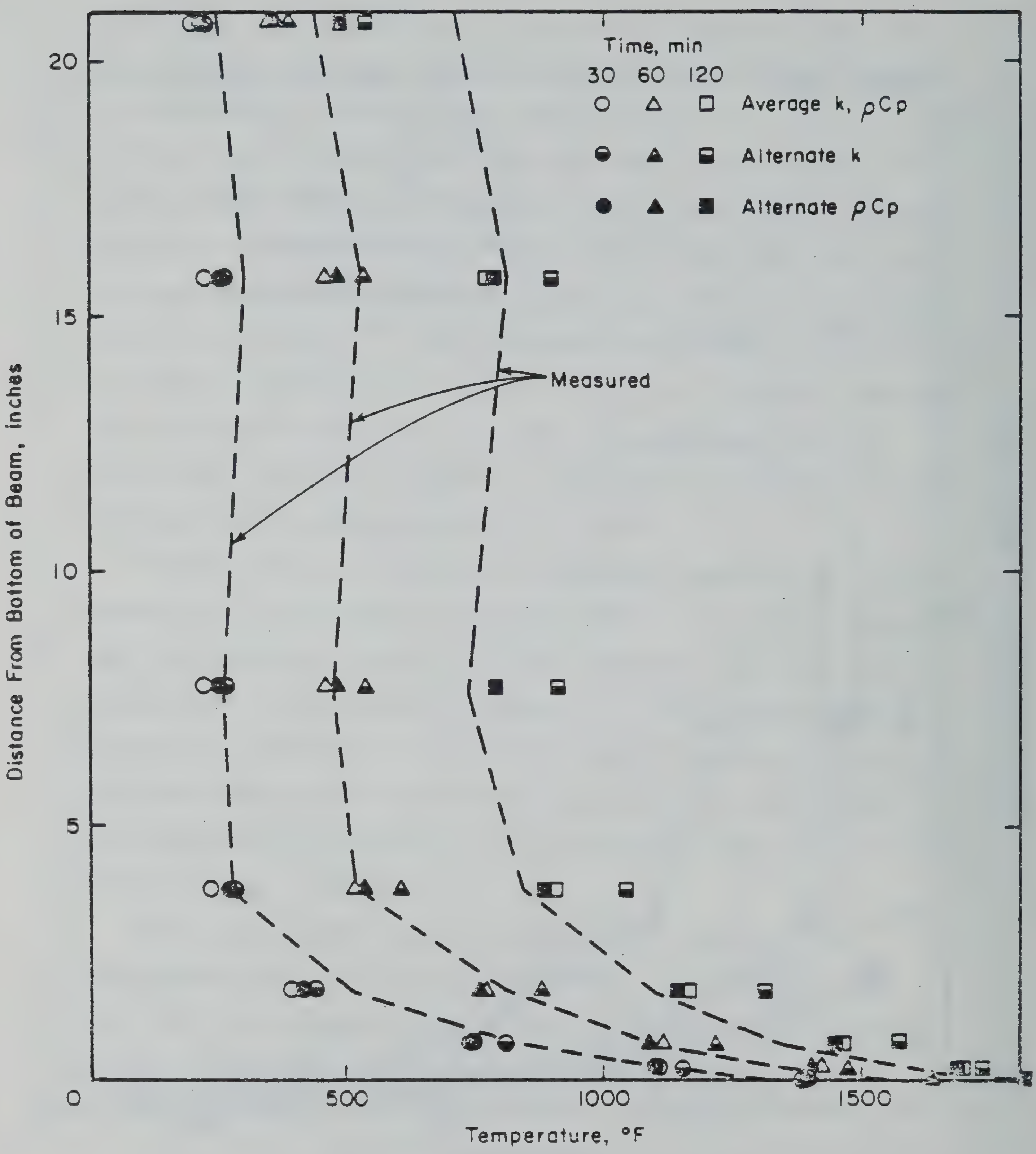

Fig. 37 Comparison of Predicted and Measured Temperatures 2.75 inches from Centerline of Cross-Section of Beam No. 1 (ASTM Fire)

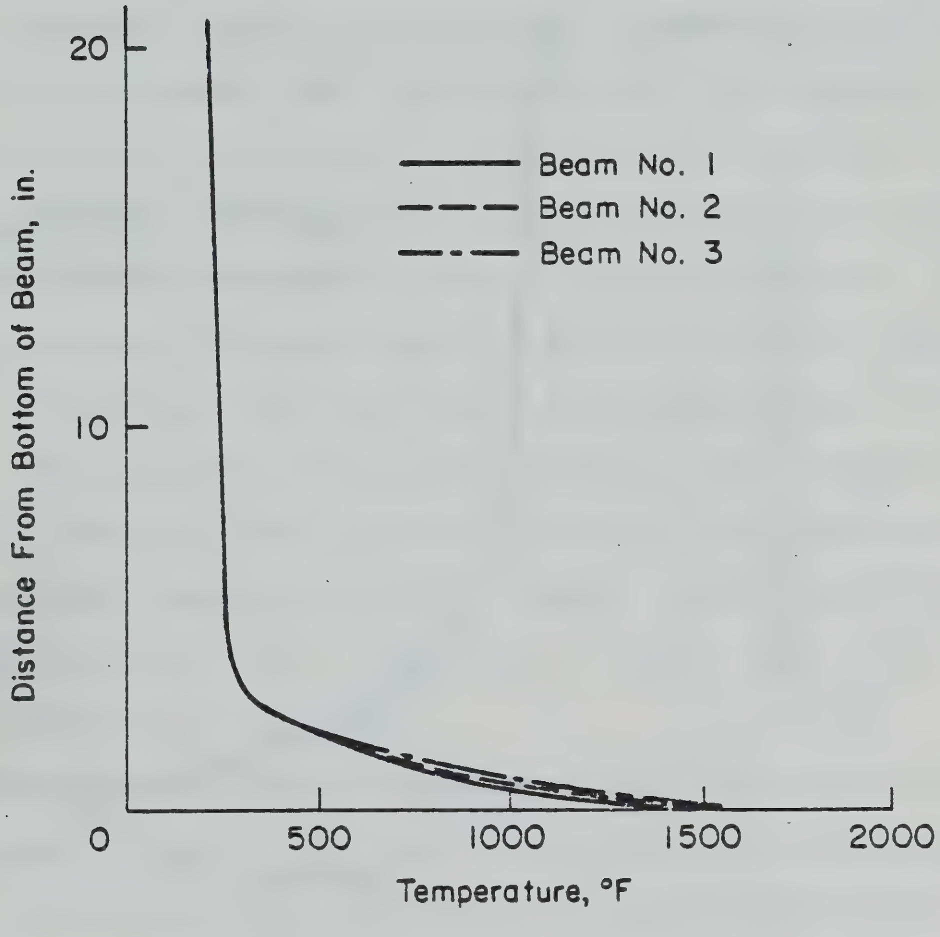

Fig. 38 Measured Temperatures in Beams 1, 2, and 3 Along the Centerline of Cross-Section @1 hr Test Time

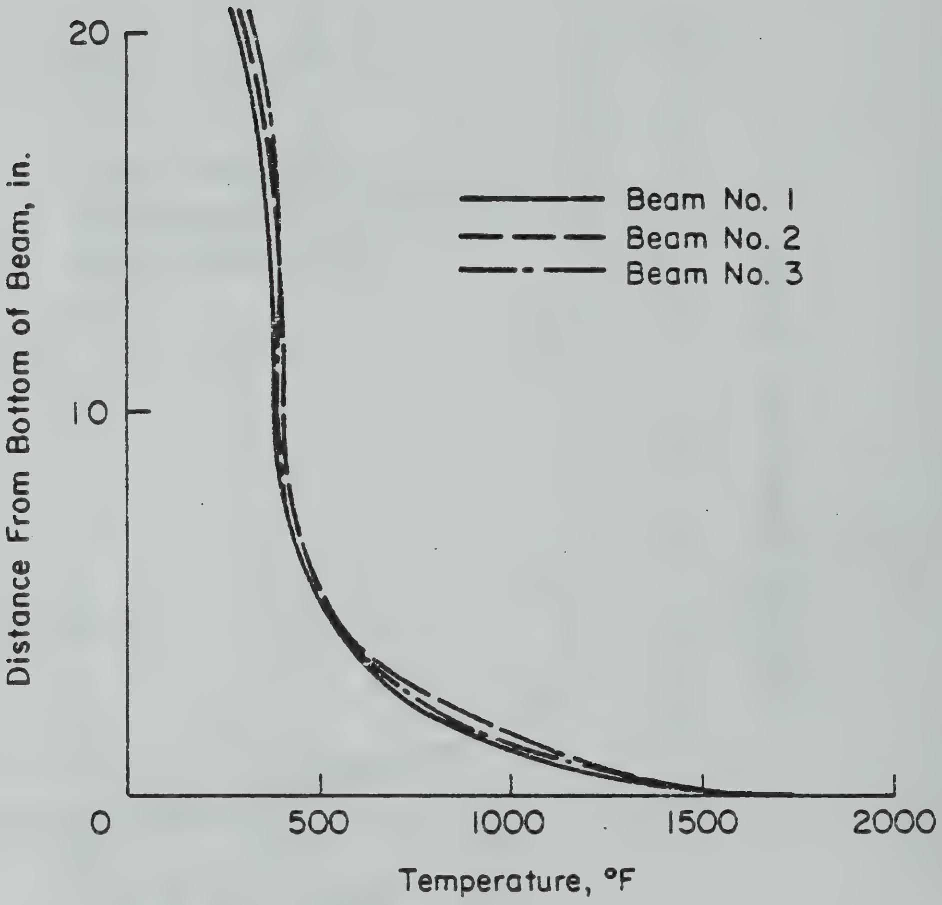

Fig. 39 Measured Temperatures in Beams 1, 2 and 3 Along the Centerline of Cross-Section @ 2 hr Test Time

Figures 40 and 41 compare the calculated and measured temperatures on Sections A-A and B-B of Beam No. 4 (See Fig. 3). The calculated temperatures on Section A-A near the top of the beam tend to be lower than the measured ones after 1 hr of fire exposure but are quite close at two hours. This indicates that perhaps the thermal conductivity at lower temperatures used in the analysis was somewhat low. At Section B-B, the measured temperatures in the interior of the beam (between 5 and 15 in. (127-318 mm) from the bottom of the beam) appeared to be higher than the temperatures nearer the exposed bottom surface of the beam. This behavior also was observed on Section B-B in Beam No. 1. It is possible that the bottom reinforcing steel with its higher thermal conductivity conducts heat longitudinally away from the section; such an effect would not be predicted by a two-dimensional thermal analysis. However, such behavior was not observed on Section B-B of Beam Nos. 2 and 3, which are nominally identical to Beam No. 1.

The predicted and observed temperatures at Sections A-A and B-B of Beam Nos. 5 and 6 are shown in Fig. 42 and 43 (See Fig. 3 and 4). Thermocouple No. 38 located at approximately 8 in. (203 mm) from the bottom of Beam No. 5 failed during the test and its temperature is not shown. The agreement between calculated and measured temperatures after approximately 1 hr of fire exposure is excellent, while the predicted temperatures

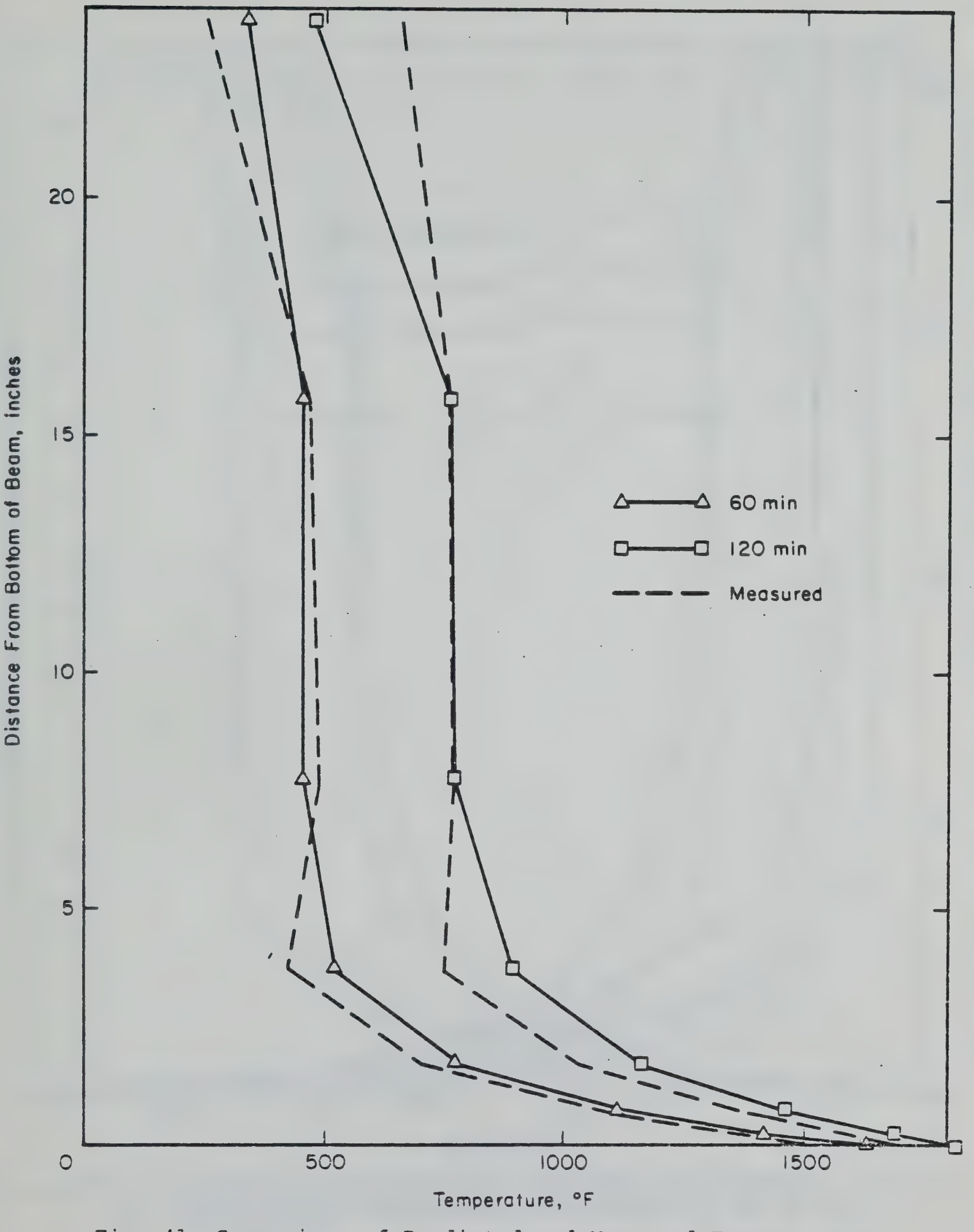

Fig. 41 Comparison of Predicted and Measured Temperatures 3.25 in. From Centerline of Cross Section of Beam No. 4

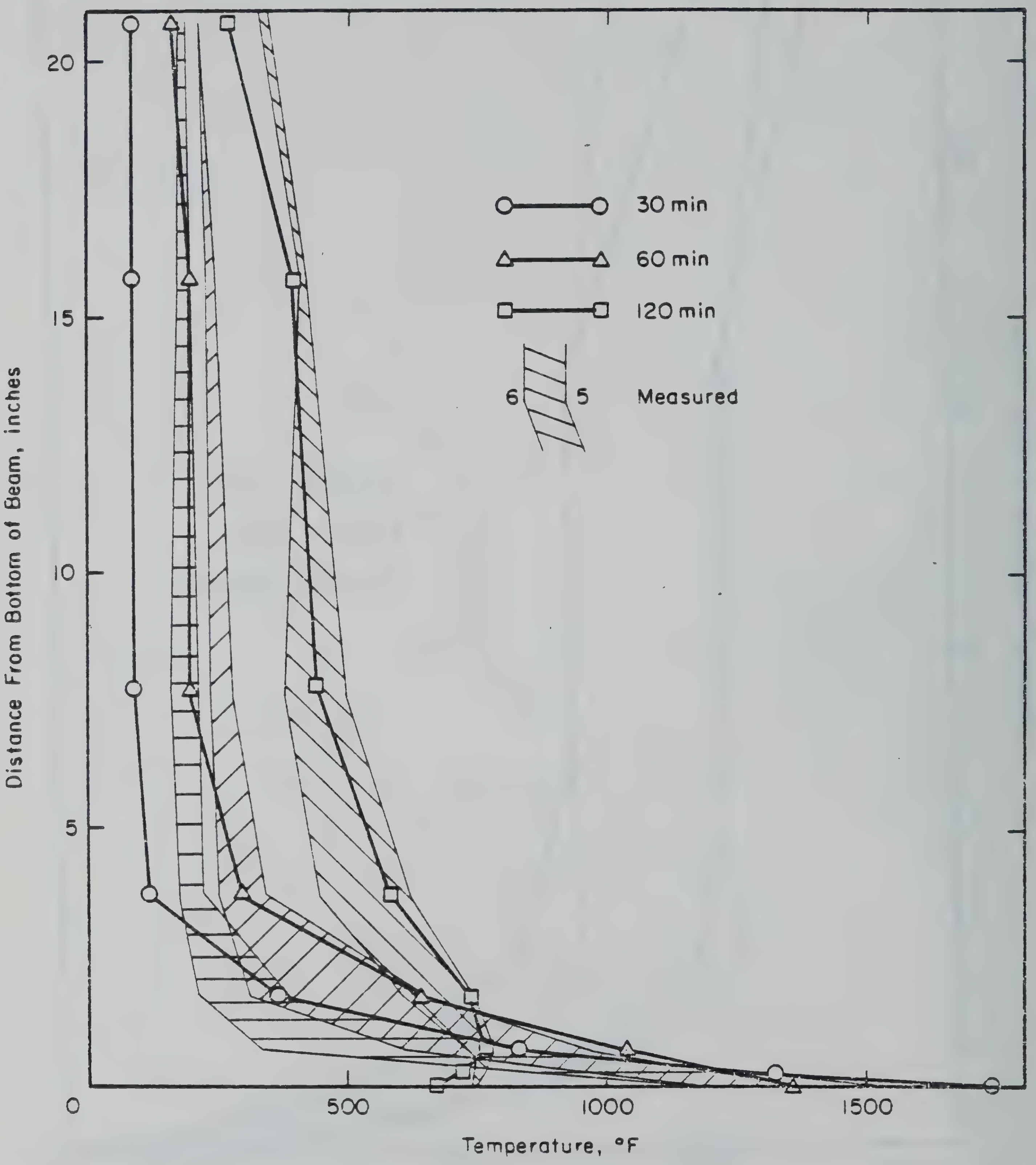

Fig. 42 Comparison of Predicted and Measured Temperatures on Centerline of Cross-Section of Beams No. 5 and 6 (SDHI Fire)

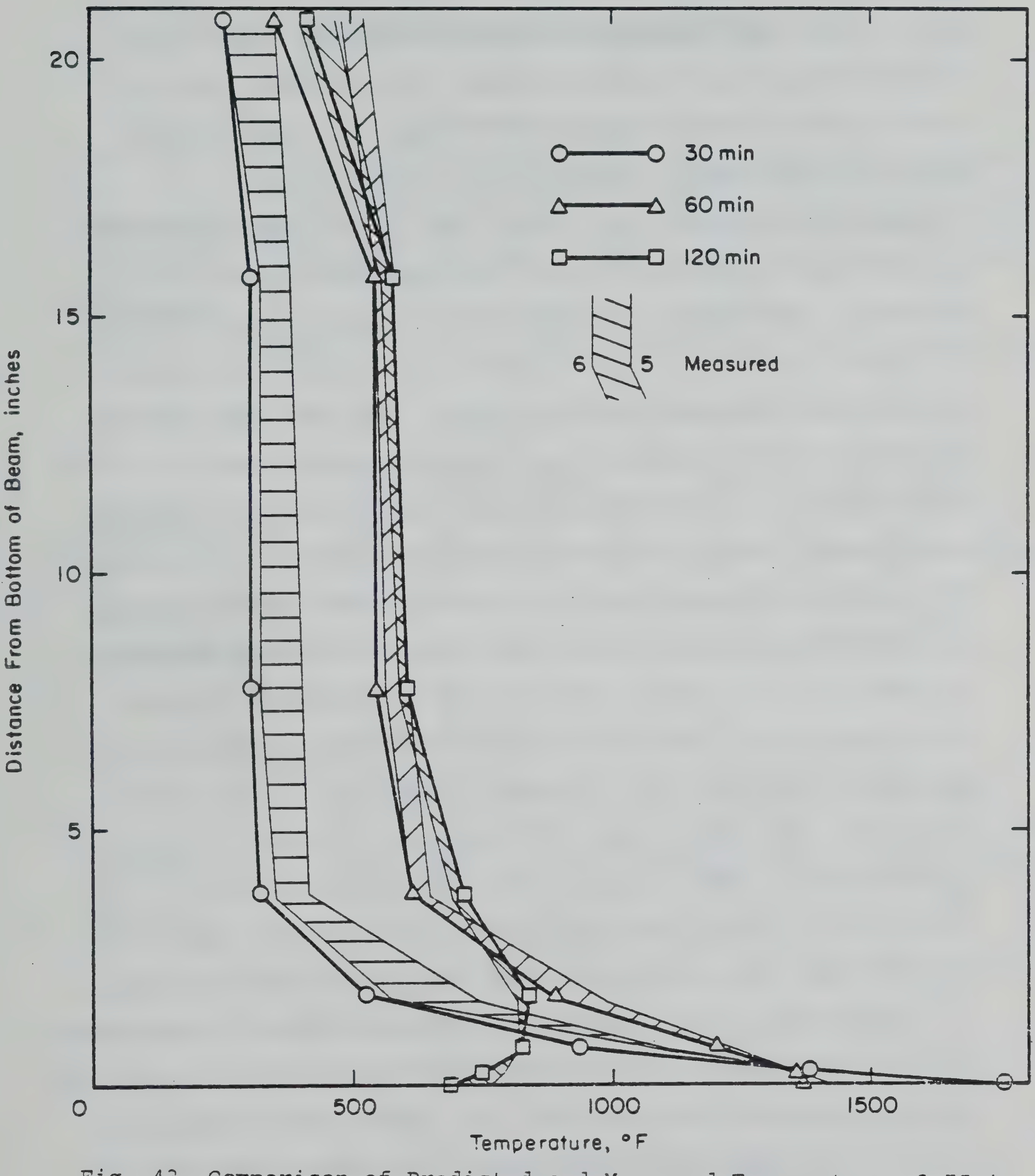

Fig. 43 Comparison of Predicted and Measured Temperatures 2.75 in. From Centerline of Cross-Section of Beam No. 5 and 6 (SDNT Fire)

at Section A-A early in the fire tend to be low. As shown in Fig. 11, the SDHI temperature reaches a maximum value at 35 minutes, after which cooling occurs. Nevertheless, Figs. 42 and 43 show that the interior of the beam continued to heat well into the cooling phase of the fire. Moreover, temperatures continued to rise in the interior of the beam for a longer period of time than in portions close to the fire boundary. For example, at Section B-B, temperatures maximized at about 1 hr 45 min, while at Section A-A on the centerline, temperatures maximized at 3 hr 30 min. The test data for Beam Nos. 5 and 6 presented in Figs. 18 to 20 confirm that significant cooling of the concrete close to the fire boundary has already occurred at two hours into the fire.

Figures 42 and 43 indicate relatively more scatter in the measured temperatures of Beam Nos. 5 and 6 than were measured in Beam Nos. 1, 2 and 3. The measured temperatures in Beam 6 were consistently lower than those in Beam No. 5. There is no apparent reason for this difference. Beam Nos. 5 and 6 were almost the same age at test (526 days and 520 days, respectively). Their relative humidities were slightly different (80 percent and 74 percent, respectively), and it is possible that this difference could be a contributing factor.

Temperatures in the top and bottom longitudinal reinforcement were measured in all beams by thermocouples placed on either side of the reinforcing bars (see Fig. 3). These temperatures are compared to temperatures predicted by the thermal analysis in Table 5 for Beam Nos. 2, 3 and 5. The agreement between

TABLE 5 - COMPARISON OF PREDICTED AND MEASURED TEMPERATURES °F IN REINFORCEMENT

5(a) Beam No. 2 (t = 3 hr)

	Top Reinforcement				Bottom Reinforcement			
Thermocouple No.	63	64	61	62	67	68	65	66
Measured	708	771	824	772	849	975	1075	1058
Avg.	740		798		912		1067	
Predicted	713		825		1024		1278	

5(b) Beam No. 3 (t = 3 hr)

	Top Reinforcement				Bottom Reinforcement			
Thermocouple No.	63	64	61	62*	67	68	65	66
Measured	639	682	712	671	850	879	998	965
Avg.	661		692		865		982	
Predicted	690		763		893		1055	

5(c) Beam No. 5 (t = 1 hr)

	Top Reinforcement				Bottom Reinforcement			
Thermocouple No.	63	64	61	62	67	68	65	66
Measured	353	452	465	--	441	516	615	584
Avg.	403		--		479		600	
Predicted	385		410		484		746	

*Thermocouple malfunction

calculated and measured temperatures is within about 12% in most cases. This is of particular importance, considering that the behavior of a properly designed reinforced concrete flexural member is governed primarily by the properties of the reinforcement. It is interesting to note that there is a significant temperature difference across the diameter of the individual reinforcing bars. The close agreement between calculated and measured temperatures lends support to the assumption that the reinforcing bars may be neglected in thermal analyses of reinforced concrete members with ordinary amounts of reinforcement.

Beam No. 3 differs from Beam 1 and 2 only in the amount of cover to the reinforcement (2-1/4 in. or 57 mm) and the location of the longitudinal reinforcement (see Fig. 1). The minimum permissible cover is 1-1/2 in. (38 mm), according to ACI Standard 318.(10) The purpose of the minimum cover requirement is to protect the reinforcement from the environment and minimize the possibility of splitting. The effect of the additional 3/4 in. (19 mm) concrete cover on the development of temperatures in the reinforcement is shown in Table 5b. The difference in temperatures in the top reinforcement in Beam Nos. 2 and 3 is on the order of 50 to 75°F throughout the fire exposure. However, the difference in temperature in the bottom reinforcement for these beams increases from 100°F at 1 hr to 200°F at 3 hr. The lower temperatures in the reinforcement would lessen the degradation in yield stress during the fire; this should be weighed against the slight reduction in load-carrying capacity that would result due to the reduction in effective depth.

STRUCTURAL ANALYSIS

Mechanical Properties of Concrete and Steel

When a structural element is exposed to fire, the element undergoes changes in length and material properties. The strengths and stiffnesses of steel and concrete invariably decrease as the temperature in the material increases. Data on mechanical properties of materials over a wide temperature range are required in analyzing structural response to fire. Much of these data on concrete at elevated temperatures were generated in the Construction Technology Laboratories of the Portland Cement Association as part of a continuing study of reinforced concrete members exposed to fire.(4,7)

The coefficients of thermal expansion for concrete and steel increase in a nonlinear fashion with increasing temperature. Figure 44 shows the thermal expansions for normal weight concretes and for steel. In general, the thermal expansion of concrete is influenced by the type of cement and aggregate and the water content.

The dependence of the modulus of elasticity of concrete made with siliceous, carbonate and light-weight aggregates on temperature is shown in Fig. 45. It appears that aggregate type and concrete strength do not significantly affect modulus of elasticity at high temperatures.(14) The modulus of

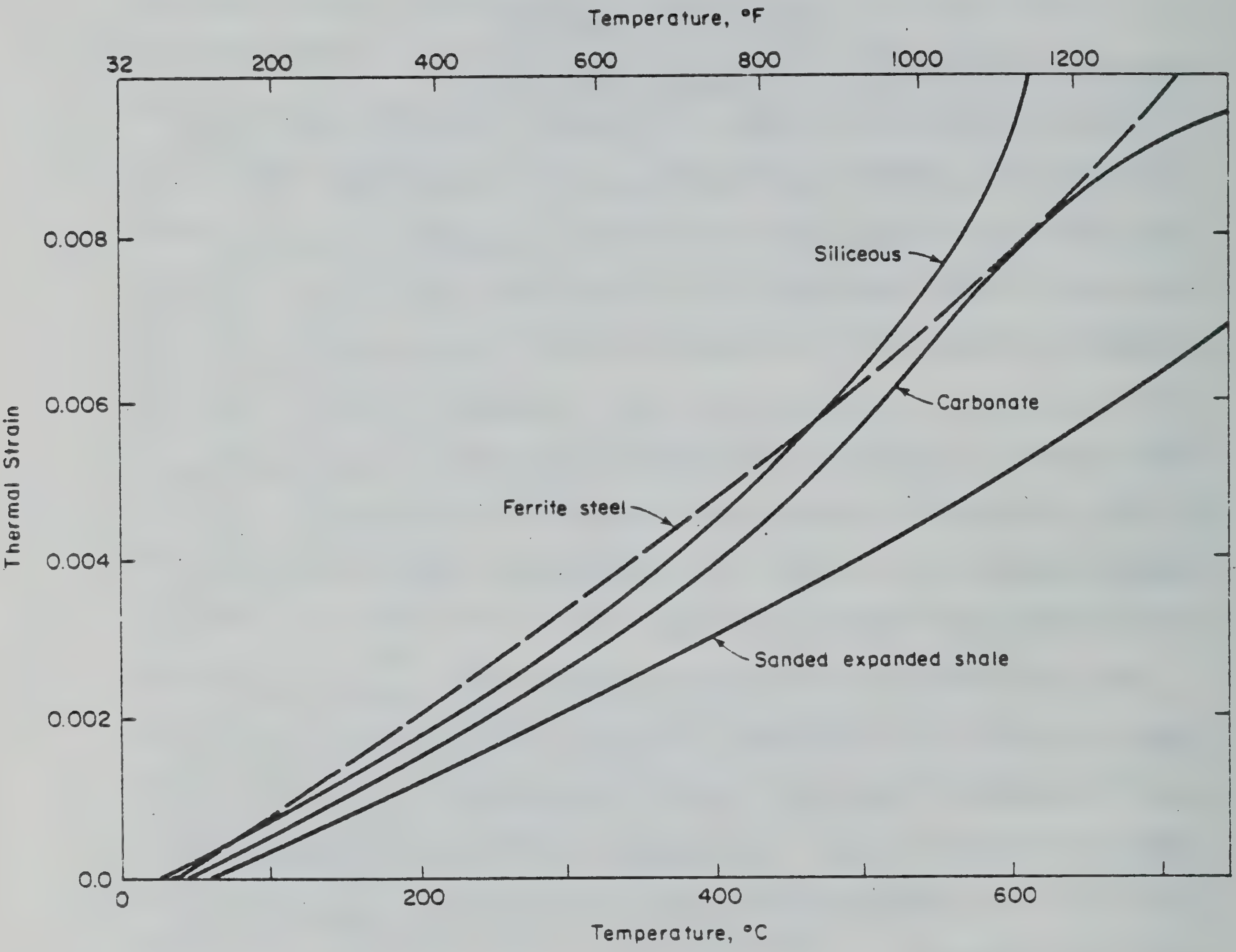

Fig. 44 Thermal Expansions of Concretes and Steel

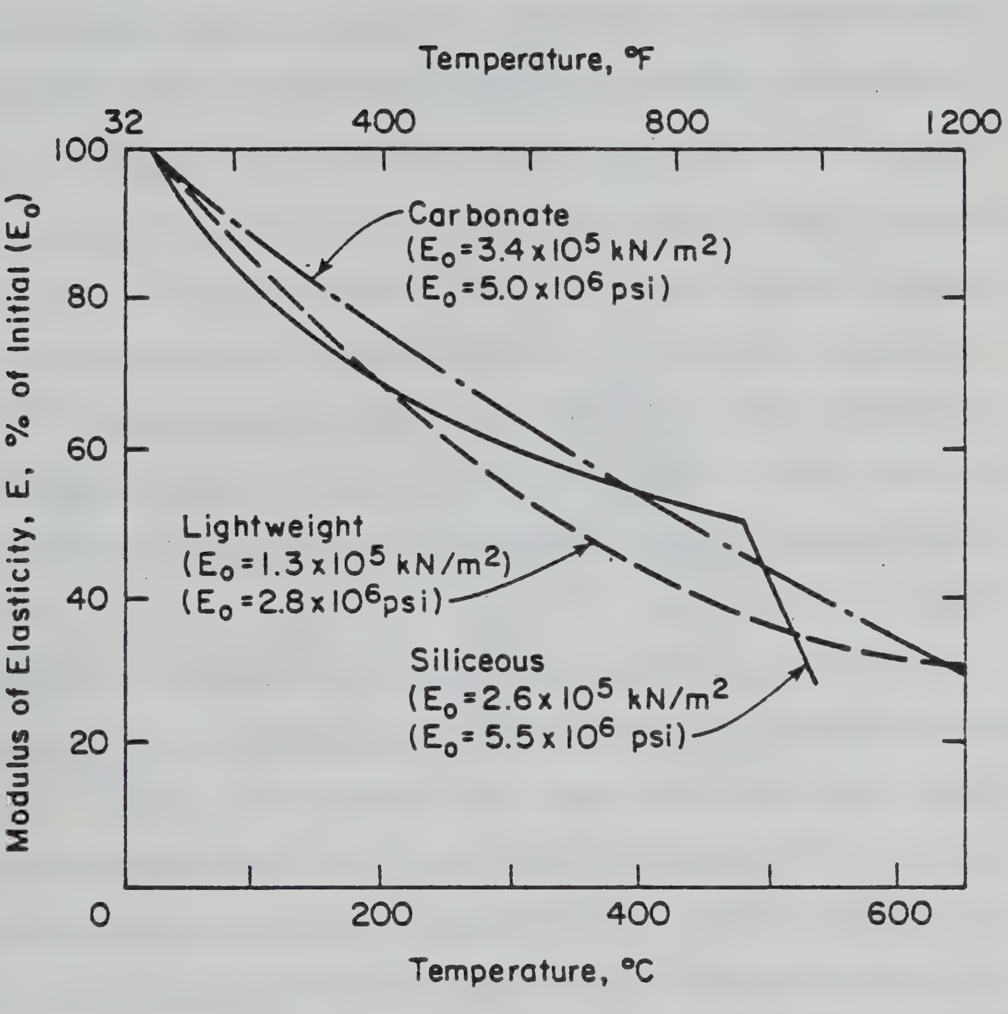

Fig. 45 Modulus of Elasticity of Concretes at High Temperatures

elasticity of steel decreases linearly with temperature to about 80% of its initial value at 500°C (932°F), and decreases rapidly thereafter.

The constitutive relation for concrete at elevated temperatures depends on the state of stress at the time of heating.(14,15) In general, concrete strength decreases with increasing temperatures.(14) However, concrete that was stressed to 0.4 f'_c during heating was stronger but less ductile than concrete that was heated without any restraint forces applied. Figure 46(a) and (b) show stress-strain relationships of concrete at high temperatures for unstressed and stressed specimens.(15) Note that in Fig. 46(b), ultimate strains are virtually independent of temperature and are close to the normal temperature value of about 0.004 in./in.

The stress-strain curve for concrete in tension is assumed to be linear up to the splitting strength. During the cooling phase, the concrete does not recover its initial strength because of internal degradation and chemical decomposition of the cement paste. Accordingly, the stress-strain curve during the cooling phase of the SDHI fire is assumed to be the same as its strength at maximum temperature.

The stress-strain curves for the steel reinforcement at elevated temperatures used in the structural analysis are shown in Fig. 47. The bilinear curves are reasonable approximations to nonlinear relations actually observed.(2,9)

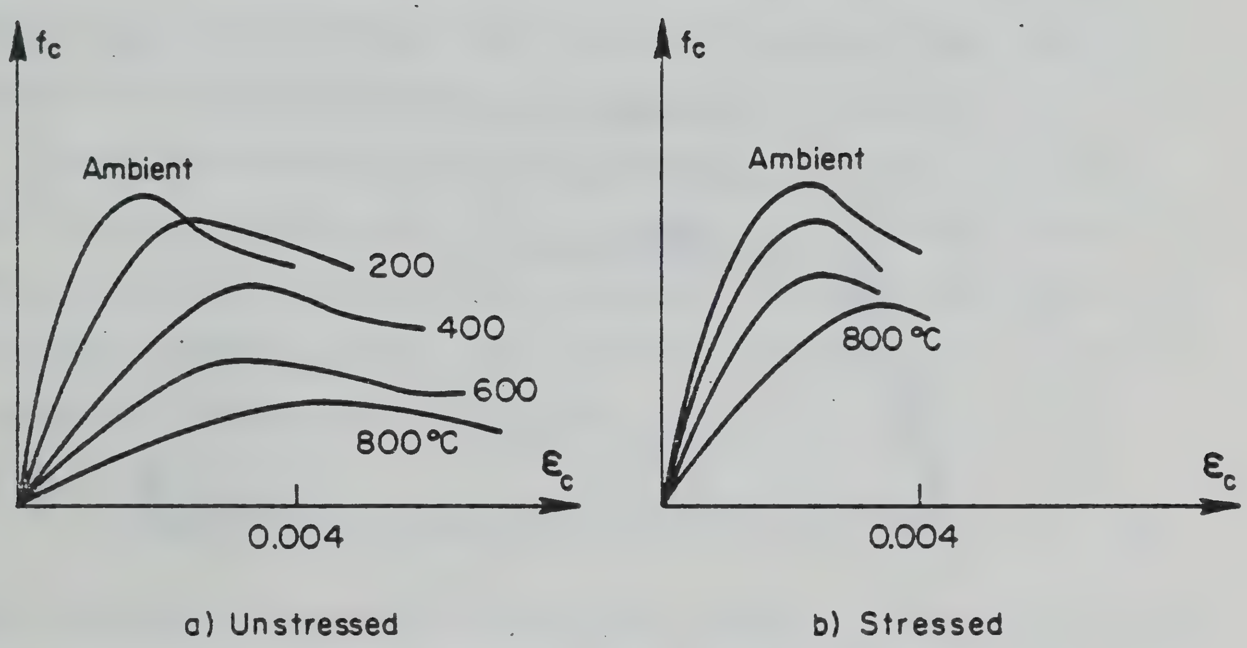

a) Unstressed

b) Stressed

Fig. 46 Stress-Strain Behavior of Concrete at Elevated Temperatures

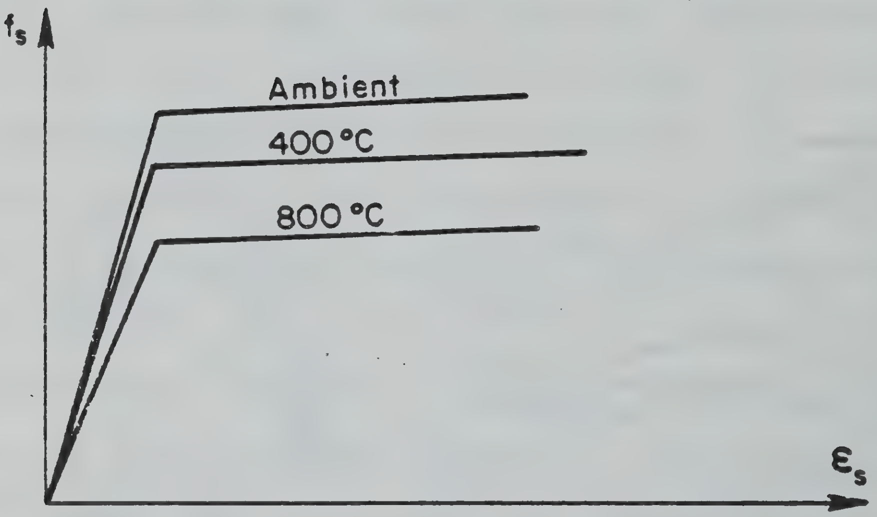

Fig. 47 Stress-Strain Behavior of Steel at Elevated Temperatures

Structural Analysis and Response

During the course of a fire, changes in material properties and creep and shrinkage at elevated temperatures and degradation of portions of the beam by cracking or crushing of the concrete cause a continual redistribution of forces in each beam. This behavior leads to a complex structural analysis problem. A computer program originally developed at the University of California$^{(2)}$ and subsequently modified at Lund Institute of Technology and at the National Bureau of Standards was used to perform the structural analysis of the six beams tested.

During the course of the fire, the total strain ε_T on any beam cross-section is the sum of strains due to thermal expansion at elevated temperatures, $\varepsilon_{th}(x,y)$, creep strains $\varepsilon_{cr}(x,y)$, transient strain $\varepsilon_{tr}(x,y)$, and mechanical strain $\varepsilon_{\sigma}(x,y)$ that is necessary to establish equilibrium;

$$\varepsilon_t(y) = \varepsilon_{th}(x,y) + \varepsilon_{cr}(x,y) + \varepsilon_{tr}(x,y) + \varepsilon_{\sigma}(x,y) \qquad (4)$$

The stresses on the cross section are computed from $\varepsilon_{\sigma}(x,y)$ using the appropriate temperature-dependent constitutive relationships shown in Figs. 46 and 47. Once the thermal, transient, and creep strains are determined as functions of the temperature, the stress-related strain ε_{σ} can be computed from Eq. 4. At elevated temperatures, $\varepsilon_{\sigma}(x,y)$ becomes highly nonlinear.

The thermal strains for concrete and steel are,

$$\varepsilon_{th}(x,y) = \int_{o}^{T} \alpha(T)\, dT \qquad (5)$$

in which α is the coefficient of thermal expansion for steel or concrete, as appropriate. The calculation of creep strains is described in Ref. (17).

The transient strain ε_{tr} is derived from a model suggested in Refs. 15 and 16. When compressed concrete is heated for the first time, the total strain is quite different from the total strain that is measured in constant temperature creep tests. An additional irrecoverable "transient strain" must be taken into account, as shown in Fig. 48. The significant parameters of this transient strain appear to be the level of stress and the thermal expansion (or, equivalently, the temperature). Accordingly, at each time step, the increment in transient strain, $\Delta\varepsilon_{tr}$, was assumed to be as the following expression$^{(16)}$,

$$\Delta\varepsilon_{tr} = -2.35 \frac{\sigma_c}{\sigma_{uo}} \Delta\varepsilon_{th} \text{, for } \sigma_c < 0 \text{ and } \Delta\varepsilon_{th} > 0$$

otherwise,

$$\Delta\varepsilon_{tr} = 0$$

in which $\Delta\varepsilon_{th}$ is the increment of thermal strain, σ_c is applied compressive stress, and σ_{uo} is the compressive strength at ambient conditions. When the transient strain is not included in the structural analysis, the result is a stiffer structural model of the beam at elevated temperatures. The computed thermal stresses become very large and can lead to a prediction of failure much earlier than would be observed.

The structural model of the beam consists of series of segments, as shown in Fig. 49. These segments usually were

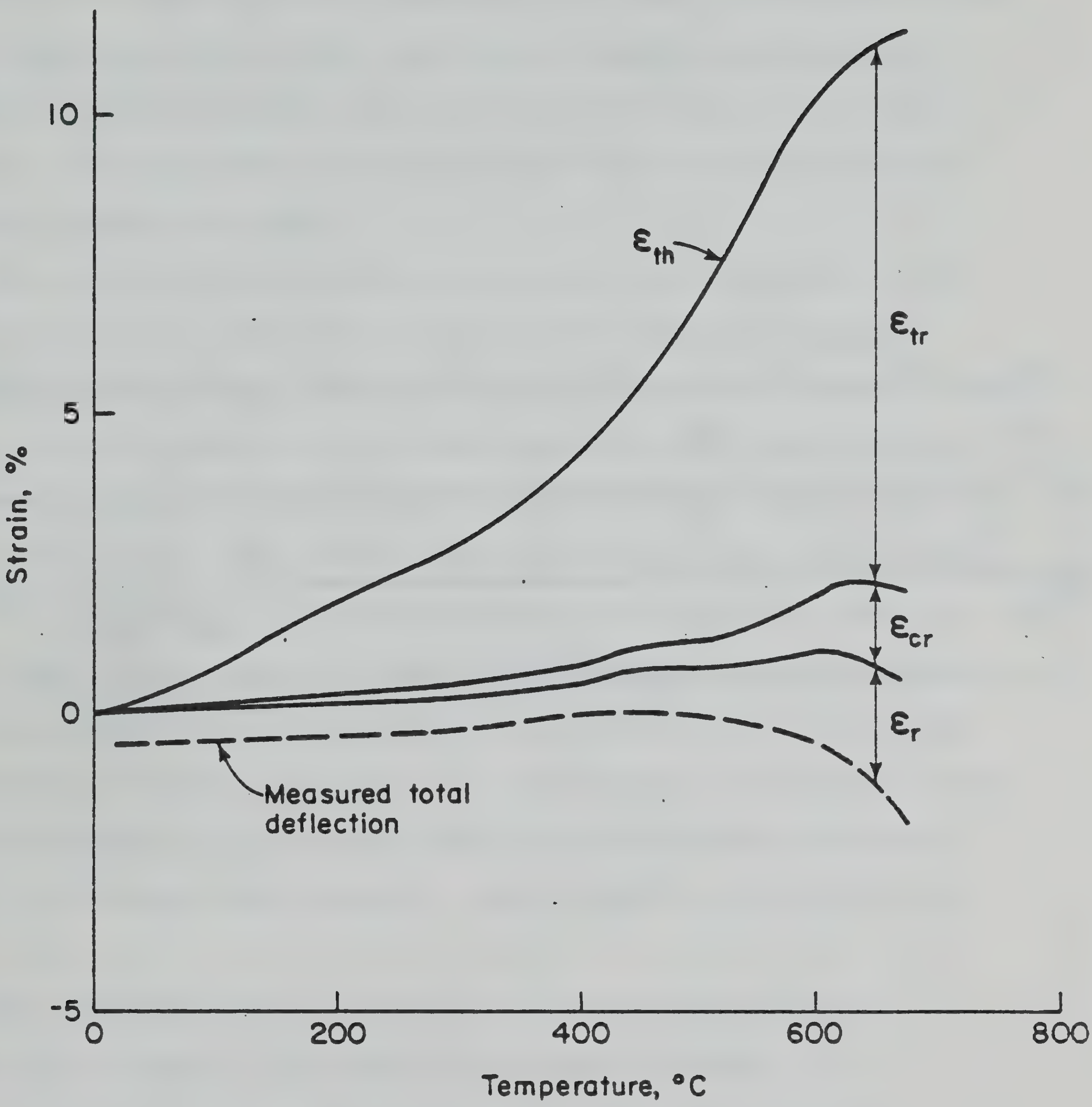

Fig. 48 Illustration of Transient Strain e_{tr} (after Ref. 15)

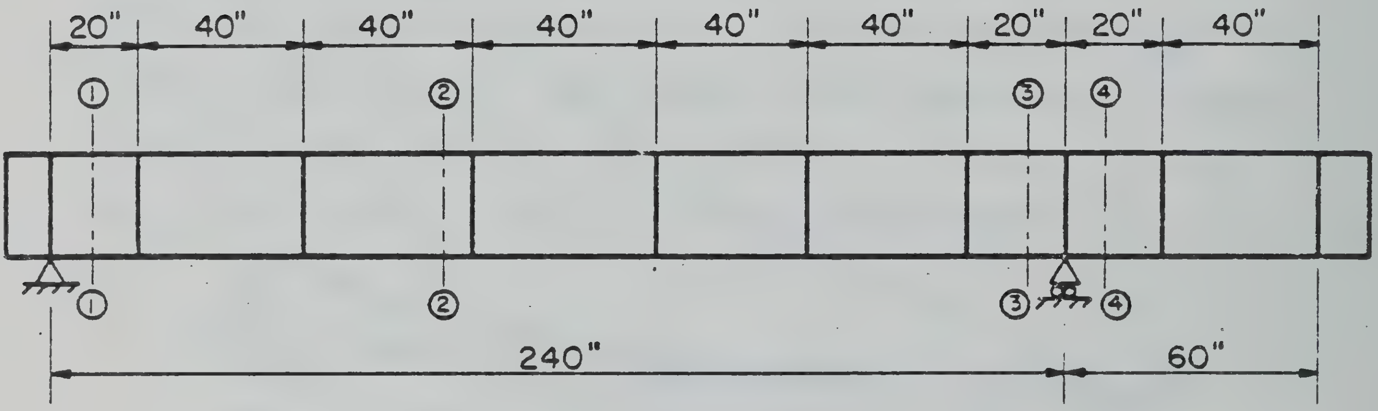

Fig. 49 Structural Modeling of Beams Tested

chosen to correspond to changes in the beam cross section due to the addition of reinforcement in regions of high moment or to point of application of concentrated loads. In regions where the moment changes rapidly, additional segments may also be required to obtain an accurate model of the beam. The cross section of each segment was discretized in a similar manner as for the thermal analyses.

The beams were analyzed at a sequence of time steps. At a particular time, a deformed shape for the beam was assumed based on deformations calculated during the previous time step. The total axial strain and curvature were then computed for each segment. The stiffness matrix for each segment was computed, taking into account the distribution of temperatures on the section, and a stiffness matrix for the beam. The load vector was formed from the applied loads and thermal effects. If each segment of the beam was in equilibrium for the assumed deformed beam shape, the time was incremented; otherwise, a new deformed shape was calculated and the procedure was repeated until convergence was obtained. More details are provided in Ref. (2).

The selection of an appropriate mesh and time step is important to ensure the stability of the solution. Unfortunately, no convergence criterion for the structural analysis portion of the algorithm is available. Thus, the mesh used to discretize the cross sections of the segments and the time step must be chosen by trial and error. Difficulties in convergence frequently were encountered if the mesh size exceeded about 1 in. (25 mm) in regions of steep thermal gradient or if the time step exceeded 5 minutes during the early stage of fire.

A common feature in all six beams tested and analyzed was the relatively poor agreement between predicted and observed deflections at ambient temperature (time t = 0 minutes). Table 6 compares the deflections predicted by the computer analysis and by the method suggested by ACI(10) with deflections measured prior to the start of the fire. The deflections predicted by the two analyses are in good agreement but in all cases are less than the measured deflections. The structural models of the beams apparently are stiffer than the beams tested. The apparent reason for this difference is the presence of several flexural cracks that appeared on the cantilever portion of the beam close to the east support when the loads were applied to the beam prior to the fire test. Such cracking was observed in all beams tested, and caused a slight loss of rotational stiffness and a concentration of curvature in the vicinity of the cantilever support. This can be seen quite clearly in the deflection profile of Beam No. 1 in Fig. 25(a). The computer program, which is based on the usual assumptions regarding continuous beam behavior, does not take localized cracking and the resulting concentration of curvature into account.

TABLE 6 - COMPARISON OF OBSERVED AND COMPUTED BEAM DEFLECTIONS AT AMBIENT CONDITIONS

Beam No.	Measured (in)	Computed, (in) Computer Analysis	 ACI 318
1	0.73	0.56	0.62
2	0.75	0.56	0.62
3	0.93	0.58	0.63
4	0.63	0.40	0.47
5	0.91	0.55	0.61
6	0.82	0.56	0.62

In the following comparisons of predicted and observed behavior, the actual deflections measured are presented without making any correction for localized cracking over the beam support so as not to introduce any artificiality into the discussion of the analysis of experiments. However, a better test of the ability of the computer analyses to simulate beam behavior accurately during fires would be obtained by initializing the predicted and experimental deflections to the same value at ambient temperature and then considering the predicted and observed incremental behavior of the beam during the course of fire. The agreement between predicted and observed beam behavior is quite good when this correction is made mentally while reviewing the comparisons in subsequent sections.

Figures 25(a) through 25(d) show deflection profiles measured during the test of Beam No. 1. Figure 50 compares the maximum predicted and measured deflections in the span as a function of elapsed time for Beam Nos. 1 and 2. The agreement between predicted and measured deflection is very close for the first 3 hr and 10 min of the fire for both beams; thereafter, the predicted increments of deflection are somewhat larger than those measured. The predicted temperatures in the bottom reinforcement are from 100°F (38 C) to 200°F (93 C) higher than measured at this late stage of the fire, which causes a reduction in the modulus of elasticity of the reinforcement and a loss in beam stiffness. The computer program predicted failure for Beam Nos. 1 and 2 at 3 hr and 45 min; tests of Beam Nos. 1 and 2 were terminated at 3 hr and 40 min and 3 hr and 26 min, respectively.

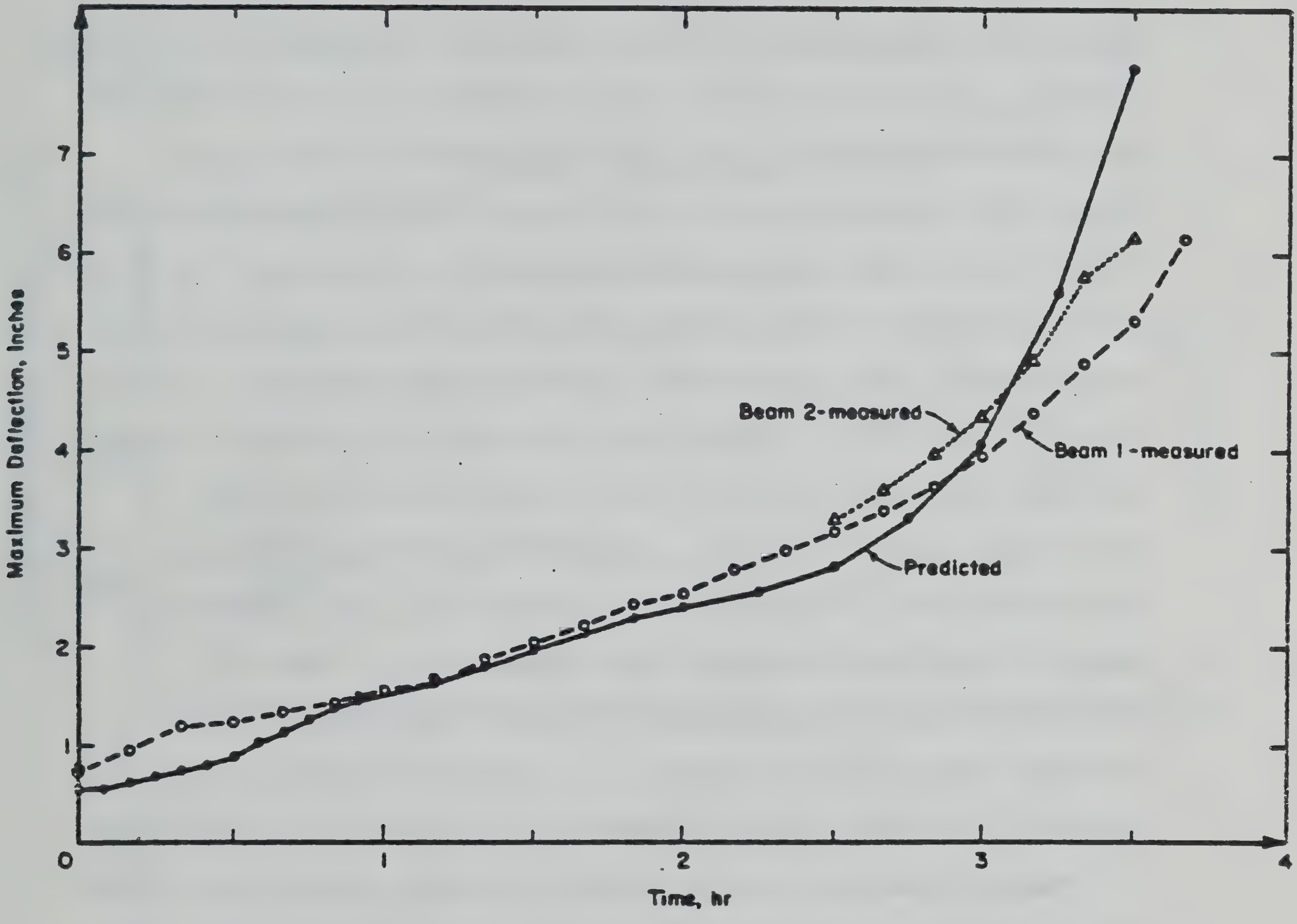

Fig. 50 Comparison of Predicted and Measured Maximum Deflections of Beam Nos. 1 and 2

At these times, the maximum rates of deflection approached 0.1 inch/minute, flexural cracks had opened to a maximum width of about 1/2 in. (13 mm) and the worst shear crack in the vicinity of the cantilever support was about 1/4 in. (6 mm) in width.

The structural analysis predicts a growth in flexural cracking in the beam during the course of the fire. Figure 51 illustrates the percentage of section cracked at several points along Beam No. 1 during the fire. The fluctuations in percentage of section cracked are due to cracks opening and closing as a result of redistribution of stresses on the sections during the fire. At the beginning of the test, prior to exposure to fire, about 35 to 45% of the section cracked, which is typical for a beam loaded to full unfactored gravity load conditions. After 1 hr of fire, 77% of the section adjacent to the simple support cracked, while about 55% of the section adjacent to the cantilever support cracked. After 2 hr of fire, these percentages of cracks adjacent to simple and continuous supports had grown to 84 and 68, respectively. Note, in contrast, that the percentage of section cracked in the unheated cantilever adjacent to its support remained constant at 43% of cracked section throughout the entire fire duration.

These increases in percentage of cracked section during the fire reduce the available area of concrete to resist shear and might increase the likelihood of a shear failure developing if it were not for the presence of stirrups at the supports. In fact, the beams did show considerable signs of shear distress. For example, in Beam No. 1, a diagonal shear crack about 4 in.

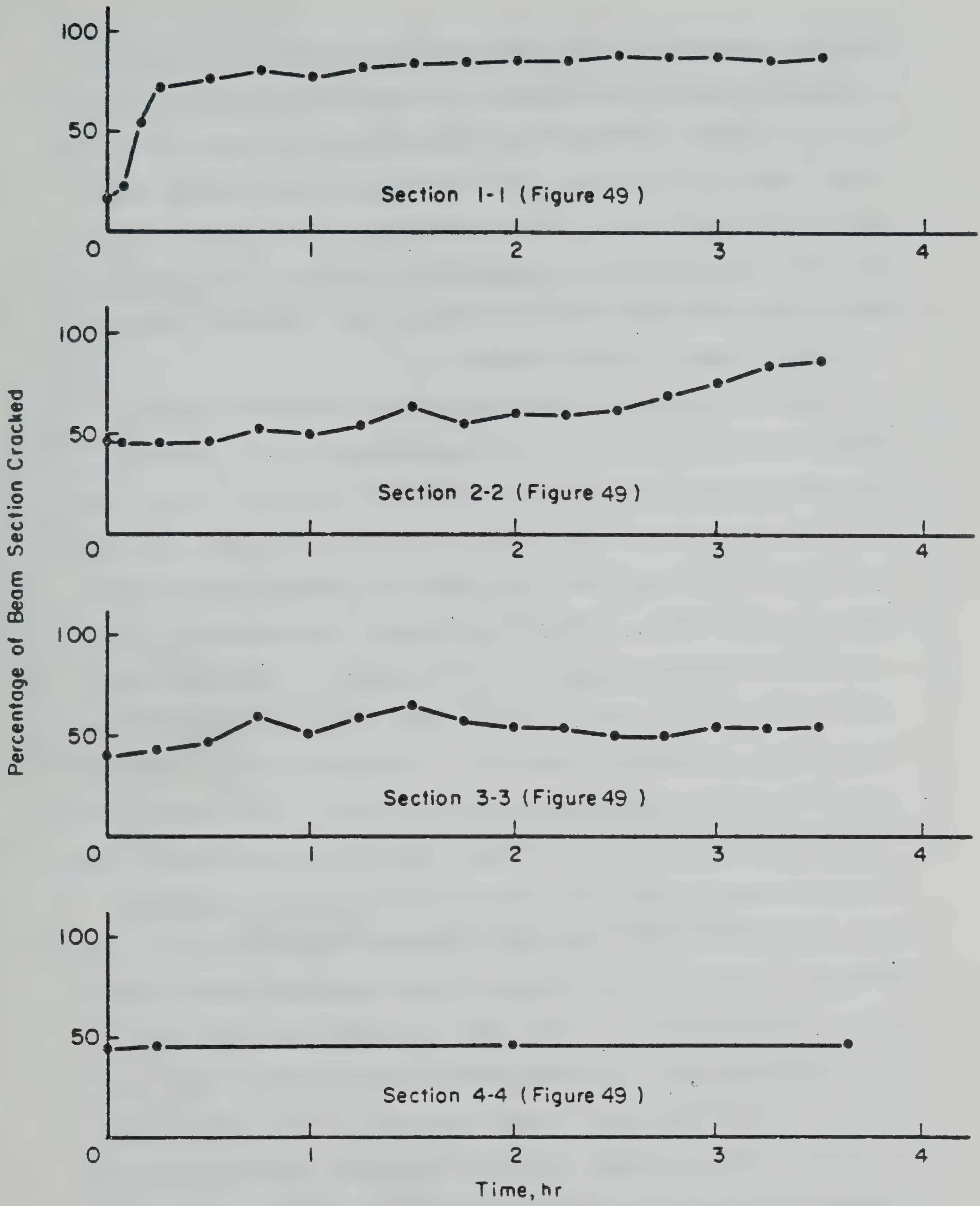

Fig. 51 Percentage of Section Predicted Crack in Beam No. 1 (See Fig. 49 for Location of Sections)

(101 mm) appeared in the lower portion of the beam about 4 ft (1.22 mm) from the east support in the furnace at 1 hr 30 min; at 1 hr 45 min, a second shear crack formed to the left of the first, and at 2 hr 10 min, two additional shear cracks were observed. The existing cracks subsequently lengthened and at the time the test was terminated at 3 hr 40 min, the worst shear crack was about 1/4 in. (6 mm) wide. However, none of the beams tested failed in shear.

Figure 52 compares the predicted and measured maximum deflection for Beam No. 3. The predicted growth in maximum deflection above the initial value over the first 3 hr of the fire was 1.63 in. (41 mm), while the observed growth was 2.59 in. (66 mm). In contrast, for Beam No. 1 these figures were 3.47 in. and 3.20 in. (88 mm and 81 mm); for Beam No. 2 they were 3.47 in. and 3.6 in. (88 mm and 91 mm). The additional 3/4 in. (19 mm) bar cover limited the increase of deflection during fire. Failure of Beam No. 3 was predicted at 3 hr 45 min; the test was terminated at 4 hr 8 min.

A comparison of predicted and measured deflections for Beam No. 4 is shown in Fig. 53. The results are quite similar to those for Beam No. 3. Beam No. 4 had the highest nominal shear strength of any beam tested and it was theorized that it might fail in shear during the fire due to greater applied load at the cantilever end. Although shear cracks formed, Beam No. 4 showed no more distress in shear than any of the other beams tested and the subsequent thermo-structural analysis indicated that the percent cracking of the various critical sections

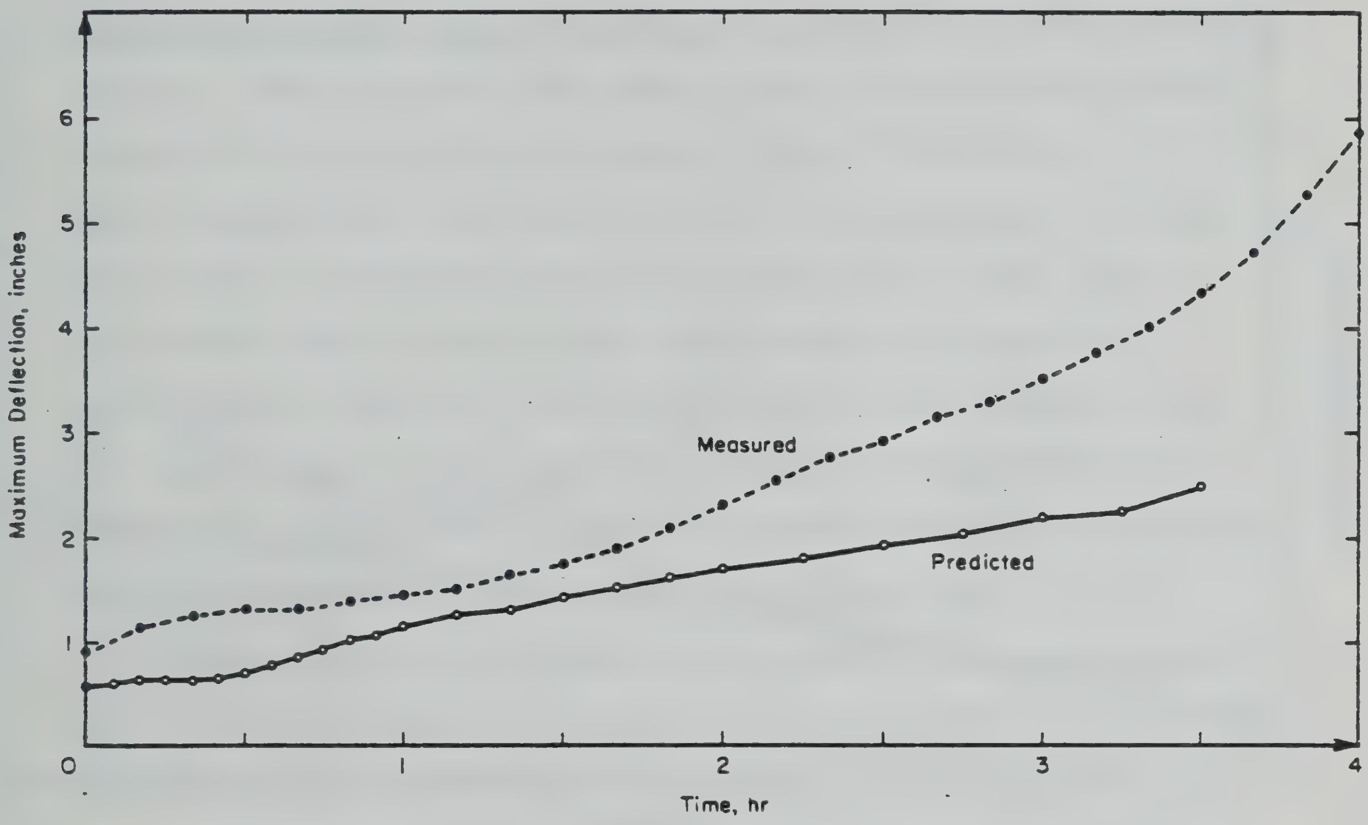

Fig. 52 Comparison of Predicted and Measured Maximum Deflections of Beam No. 3

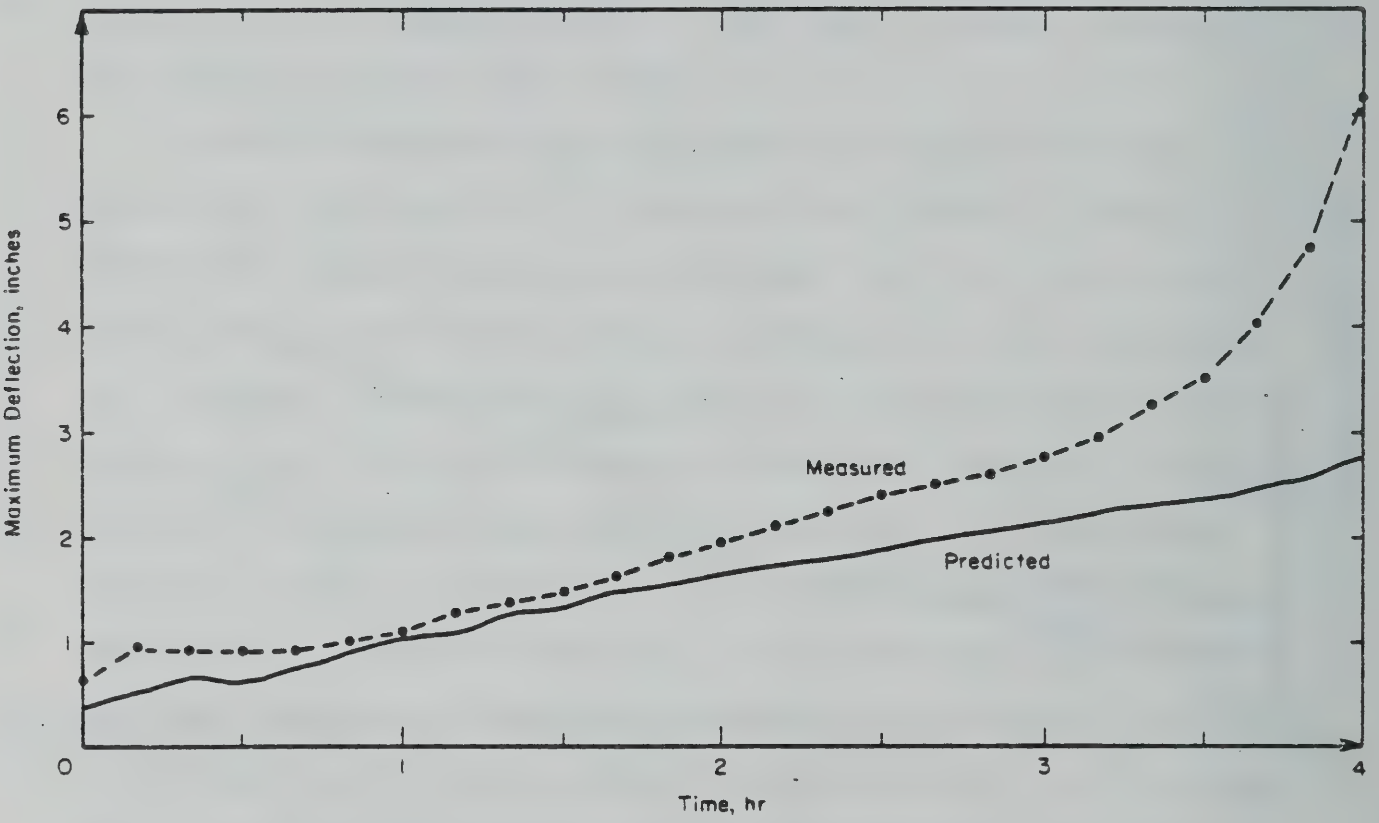

Fig. 53 Comparison of Predicted and Measured Maximum Deflections of Beam No. 4

along the span was quite similar to that shown for Beam No. 1 in Fig. 51. The computer simulation of the fire test of Beam No. 4 ran for the full 4 hr without predicting failure. The test of Beam No. 4 was terminated at 4 hr 8 min.

Beam Nos. 5 and 6 were tested with the SDHI fire exposure. The predicted and observed behavior of these beams during test is quite different from the behavior of the first four beams tested. Figures 54 and 55 compare the predicted and observed maximum deflections for Beam Nos. 5 and 6. A rotary potentiometer that was used to measure the maximum deflection in Beam No. 5 recorded erratically during the test. Thus, a polynominal was fitted to the data obtained at adjacent potentiometer stations, and the deflection was obtained from the polynominal by interpolation. When the discrepancy at ambient is removed, the agreement between predicted and observed deflections is quite good during the entire fire.

Several points of interest can be noted from Figs. 54 and 55. First, the maximum deflection during the SHDI fire exposure is substantially less than that observed during the ASTM fire, being approximately 2-3 in. (51-76 mm) for the SHDI fire and 6 in. (152 mm) for the ASTM fire. Second, unlike the beams tested with the ASTM fire exposure, the effect of increasing the concrete cover over the reinforcing bars has a much less pronounced effect on the maximum deflection during the test. The time at which Beam No. 6 attains its maximum deflection is greater than Beam No. 5 (in excess of 3 hr as opposed to 2 hr in Beam No. 5), but the maximum deflections are within about

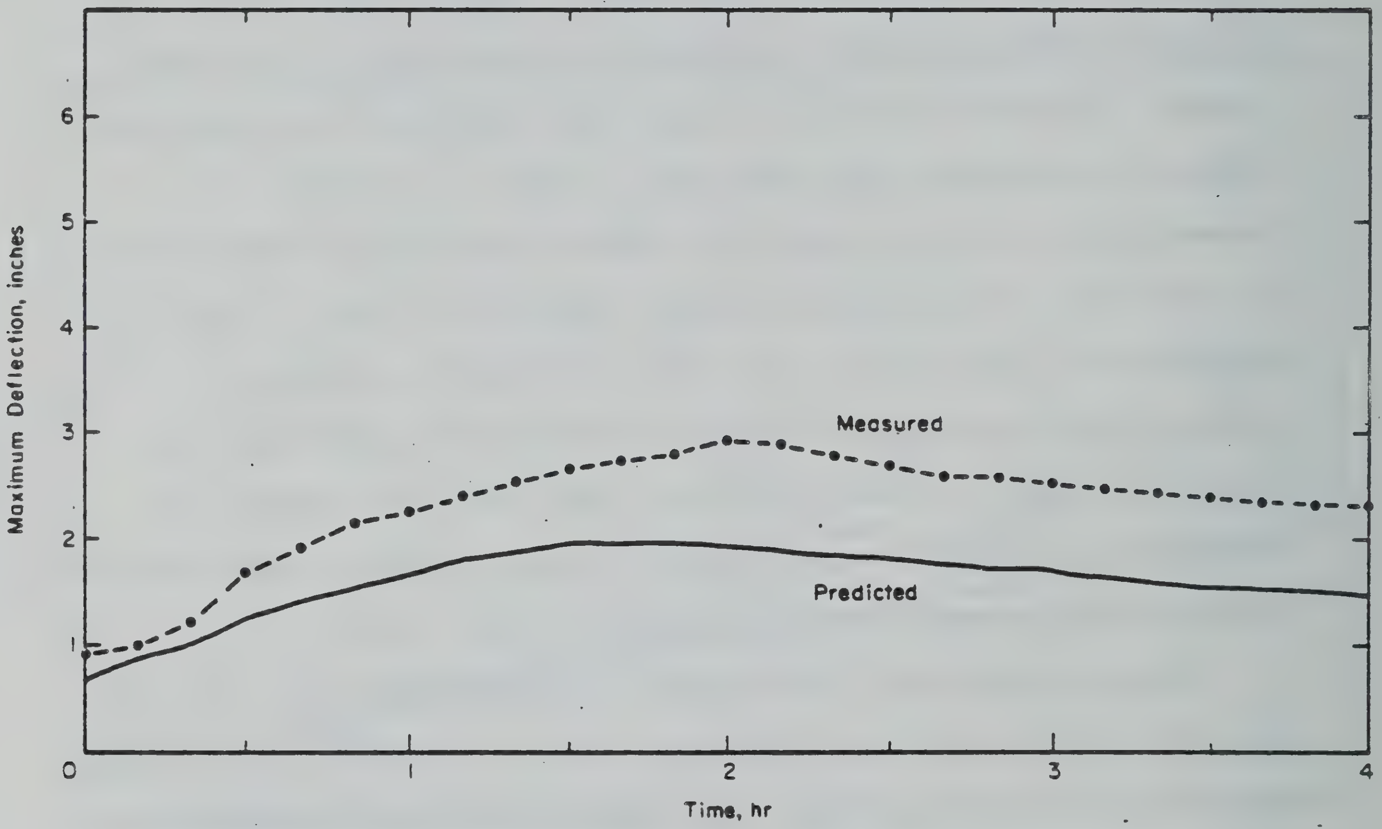

Fig. 54 Comparison of Predicted and Measured Maximum Deflections of Beam No. 5

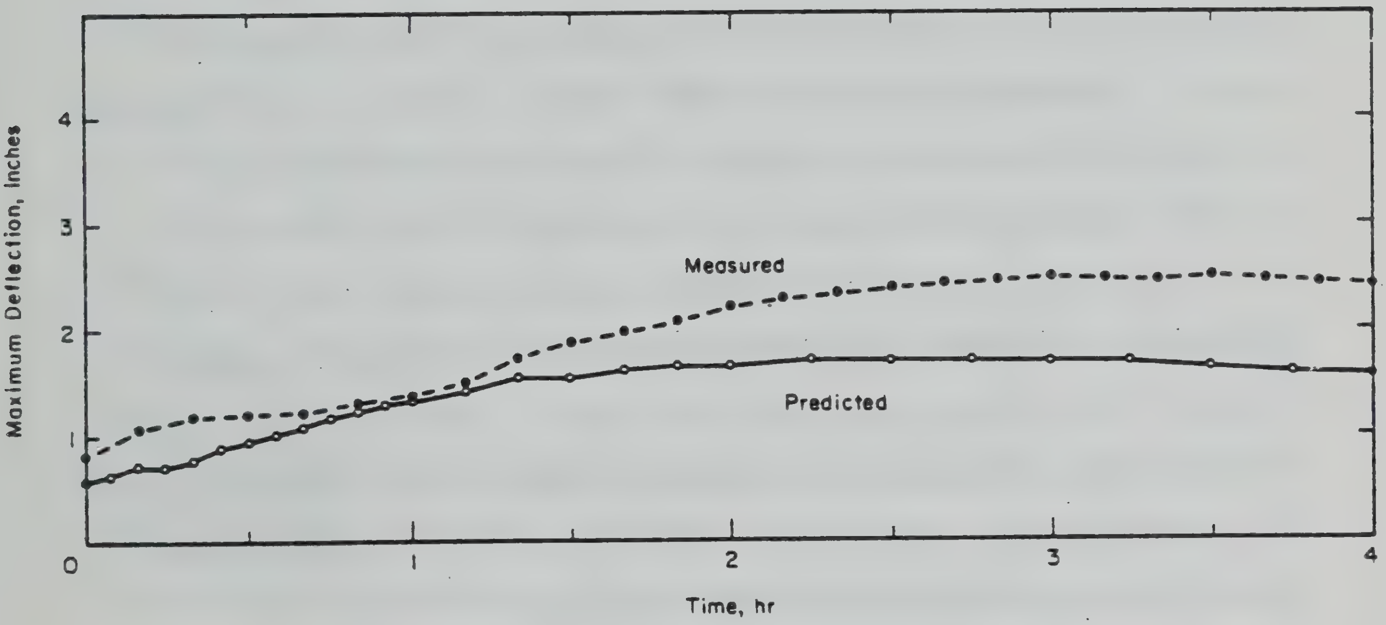

Fig. 55 Comparison of Predicted and Measured Maximum Deflections of Beam No. 6

1/4 in. (6 mm) of each other. Thus, in a realistic fire exposure, the increased bar cover appears merely to delay the time at which maximum deflection occurs rather than the magnitude of the deflection. Perhaps most significant, neither Beam No. 5 nor Beam No. 6 came close to imminent collapse during the SDHI fire exposure.

The behavior of concrete beams exposed to realistic exposure such as the SHDI fire appears to be characterized by a period of relatively stable behavior following the initial heating phase. Although the gradients of thermal strain on the section are greater in the early stages of the fire, they are more uniform during the extended cooling phase. This uniformity in thermal strain leads to extended period of relatively stable behavior of the beam, in contrast to the continually changing behavior seen during the ASTM fire test. However, this observation would not apply to structural members with thin sections or higher thermal conductivity; the behavior of such members would follow the SDHI curve more closely.

SUMMARY

In this program, six 27-ft (8.2 m) long, reinforced concrete beams were fire tested. Five beams were 21-in. high by 9-in. (533x224 mm) wide and one beam was 24-in. high by 10-in. (610x254 mm) wide. An ASTM Designation: E119 fire was used in four of the tests and a SDHI fire in the remaining two tests.

Applied loads, furnace atmosphere, concrete and steel temperatures, deflections, expansions, and slopes were measured in each test. These data were needed to validate the computer program developed in the Center for Building Technology of the National Bureau of Standards.

All beams developed shear cracks as early as 90 minutes after the start of the fires. Flexural cracks formed in the positive moment region approximately 30 min. later extended rapidly. As a result, none of the beams tested failed by shear but rather by flexure. Thus, shear strength of beams at elevated temperatures does not appear to be a problem.

Tests were terminated when the rate of increase in deflection reached the point where flexural failure became imminent. Test durations ranged from 3 hr 26 min. to 4 hr 8 min.

This investigation has shown that thermo-mechanical structural analysis, coupled with appropriate material constants, can predict the behavior of reinforced concrete structural elements exposed to different fire exposures, at least within the limits of accuracy required for states limit states design. The ability of the analysis to predict structural behavior is limited by the quality of data available on the structural materials at elevated temperatures, and to a lesser extent by the analytical model which neglects the effect of localized cracks and spalling of concrete.

The most important factor affecting predicted beam behavior is the calculated temperature history in the reinforcement.

The computation of these temperatures directly from temperatures in the concrete obtained from a two-dimensional thermal analysis tends to be conservative because the capacity of the reinforcement to conduct heat longitudinally is not taken into account. In contrast, accuracy in predicting temperature distribution in the concrete is not as important in predicting load-carrying capacity of reinforced concrete beams.

REFERENCES

1. ASTM Designation: E119, "Standard Methods of Fire Tests of Building Construction and Materials," American Society for Testing and Materials, Philadelphia, Pa.

2. Becker, J. and Bresler, B., "FIRES - RC - A Computer Program for the Fire response of Structures - Reinforced Concrete Frames," Report No. UCB-FRG 74-3, University of California, Berkeley, California, July, 1974.

3. Woods, Hubert, "Research on Fire Resistance of Prestressed Concrete," Journal of the Structural Division, ASCE, Vol. 86, No. ST11, Nov., 1960, pp. 53-64.

4. Lin, T. D., Gustaferro, A. H., and Abrams, M. S., "Fire Endurance of Continuous Reinforced Concrete Beams," 1981, PCA Bulletin RD072.01B.

5. ASTM Designation" A615-74A, Standard Specification for Deformed and Plain Billet-Steel Bars for Concrete Reinforcement, American Society for Testing and Materials, Philadelphia, Pa.

6. Monfore, G. E., "A Small Probe-Type Gage for Measuring Relative Humidity," Journal of the PCA Research and Development Laboratories, Bol. 5, No. 2, pp. 41-47, May 1963; PCA Research Department Bulletin 160.

7. Lin, T. D., and Abrams, M. S., "Fire Tests of Reinforced Concrete Beams," 1981, PCA Research Report.

8. Magnusson, S. E. and Thelandersson, S., "Temperature-Time Curves of Complete Process of Fire Development, Theoretical Study of Wood Fuel Fires in Enclosed Spaces," Acta Polythenica Scandinavica, Ci 65, Stockholm, 1970.

9. Ellingwood, Bruce and Shaver, J. R., "Analysis of Reinforced Concrete Beams Subjected to Fire," 1976, Building Science Series No. 76, Nationals Bureau of Standards, Washington, DC 20234.

10. "Building Code Requirements for Reinforced Concrete, ACI Standard 318-77, " American Concrete Institute, Detroit, MI, 1977.

11. Harmathy, T. Z., "Thermal Properties of Concrete at Elevated Temperatures," 1970, Journal of Materials, JMLSA, Vol. 5, No. 1.

12. Ellingwood, B. and Shaver, J., "Effects of Fire on Reinforced Concrete Members," Journal of the Structural Division, ASCE, Vol. 106, No. ST11, November 1980, pp. 2151-2166.

13. Wickstrom, U., "TASEF-2: A Computer Program for Temperature Analysis of Structures Exposed to Fire," Department of Structural Mechanics, Lund Institute of Technology, Report No. 79-2, Lund, Sweden, 1979.

14. Abrams, M. S., "Compression Strength of Concrete at Temperature and Concrete, American Concrete Institute SP 25, Detroit, MI, 1971.

15. Schneider, U., "Behavior of Concrete Under Thermal Steady State and Non-Steady State Conditions," Fire and Materials, 1, 1976, pp. 103-115.

16. Anderberg, Y., and Thelandersson, S., "A Constitutive Law for Concrete at Transient High Temperature Conditions," Lund Institute of Technology Report, Lund, Sweden, 1978.

17. Harmathy, T. Z., "A Comprehensive Creep Model," Journal of Basic Engineering, ASME, September 1967, pp. 496-502.

NBS-114A (REV. 2-80)

U.S. DEPT. OF COMM. **BIBLIOGRAPHIC DATA SHEET** *(See instructions)*	1. PUBLICATION OR REPORT NO. NBS/GCR-87/536	2. Performing Organ. Report No.	3. Publication Date November 1987

4. TITLE AND SUBTITLE

Flexural and Shear Behavior of Reinforced Concrete Beams During Fire Tests

5. AUTHOR(S)

T.D. Lin, Bruce Ellingwood, Olivier Piet

6. PERFORMING ORGANIZATION *(If joint or other than NBS, see instructions)*

Portland Cement Association
5420 Old Orchard Road
Skokie, IL 60077

7. Contract/Grant No.

G8-9027

8. Type of Report & Period Covered

Final

9. SPONSORING ORGANIZATION NAME AND COMPLETE ADDRESS *(Street, City, State, ZIP)*

Center for Fire Research
National Bureau of Standards
Gaithersburg, MD 20899

10. SUPPLEMENTARY NOTES

This report includes extended analysis of tests conducted by PCA under the above grant.

☐ Document describes a computer program; SF-185, FIPS Software Summary, is attached.

11. ABSTRACT *(A 200-word or less factual summary of most significant information. If document includes a significant bibliography or literature survey, mention it here)*

The results of fire resistance tests of six reinforced concrete beams exposed to the standard ASTM E119 test conditions and to a short duration high intensity fire are described and summarized. The measured temperatures, deflections, expansions and slopes together with the thermal and structural properties of concrete and steel were used to validate predictive thermal structural analysis computer programs.

12. KEY WORDS *(Six to twelve entries; alphabetical order; capitalize only proper names; and separate key words by semicolons)*

ASTM E119; fire resistance testing; flexure strength; reinforced concretes; shear strength; structural design; thermal analysis

13. AVAILABILITY

☒ Unlimited
☐ For Official Distribution. Do Not Release to NTIS
☐ Order From Superintendent of Documents, U.S. Government Printing Office, Washington, D.C. 20402.
☒ Order From National Technical Information Service (NTIS), Springfield, VA. 22161

14. NO. OF PRINTED PAGES

104

15. Price

$18.95